Title	Application of Hyperspectral Remote Sensing to Estimate Eutrophication in Shallow Lakes and Reservoirs
Author(s)	Abdoul Nasser IBRAHIM
Citation	高知工科大学，博士論文.
Date of issue	2006-09
URL	http://hdl.handle.net/10173/202
Rights	
Text version	author

Application of Hyperspectral Remote Sensing to Estimate Eutrophication in Shallow Lakes and Reservoirs

Abdoul Nasser IBRAHIM

A dissertation submitted to
Kochi University of Technology
in partial fulfillment of the requirements
for the degree of

Doctor of Philosophy

Department of Engineering
Graduate School of Engineering
Kochi University of Technology
Kochi, Japan

August 2006

Acknowledgement

My research work and my personal life in Kochi have benefited from the help, advises, and friendship of many people and organizations including Kochi University of Technology (KUT), International Relation Center (IRC), Nakajima Foundation, Tohoku University, Chiba Natural History Museum, and Japan International Cooperation Agency (JICA).

First, I would like to address my gratitude to my advisor Professor Masahiro Murakami of the Department of Frontier Engineering at KUT. His support and his help to my research and my personal life in Kochi have been essential for carrying out and for completing this research.

Thanks also to my PhD committee members comprising Professor Shunji Kusayanagi, Professor Seigo Nasu, Professor Kasuo Ouchi, Professor Tsunemi Watanabe, Professor Masaki Sawamoto, and Professor Masahiro Murakami.

The International Relation Center of KUT and the Nakajima Foundation granted me scholarships for 1 year and 2 years respectively to complete my PhD program and I would like to address my gratitude and special thanks to both organizations.

Professor Masaki Sawamoto and Professor So Kazama have welcomed me to Tohoku University in many occasions. Their excellent guidance and advises have been essential to develop and to improve my research.

Doctor Norio Hayashi, curator at the Chiba Natural History Museum, has played a pivotal role in the algae classification aspect of this research. I have tremendously benefited from his large experience as a pioneer and leading researcher in eco-engineering specialty in Japan. I would like to say many thanks to Dr. Hayashi.

My thanks to Dr Ishikawa and to Dr Ariga who have contributed to my understanding of algae culturing in laboratory.

I have benefited from JICA training courses and field excursions for 3 years. Besides the knowledge which I have gained, I have met many friends through the JICA training program and I still keep contact with many people from around the world.

Finally, I would like to say my thanks to all students in Murakami Lab and in Watanabe Lab for their help and their friendship.

Abstract

Remote sensing is a tool for exploring “earth” and it involves the use of instruments or sensors to “capture” the spectral characteristics of objects and materials observable at a distance.

Rapid advances in sensor technology have made it recently possible to collect remote sensing data with spectral bands, which can span from 220 bands with 20-m spatial resolution. This study investigates whether the hyperspectral remote sensing can be used as an appropriate technology to monitor the water quality (Eutrophication) in the shallow lakes and reservoirs.

The background objective of this study is to protect the life of people by securing safe drinking water, of which the primary source is dependant on lakes and reservoirs, through monitoring of the eutrophication problem.

The purpose of this research is to find out the way of estimation and monitoring of the eutrophication in the shallow lakes and reservoirs by using the hyperspectral remote sensing technology.

To achieve this objective, the research sets the following steps: (i) set up classified phytoplankton specimens using the hyperspectral remote sensing technology, (ii) estimate the chlorophyll density in the classified specimens with appropriate accuracy using the hyperspectral remote sensing technology, and (iii) up-scale the findings of this research with the hyperspectral spectrometer to the field application including the satellite remote sensing.

To use the remote sensing technology for monitoring the eutrophication in the shallow lakes and reservoirs, *stage 1* and *stage 2* in the study framework (see Fig. A.1), should be achieved first. Then *stage 3* in the future studies. To achieve *stage 3*, the findings of the

laboratory experiment using the hyperspectral spectrometer need to be taken into account for real field applications of satellite hyperspectral remote sensing.

The goal of monitoring the eutrophication in the shallow lakes and reservoirs using remote sensing technology will be fully achieved to integrate problems of classification of phytoplankton (stage 1), chlorophyll density estimation (stage 2), and the problems of up-scaling the laboratory results to satellite hyperspectral remote sensing (stage 3) are solved together.

Major findings in this research include:

(1) Potentially harmful phytoplankton specimen "*Mycrocystis aerugunosa"* could be discriminated and classified into a separate group of phytoplankton by using simple classifiers. This is an important finding to help manage the eutrophication in shallow lakes and reservoirs by using hyperspectral remote sensing technology. However remaining problems include (i) how to obtain spectral data from pure phytoplankton species and use this information for accurate classification (ii) How to choose the classifier to obtain good discrimination between the species?

(2) The accuracies of classification and chlorophyll density estimation were not enough to support the eutrophication monitoring objectives owing to large amount of error in the raw spectral data. Important problems to be solved include: (i) the ancillary data measurement error and (ii) the influence from water column constituents such as dissolved substances, suspended sediments, difference in the species in phytoplankton community, and bottom sediments re-suspension problem.

This research suggests the potential possibility of phytoplankton classification and chlorophyll density estimation by using the hyperspectral remote sensing technology with a limited accuracy.

At this preliminary and pioneering stage of the research, the major problems affecting the accuracies of phytoplankton classification and chlorophyll density estimation are delineated and clear directions are set to solve the problems.

Unless the problems affecting the phytoplankton classification accuracy, the problems affecting the chlorophyll density estimation accuracy and the problem of up-scaling the findings to field remote sensing are solved together, the remote sensing technology will not fit the necessary accuracy for routine use in monitoring of the eutrophication in the shallow lakes and reservoirs.

It is recommended in future studies to i):evaluate the spectral contributions of skylight and the variations in sunlight intensity, ii) evaluate the interference of the water column constituents on the chlorophyll density estimation by using hyperspectral remote sensing, iii) of this research to field remote sensing, and iv) evaluate the cost effectiveness of monitoring by using remote sensing technology.

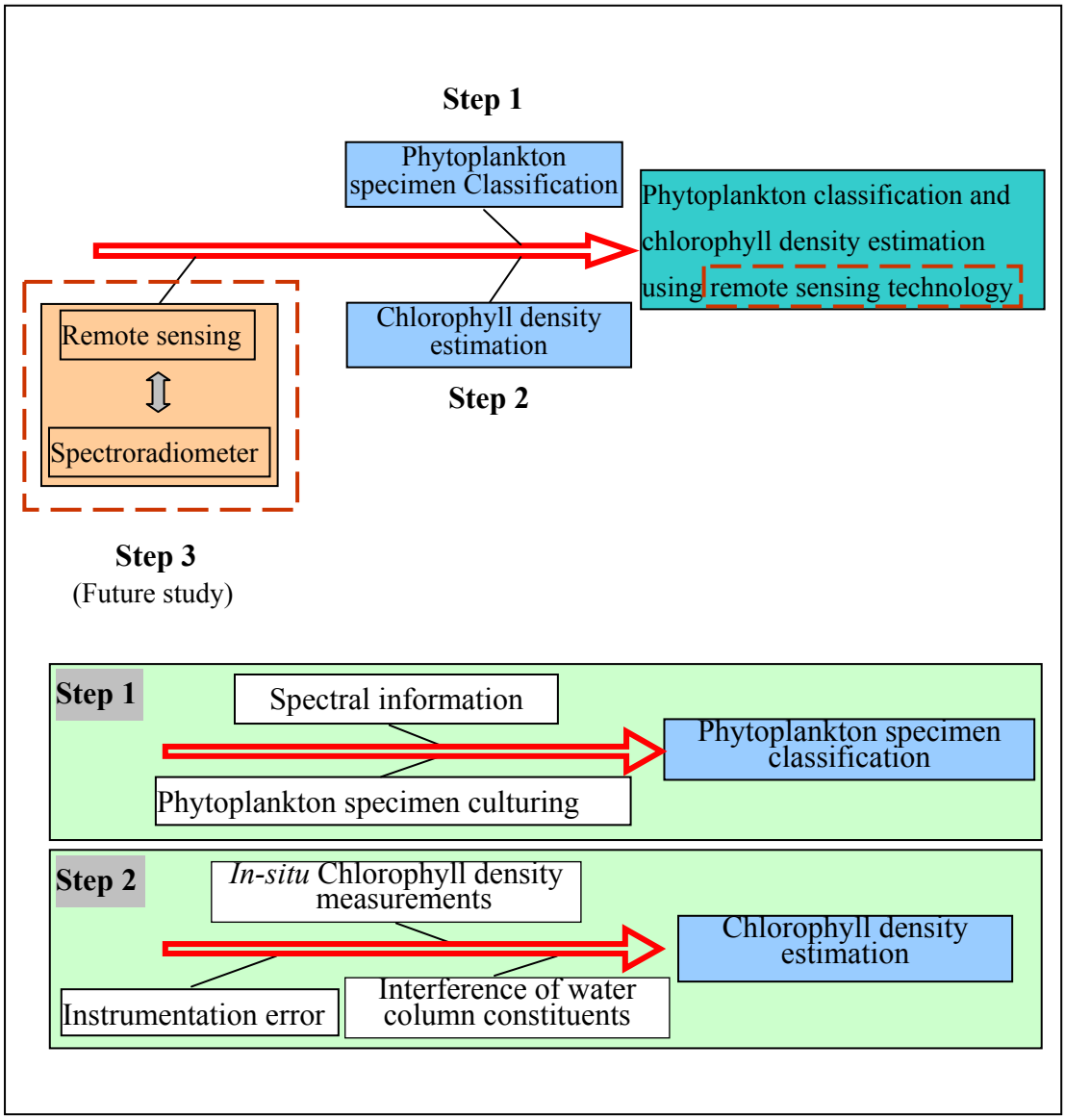

Fig. A.1. The study framework

Contents

List of figures

Chapter 1
Introduction

1.1 Background and purpose of the study

Eutrophication is a global issue and it is more widely known in relation to human activities, where the artificial concentration of nutrients, particularly the phosphorus and nitrogen in the freshwater systems, has lead to the proliferation of algae and aquatic plants. Eutrophication ranks with other major anthropogenic effects such as global warming, ozone layer depletion, and large-scale environmental disturbances, in relation to its potentially harmful effect on natural ecosystems (Cullen et al. 1997; Holligan, 1983. Marra, 1992, ReVelle et al. 1988, Richerson et al. 1998; Scheffer, 1997, Smith et al. 1990). Although the problem is global, there is a discrepancy between developed and developing countries over the ways of dealing with the eutrophication process.

Developed countries produce more pollutants (Nitrogen and phosphorus) but they are more efficient than the developing countries to manage the eutrophication problem. Important reasons for the discrepancy include economics and/or awareness on the need to keep the water environment clean.

The developed countries are economically able to treat wastewater, to monitor drinking water quality, to create and to enforce regulations on water environment. The developing countries are economically restricted, they have few or no wastewater treatment, they have few or no water quality monitoring programs, and they are not able to enforce environmental regulations.

As a consequence, the present water quality status in the developing countries is unknown, the water quality is degrading step by step and the public health is highly impacted. This diagnostic analysis shows that the monitoring of eutrophication problem is vital for the developing countries to compare to the developed countries. Monitoring is important to (i) warn people against the exposure to un-safe drinking water (ii) rise their consciousness and (iii) help people in the developing countries to restore and to secure their valuable water resources. The eutrophication problem is still unsolved both in the developed and developing countries. This is because appropriate treatment technology to remove the nutrients (nitrogen and phosphorus) from wastewater is still lacking. Consequently the nutrients end up in the freshwater systems to trigger the eutrophication process.

The wastewater treatment process consists of three steps (Moore et al. 1988; USEPA, 1999, USEPA, 2000): (i) primary treatment removing the solids, (ii) secondary treatment using the activated sludge method to remove 90% of the organic matter, and (iii) tertiary treatment to remove nutrients including nitrogen and phosphorus.

Conventionally accepted technologies in the wastewater treatment are the primary and the secondary treatment processes. The tertiary treatment process consists of many methods, which are still under intensive research or on trial at pilot stage or on trial in some environmental conservation projects including the Tokyo bay project. Tertiary wastewater treatment technologies are still not available on routine basis to remove the nitrogen and phosphorus in the conventional wastewater treatment system.

The background objective of this study is to save the life of people by securing safe drinking water, of which the primary source is dependent on shallow lakes and reservoirs, through monitoring of the eutrophication problem.

1.2. Research objectives

The objective of this research is to find out the way to estimate and to monitor the eutrophication in shallow lakes and reservoirs by using the hyperspectral remote sensing technology.

To achieve this objective, the research sets the following steps:

(i) Set up a classification scheme for phytoplankton specimens using the hyperspectral remote sensing technology,

(ii) Estimate the chlorophyll density with appropriate accuracy using the specimens classified with the hyperspectral remote sensing technology, and

(iii) Up-scale the findings of this research with the hyperspectral spectrometer to the field application including the satellite remote sensing.

This research will focus on the following points to achieve the objectives:

- Look into the optical characteristics of the phytoplankton in order to get useful information for the classification of phytoplankton species and the estimation of chlorophyll density in the shallow lakes and reservoirs
- Analyze hyperspectral remote sensing data to find out if this technology accurate enough to be used for the eutrophication monitoring goal set in this study
- Identify key limiting factors and set directions to solve potential problems that may be encountered in the field application of the remote sensing technology

1.3. Study framework

S*tage 1* and *stage 2* in this study framework (see Fig 1.1) should be achieved first, in order to use the remote sensing technology for monitoring the eutrophication in the shallow lakes and reservoirs.

Then in a third stage (*stage 3*), the outcome of laboratory experiment by using spectrometer (findings in *stage 1* and *stage 2*) will be applied to real field applications of satellite hyperspectral remote sensing (*stage 3*). The goal of monitoring the eutrophication in Shallow lakes and reservoirs using remote sensing technology will be achieved when the problems of classification of phytoplankton (stage 1); the problem of chlorophyll density estimation (stage 2); and the problems of up-scaling the laboratory results to satellite hyperspectral remote sensing (stage 3) are solved together.

1.4. Major findings

Major findins in this research include:

(1) Potentially harmful phytoplankton specimen "*Mycrocystis aerugunosa"* could be discriminated and classified into a separate group of phytoplankton by using simple classifiers. This is an important finding to help manage the eutrophication in shallow lakes and reservoirs by using hyperspectral remote sensing technology. However remaining problems include (i) how to obtain spectral data from pure phytoplankton species and use this information for accurate classification (ii) How to choose the classifier to obtain good discrimination between the species?

(2) The accuracies of classification and chlorophyll density estimation were not enough to support the eutrophication monitoring objectives owing to large amount of error in the raw spectral data. Important problems to be solved include: (i) the ancillary data measurement error and (ii) the influence from water column constituents such as dissolved substances, suspended sediments, difference in the species in phytoplankton community, and bottom sediments re-suspension problem.

1.5. Thesis outline

Chapter 1 describes the objectives and the framework of this study. The original points and the roadmap of the study are presented in chapter 2. The experimental methodologies, which are used in the research, are described in Chapter 3. Chapter 4 discusses the classification of phytoplankton species by using hyperspectral spectrometer and delineates the problems affecting the accuracy of the classification. Some directions to solve the problems are also discussed. Chapter 5 discusses the chlorophyll density estimation by using the hyperspectral spectrometer and delineates the potential problems that are to be encountered in the field applications. Some directions to solve some of the problems are also discussed. Chapter 6 presents the findings of the research. Chapter 7 concludes the study, and recommends future studies.

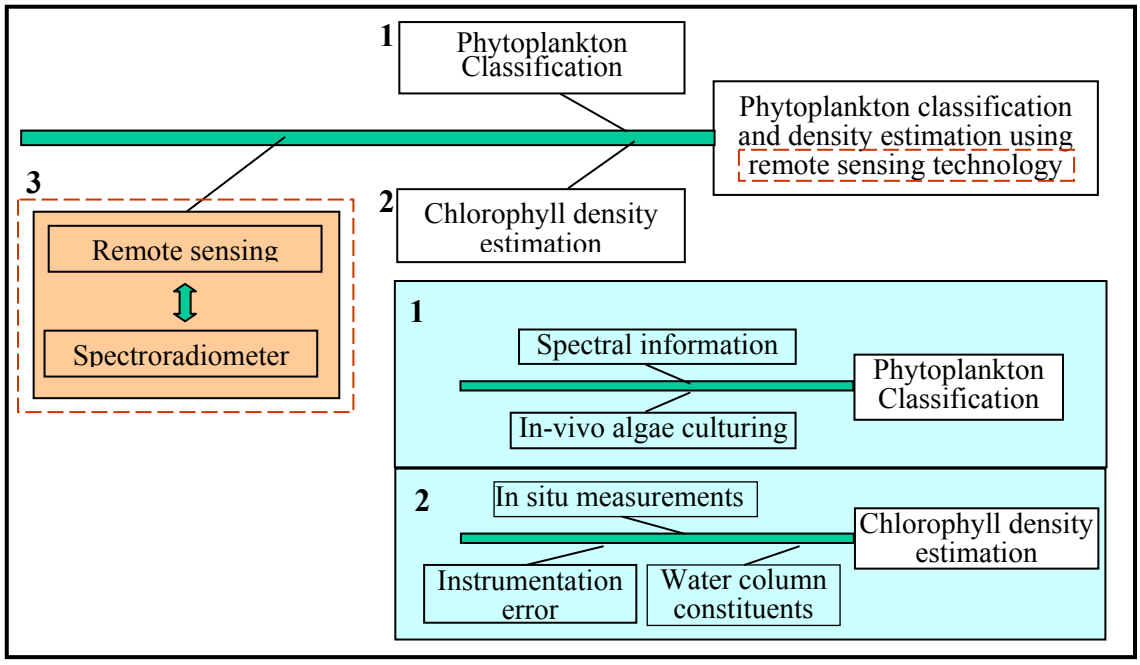

Fig.1.1. Framework of the study

Chapter 2

Basic concept and structure of the Study

2.1 Basic concept

This study combines the fields of physics, chemistry, and biology, by attempting to find out a relationship between: (i) the optical characteristics (spectral signatures) and (ii) the chemical characteristics (chlorophyll density), and the biological characteristics (phytoplankton species characteristics). The research suggests that the optical characteristics of the phytoplankton can be used to classify phytoplankton species and to estimate the chlorophyll density in the water column with limited accuracy.

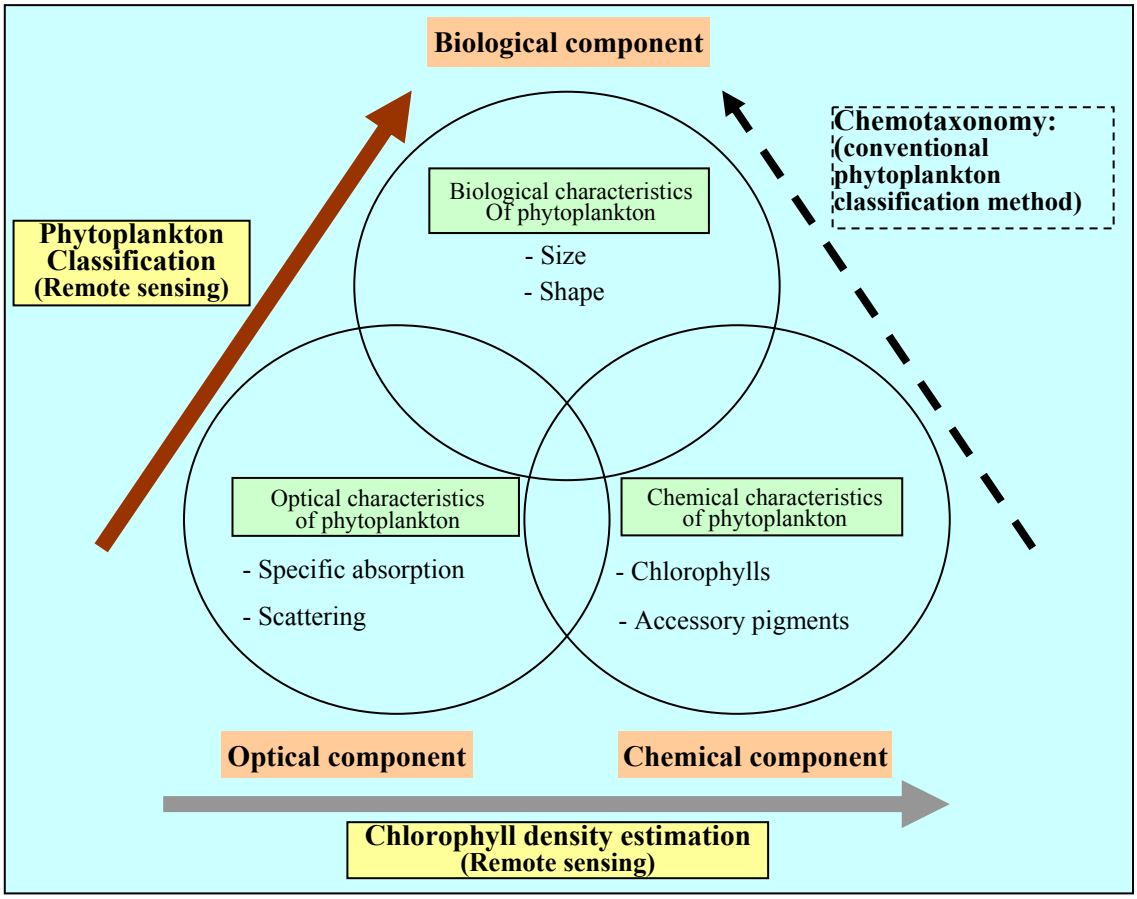

Fig. 2.1. Concept of this study

2.2 Study roadmap and major points of this study

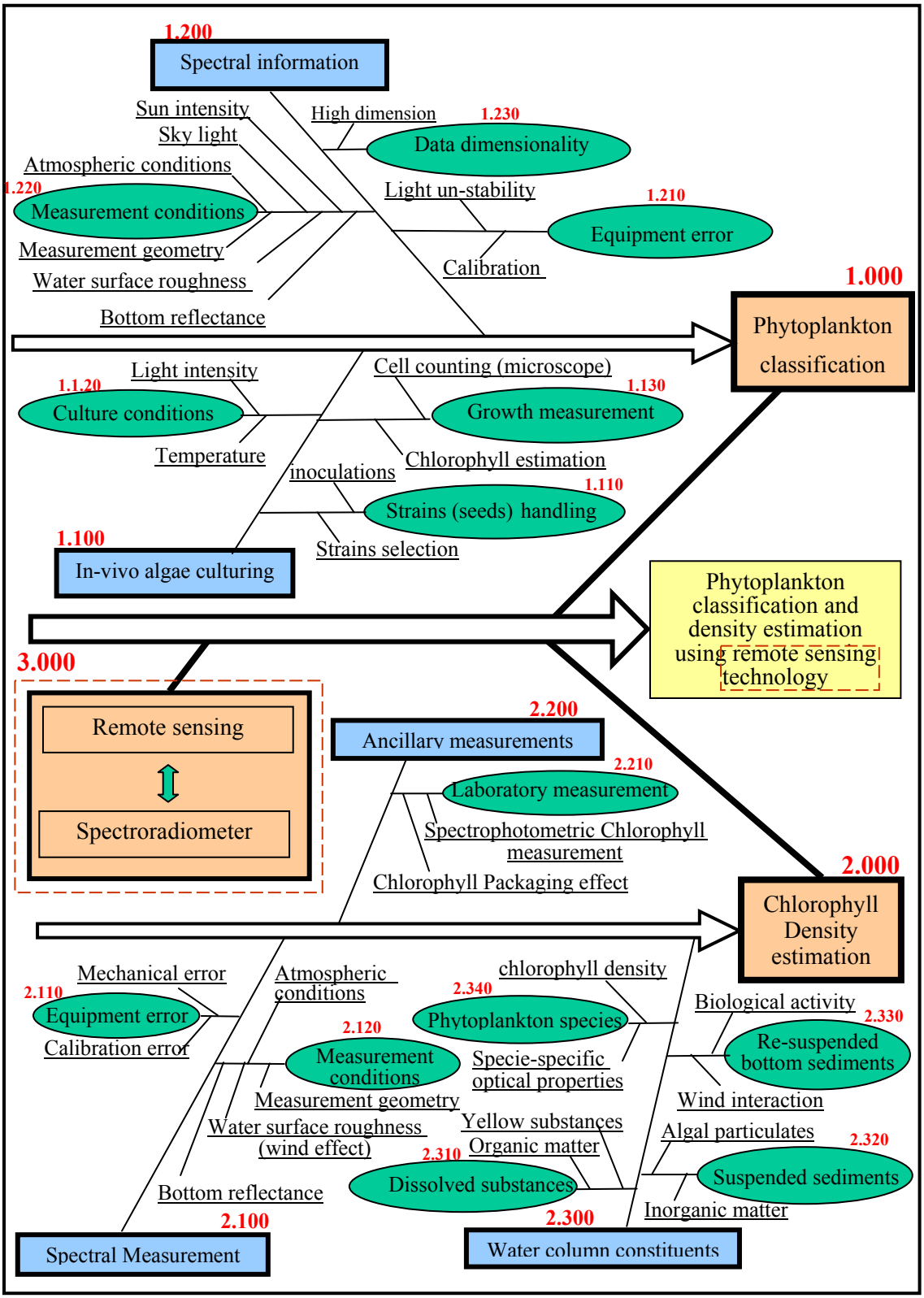

Fig. 2.2. Study roadmap

The study roadmap is shown in Fig 2.2. To achieve the goal of monitoring the eutrophication in shallow lakes and reservoirs the following objectives should be achieved:

(1) Classification of phytoplankton species at the laboratory scale using hyperspectral spectrometer. This classification should be accurate enough to achieve the goal.

(2) Estimation of the phytoplankton's chlorophyll density at laboratory scale using hyperspectral spectrometer. This estimation should be accurate enough to achieve the goal.

(3) The laboratory study results using spectrometer need to be up-scaled to the field application using hyperspectral remote sensing.

Figure 2.2.1 shows various items, which are highlighted in blue color. These are the controlling factors of the phytoplankton classification accuracy (1.100, and 1.200) and the phytoplankton's chlorophyll density estimation accuracy (2.100, 2.200, and 2.300) Each of the items is further subdivided into influential sub-items. The items and sub-items are discussed in detail in chapter 4 and chapter 5.

Chapter 3

Methodology of experiment

3.1. Methodology of water sampling

Water samples for the laboratory testing were collected from an oligotropic reservoir, and from tap water. One replicate using reservoir water and another replicate using tap water were prepared for each sample. Thirty-five (35) samples and seventy (70) replicate samples were prepared by steps; adding the chlorophyll pigment and the total suspended sediments (Kaolin) to obtain a large variation of optically active components. The chlorophyll concentration and turbidity level in the 35 samples are shown in Fig. 3.1. The 70 replicates were also prepared by adding the same amount of chlorophyll and suspended sediments (Kaolin).

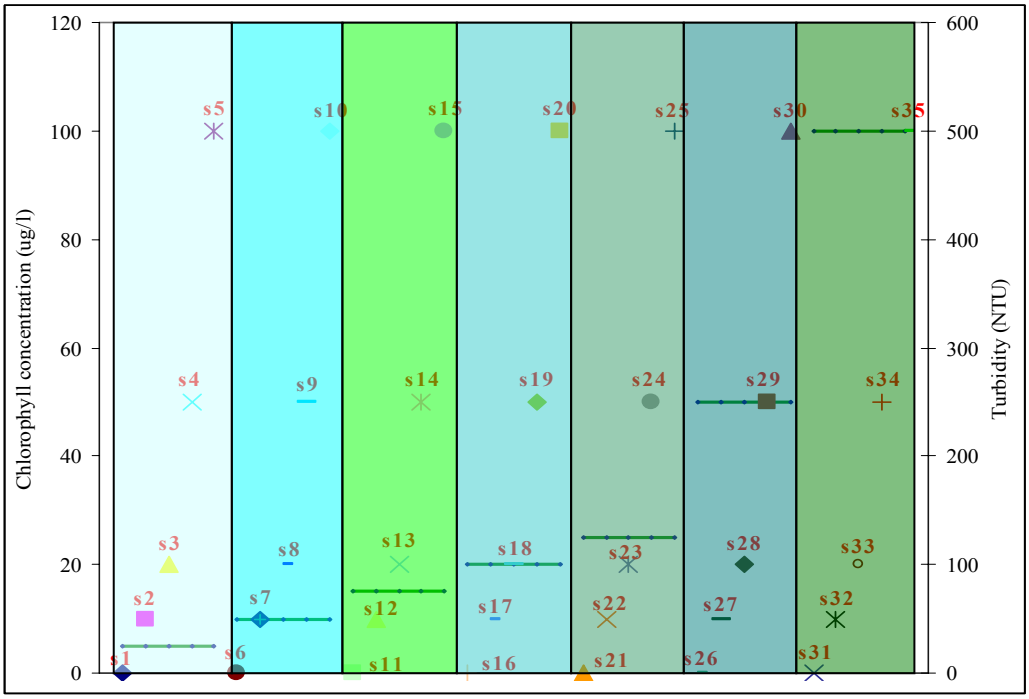

Fig. 3.1 Chlorophyll and turbidity concentrations of the testing water samples

3.2. Methodology of phytoplankton cell counting by microscope

Cell counting has two principal aims (Anderson et al. 2005): (i) to estimate the size of the population of the cultured phytoplankton species as a total number of cells (colonies) in the culture as a whole or, as individuals per unit volume of the culture, and (ii) to estimate the rate of culture augmentation, equivalent to the rate of population increase.

The practical aim is to tally all the cells in a known volume of the cultured material when they are settled in the same plane, or nearly one plane, within the depth of the focus of the objective-ocular system of the microscope (Anderson et al. 2005)

Counting method:

(1) Of the cultured material, place 0.05 mL (=0.05cm^3 = 50mm^3) onto the slide (Note that 0.05 mL = 1/20 mL, which is about 1 drop from pipettes or droppers).

(2) Cover the drop with a 20x20 mm^2 coverslip (400 mm^2 area). The liquid should fill the space under the coverslip without significant outflow (Note that each area of the coverslip hold cells from 1/400x1/20mL = 1/8000 mL = $1.25x10^{-4}$ mL of culture.

(3) If *n* cells are on average counted under 1 mm^2 of the coverslip, then the culture has *n* x 8,000 cells per mL

3.3. Chlorophyll measurement by water quality logger YSI 6600

The YSI-6600 instrument shown in Fig 3.2 is a multi-parameter water quality sonde. The YSI multi-parameter sonde allows direct measurement of up to 8 different parameters simultaneously, including 2 optical ports for self-cleaning turbidity, chlorophyll and rhodamine. An internal battery pack is included for long-term monitoring applications. With 15-minute intervals, the sonde will simultaneously log all parameters for 75 days. The YSI-6600 is useful tool for long-term in-situ monitoring. It is also equipped with a temperature and conductivity sensor. The YSI's chlorophyll sensor provides a convenient in situ monitoring system for detecting chlorophyll content in phytoplankton, which can be used to predict algae blooms and nutrients loading in

water. The YSI-6600 is equipped with the EcoWatch for Windows software, which provides user-friendly data analysis and statistics applications.

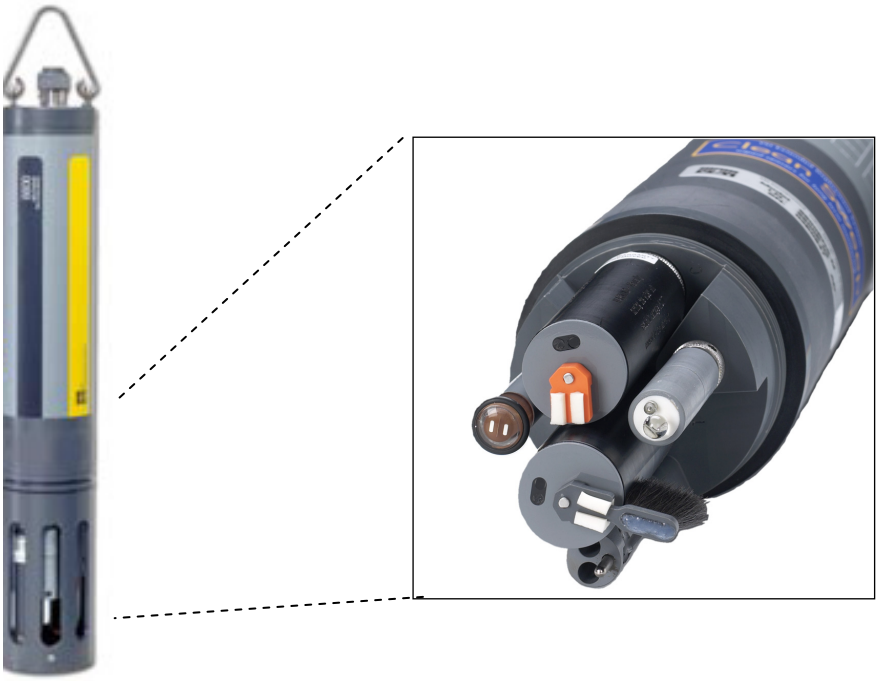

Fig. 3.2. water quality logger YSI 6600

3.4. Chlorophyll measurement by spectrophotometer

Chlorophyll measurements were performed by acetone extraction and absorbance rates measurements at four discrete wavelengths 750nm, 663nm, 645nm, 630nm using a standard type of laboratory spectrophotometer. On the basis of these absorption rates measurements, the absorption factors for each sample at three discrete wavelengths 663nm, 645nm, and 630nm are calculated using equations 4.9 to 4.11:

$$E_{663} = AR_{663} - AR_{750} \quad (4.9)$$

$$E_{645} = AR_{645} - AR_{750} \quad (4.10)$$

$$E_{630} = AR_{630} - AR_{750} \quad (4.11)$$

Then from the absorption factors, the concentrations of three forms of chlorophyll pigment namely Chlorophyll-a, chlorophyll-b, and chlorophyll-c can be calculated using the following empirical formulae proposed by the American Environmental Protection Agency (Arar et al. 1994; Axler et al. 1994; Baker, 1983; Evans et al. 1983; EPA, 1995; Holm-Hansen et al. 1965; Kiefer et al. 1989; Kiyosawa et al. 1995; Lorenzen et al. 1966; Vyhnalek et al. 1993; Welschmeyer, 1994; White, 1972; Yentsch, 1963):

$$\text{Chl-a} = 11.64E_{663} - 2.16E_{645} + 0.10E_{630} \quad (4.12)$$

$$\text{Chl-b} = -3.94E_{663} + 20.97E_{645} - 3.66E_{630} \quad (4.13)$$

$$\text{Chl-c} = -5.53E_{663} - 14.82E_{645} + 54.22E_{630} \quad (4.14)$$

3.5. Spectral data measurement by hyperspectral radiometer

The methodology used to measure spectral reflectance of the water samples in the laboratory is described in this section. The FieldSpec-Pro radiospectrometer reflectance measurement probe is positioned in nadir pointing direction at a constant distance of 1 m above the water surface using a tripod as shown in Fig. 3.3.

The experiment is carried out in the laboratory using two halogen lamps to control the illumination and to avoid spectral contamination by other light sources. Reflectance values are measured for the wavelengths ranging from 350nm to 2500nm by three different scanning diodes.

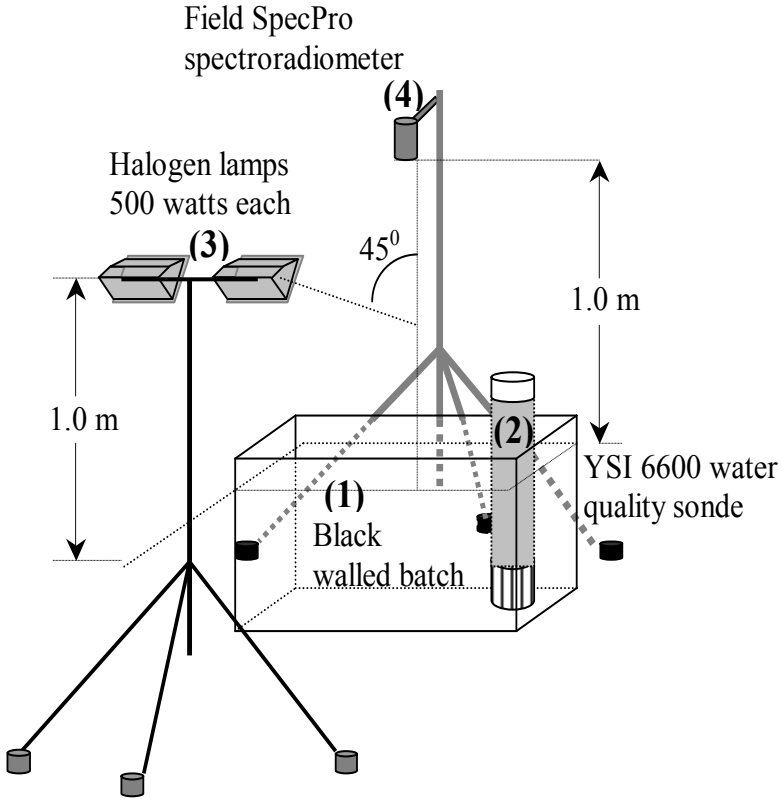

Fig 3.3. Experimental apparatus for spectral measurements

A reference spectrum is collected using the white reference panel (spectralon), which can reflect 98% of incident light. The spectralon panel is placed horizontally at the same level as the water surface. The spectral measurement probe is placed at 1 m distance to the white reference board in nadir (vertical) view. The batch is filled with the water sample until the level reaches 1 m distance from the nadir pointing reflectance

measurement probe. The halogen lamps are warmed up until to confirm the stabilization of the measurement system. Once the spectrometer stabilized, ten reflectance measurements under halogen lamps illumination ($WRef_H$) and ten spectral measurements in complete dark ($WRef_D$) are collected from the white reference panel.

Light, which is reflected from the water surface, is measured as $SRef_H$ by ten times. Prior to spectral measurements, each sample is manually stirred for three minutes to obtain homogenous distribution of the suspended sediments and chlorophyll concentration.

Dark current is measured once for each sample. Finally, radiance reflectance is calculated applying equation (3.1).

$$R=0.98(SRef_H-SRef_D)*IT_S/(WP_H-WP_D)*IT_{WP} \quad (3.1)$$

SRefH and SRefD are the averages of the reflectance measurements of the sample in light and in dark condition respectively. WPH and WPD are the averages of reflectance measurements of the white reference spectralon panel under halogen lamp illumination and in the complete dark conditions respectively. ITS and ITWP are the integration time of the water sample and the integration time of the white reference spectralon panel respectively.

Chapter 4

Phytoplankton Classification

4.1 Importance of phytoplankton classification in managing the eutrophication problem by using the hyperspectral remote sensing technology

Phytoplankton is a generic term to include about 2000 species of which 30 are potentially harmful toxin producers. Phytoplankton species have significant differences as for their shapes, their sizes and their pigments composition, and thus their optical properties. Phytoplankton pigments including the chlorophylls and accessory pigments absorb the light energy in form of photons to perform the basic process of photosynthesis. All phytoplankton have in common the chlorophyll-a, but the other types of chlorophyll-(b,c, or d), and the accessory pigments vary from one species to another. Some accessory pigments are typical to some species, and are termed biomarkers. For instance the accessory pigment phicobiliprotein is the biomarker of one typical harmful phytoplankton called "*Microcystis aerugunosa*".

Light energy absorption by the phytoplankton greatly depends on the pigments association, which gives characteristic shapes to the absorption spectra of pure phytoplankton species.

The amount of chlorophyll and accessory pigments varies from one phytoplankton specie to another, therefore the quantification of algae biomass through the chlorophyll pigment requires *a-priory* knowledge of the phytoplankton specie to be quantified.

This is the reason why it is necessary to understand the distribution on phytoplankton species before quantification of their biomass.

Consequently, the use of optical remote sensing to manage the eutrophication of freshwater systems requires understanding the distribution of phytoplankton species on both temporal and spatial scales.

This study is carried by using simple systems consisting of laboratory cultures of 4 typical species of phytoplankton. Direct microscopic examination of cultured medium is used during the culturing process to assure that the phytoplankton specimen is not contaminated by other phytoplankton species.

Regression analysis, between spectral data and in-situ chlorophyll concentrations of the phytoplankton specimen, is used to develop unique spectral signatures for the phytoplankton specimens of interest.

Hyperspectral radiometry is used to detect specific spectral features of the phytoplankton specimens, which are cultured *in-vivo*. Subsequently, the potentiality of the technique to discriminate the phytoplankton specimen is assessed.

4.2 Rational of using the spectral data for classification purpose

The rational for using the hyperspectral data to classify the phytoplankton specimens being observed is that: (i) the hyperspectral signatures may characterize the specimen being observed, and (ii) the hyperspectral data are influenced by the optical properties of the phytoplankton specimen being observed. Thus the optical characteristics of the phytoplankton specimen living in the water columns of lakes and reservoirs influence how radiance is transmitted through, absorbed by, scattered by and/or reflected from the

water column. The spectral reflectance signatures may thus help in determining whether two different specimen can be distinguished from each other, and if so in which part of the spectrum the spectral characteristics differ. This chapter discusses the possibility of phytoplankton specimen classification by using the hyperspectral remote sensing technology.

4.3 Identification and description of the factors and problems affecting the phytoplankton classification

This research identifies 6 important factors that may potentially affect the possibility of phytoplankton classification by using the remote sensing technology (see Fig.4.1): These factors are classified into 2 groups:

(1) The algae culturing process which includes the culturing conditions, the strains handling and the growth measurement, and

(2) The spectral information, which includes (i) the spectral measurement conditions, (ii) the equipment error, and (iii) the choice of the classifier. These factors are reviewed in this chapter and are described in details as for their influences on the phytoplankton classification accuracy.

In this chapter the influential factors are reviewed and analyzed. It was attempted to quantify the respective influences of the factors and to identify residual problems to be solved in future studies. Directions to solving the residual problems are also proposed.

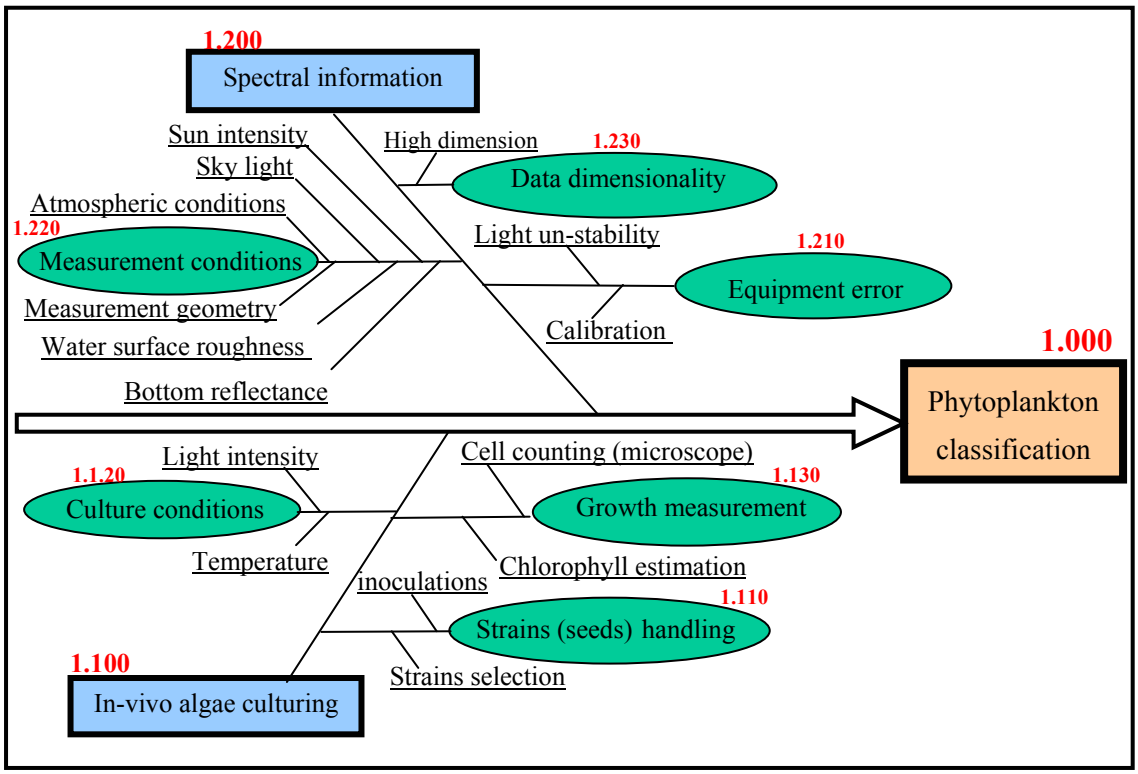

Fig.4.1. Factors affecting the phytoplankton classification accuracy

4.3.1. Algae culturing *in-vivo*

Four (4) referenced phytoplankton seeds (strains) were ordered from the National Institute for Environmental Studies (NIES) in order to grow phytoplankton specimen in-vivo in the laboratory and to collect useful information on their optical characteristics and to understand and suggest phytoplankton classification scheme on the basis of the optical characteristics. For detailed reference on the strains refer to Appendix F. The species include *Chlorella saccharophyla, Chlosterium paracerosum, Cyanophora tetracyanea, and Microcystis aerugunosa*.

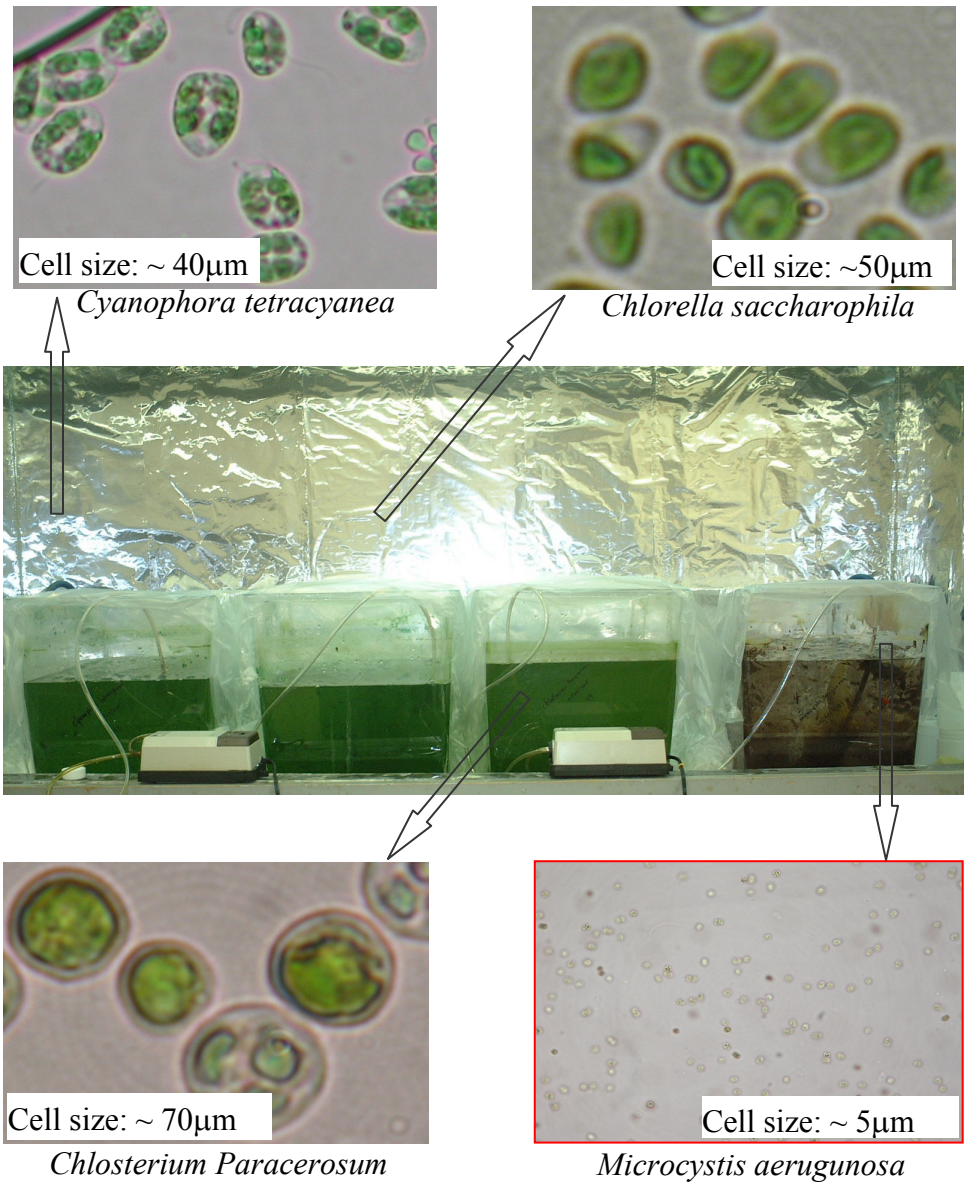

Note: from left to right: *Cyanophora tetracyanea*, *Chlorella saccharophila*, *Chlosterium paracerosum*, and *Mycrocystis aerugunosa*.

Plate 4.2 Batch monocultures of four different species of phytoplankton.

After receiving the strains these species were cultured in-vivo following the guidelines which are provided by the National Institute for Environmental Studies (see Appendix F). All algae culturing procedures were performed under aseptic conditions to avoid any

contamination(Bidigare et al. 1990; Fairchild et al. 1998; Goulder, 1969; Mayer et al. 1997; Mjelde et al. 1997; Olso et al. 1996; Paasche et al. 1973; Reed et al. 1996; Stramski et al. 2002). All preparations of media and culture inoculations were performed under sterile conditions within a laminar flow cabinet. Sterile, autoclaved glassware, plastics and pipettes were used for each sample. Surfaces were wiped with 80% ethanol before and after use to remove dust, spillage and microorganisms. For washing or any dilution work performed, sterile, filtered water was used.

4.3.1.1. Culture conditions

There are two important parameters that should be properly handled for a successful in-vivo phytoplankton culturing. These two parameters are: (i) the water temperature, and (2) the light intensity.

4.3.1.1.1. Temperature

4.3.1.1.1.1.What is the problem?

The same phytoplankton specimens that are cultured under different temperature conditions may have variable chlorophyll concentrations because the temperature parameter regulates the ratio of carbon to chlorophyll (Schwarz et Grossman 1998, Fujita et al. 1994; Escoubas et al. 1995). This kind of relationship is not investigated in this study.

4.3.1.1.1.2. How to solve the problem?

Laboratory experiment at varying temperature can help to find out the relationship between the chlorophyll concentrations and the temperature parameter.

4.3.1.1.2. Light intensity

4.3.1.1.2.1. What is the problem?

Phytoplankton needs light energy to perform the vital process of photosynthesis whereby the sunlight energy is harvested by the chlorophyll pigment and is used to produce sugar which cellular respiration converts into ATP, the "fuel" which is used by all living things. Phytoplankton adapts to variation in the light intensity by increasing or by decreasing the amount of chlorophyll. For instance, the up-regulation of chlorophyll pigment synthesis at lower light intensities, leading to increased pigment content, has been well-documented for both prokaryote and eukaryote algae (Falkowski and La Roche, 1991).

4.3.1.1.2.2. Direction to solve the problem?

This phenomenon of photoadaptation is not studied experimentally herein but interested readers are referred to: (Stramski et al. 2002, Le Floc'h et al. 2000, Geider et al. 1998, Cullen et al. 1998, Falkowski et al. 1991).

These changes in chlorophyll content can be directly measured in laboratory and also in environmental phytoplankton samples as an increase in the concentration of chlorophyll per unit cell biomass (Sigee, 2004).

4.3.1.2. Strains handling

4.3.1.2.1. What is the problem?

Mains issues that were identified in this study as for the strains handling include: (i) how to select phytoplankton species with similar culture conditions requirements and at the same time with different appearance as for color and/or shape on which the classification rely, and (ii) how to transfer the seeds from the test tube to the batch

culture without contaminating the strains. This second point is important to assure that the subsequent measurements will keep on providing optical and chemical characteristics of one single pure monoculture of phytoplankton.

4.3.1.2.2. How to solve the problem?

Referenced phytoplankton seeds (strains) are used in this study. Precise guidelines are sent along with the strains order. These guidelines describe in details how to culture the phytoplankton, how to prepare the suitable culture medium, and the requirements for important controlling parameters including light intensity and temperature.

4.3.1.2.1. Strains (seeds) selection issue

4.3.1.2.1.1. What is the problem?

Strains selection is a difficult task because the phytoplankton species, which were grown and examined in this study, have very different culture conditions but should grow under the constraint of incubator availability.

4.3.1.2.1.2. How to solve the problem?

The only possibility is to optimize the culture conditions in order to keep all the species growing. However for this option risk is high to stress part or all of the phytoplankton species which cannot adapt to a high range of temperature and light variability

4.3.1.2.2. Strains (seeds) inoculation

4.3.1.2.2.1. What is the problem?

Strain inoculation is the only way to avoid the contamination of pure phytoplankton samples by other phytoplankton species. However for mass culturing, as carried out in

this study, this type of inoculation cannot be performed but rather the strains are transferred directly to the batch, increasing the risk of contamination.

4.3.1.2.2.2. How to solve the problem?

In this study, the culture batches were wiped with 5% ethanol solution, culture media were prepared directly in the batch by mixing manually distilled water and vitamins with asceptized spoon. After the medium is prepared, the inoculum is transferred directly in the culture medium. The batch, which contains the newly inoculated culture medium is covered by a transparent film (see Plate 4.2.). An air diffuser is placed in the medium, at the bottom of the batch, to assure the oxygen supply to the cultured phytoplankton.

4.3.1.3. Growth measurement

4.3.1.3.1. What is the problem?

Growth measurement is a means to verify that the phytoplankton is growing normally without major stress. Growth measurement is particularly useful to establish a conversion curve between the cells counts and the corresponding chlorophyll concentrations so to avoid recounting the cells when repeating the experiment.

4.3.1.3.2. How to solve the problem?

The growth measurement is not studied herein, however a general methodology consists of sampling the culture medium at regular time interval like once a day or once every 3 days to measure the chlorophyll concentration and to count the cells number per mL of the culture medium. Thereafter, a correspondence curve between the cells counts and the corresponding chlorophyll concentrations is established.

4.3.1.3.1. Cell counting by microscope

4.3.1.3.1.1. What is the problem?

In the natural conditions the phytoplankton species are living in communities and are unevenly distributed in the water body to be studied. Moreover, the sizes of the phytoplankton populations for each species depend on the ability of that specie to adapt and colonize the environment. The dominant species which have bigger population sizes will determine the optical properties of the water column. Therefore, it is important to know the repartition of the dominant species in the water body.

4.3.1.3.1.2. How to solve the problem?

The practical aim of cell counting is to tally all of the cells in a known volume of the cultured material when they are settled into one plane, or nearly one plane, within the depth of focus of the objective-occular system of the microscope. Of the cultured material , place 0.05mL (=0.05cm3 = 50mm3) onto a slide. (Note that 0.05nL = 1/20 mL, which is about one drop from many pipettes or droppers). Cover the drops with a 20x20mm2 coverslip (400mm2 area); the liquid should fill the space under the coverslip without serious outflow. Therefore, each 1mm2 of coverslip area holds cells from 1/400x1/20mL = 1/8,000mL =1.25x10-4mL of culture. If n cells are on average counted under 1mm2 of coverslip, then the culture has nx8,000 cells per mL.

4.3.1.3.2. Chlorophyll estimation by spectrophotopmeter

4.3.1.3.2.1. What is the problem?

Chlorophyll, in various forms, is bound within the living cells of phytoplankton, and other plants, which are found in water environment. In general, the amount of chlorophyll in a collected water sample is used as a measure of the phytoplankton

biomass, the magnitude of which can significantly affect the overall quality of the water. The estimation of chlorophyll then depends on the sample matrix. Moreover there are differents equations to estimate chlorophyll from the absorption rates, which are measured by the spectrophotometer. These equations seem to return different results of chlorophyll estimation from absorption rates.

4.3.1.3.2.2. How to solve the roblem?

One way to solve the problem is to compare between available chlorophyll estimation methods and check which method gives the best repeatability and lowest standard error of estimation. Important thing is also to keep the same equations for estimation of chlorophyll density from absorption rates.

4.3.2. Spectral information

The spectral data contains significant noise which originate from:

(1) the spectral measurement conditions, including the sunlight intensity, the skylight intensity, the atmospheric conditions, the measurement geometry, the water surface roughness due to wind effect, and the bottom reflectance

(2) the equipment error due to calibration problem and light source un-stability problem

(3) the choice of the classifier to discriminate the characteristics of different species of phytoplankton.

4.3.2.1. Measurement condition

The effects of sunlight intensity, skylight intensity, and atmospheric conditions are not studied experimentally in this research. The effect of the water surface roughness on the

accuracy of the classification and estimation of chlorophyll density is not studied experimentally. However an explanation based on theory is provided and directions to solving the problem are proposed. The effects of the measurement geometry and the choice of the classifier are studied experimentally and their effects on the classification accuracy are evaluated.

4.3.2.1.1 Measurement geometry

4.3.2.1.1.1. What is the problem?

Variations in the zenith angles of the illumination source (sun, halogen lamps…), and the zenith angle of the sensor can result in error in the spectral measurement.

4.3.2.1.1.2. How to solve the problem?

The spectral measurement procedure by using the spectrometer should be standardized by keeping the same measurement geometry. This includes a constant distance between spectrometer and the surface, and leveling the instrument and standard, and also target surface when possible. During the measurement cycle, stand away from the instrument to avoid adding a component of light reflected from clothing to the surface being measured. In addition to duplicate runs, take multiple measurements over the area or feature being measured. Do not assume homogeneity. To evaluate the spectrometer's performance in the field, keep a copy of the plot from the reference standard made right after the instrument was recalibrated.

4.3.2.1.2 Water surface roughness (wind effect)

4.3.2.1.2.1. What is the problem?

The spectral reflectance of measured samples can show large variations owing water surface irregularities like waves which are generated by the interaction between the water surface and the wind.

4.3.2.1.2.2. How to solve the problem?

Although the influence of the water surface roughness on the reflectance data is not examined in this study, the bibliography on this topic is well documented. Surface roughness can be defined in terms of wavelength of the radiation concerned. For a surface to "appear" smooth at a given wavelength, it must be flat to within about a quarter of the wavelength of the radiation at which it is measured. Under this condition, most of the incoming radiation is reflected at an angle that equals the angle of incidence, i.e., specular reflection. If the surface variations exceed this, then proportionally more of the energy is scattered in other directions. This is called the diffuse component. As the surface variations increase, more energy is scattered in other directions, i.e., the diffuse component gets larger, and the specular component gets smaller.

The water surface roughness and the sensor's viewing angle are closely related in that the influence of surface structure is dependent on viewing angle of the sensor in relation to the sun. For remote sensors using reflected sunlight, the wavelengths fall between 400 nm and 2500 nm, or between 0.4 and 2.5 μm.

Laboratory experiment can be carried out to evaluate this type of influence. The wave effect can be generated by blowing air under variable pressure on the water surface to generate waves which have variable heights. Then the influence of this phenomenon can be checked directly on the spectral information to evaluate the wind effect on the remote sensing data.

4.3.2.1.3 Bottom reflectance

4.3.2.1.3.1. What is the problem?

In the natural condition, even if the water body such as lake or reservoir contains the same dominant specimen of phytoplankton, there is great chance that the bottom may vary. In that case the spectral measurements may not be useful for identification of phytoplankton species.

4.3.2.1.3.2. How to solve the problem?

Bottom reflectance is a difficult noise to deal with. The bottom reflectance contribution to the remote sensing signal can amount to 80%. The contribution is dependant on many factors such as the water depth, the bottom type and texture and the type of material suspended and/or dissolved in the water column. The contribution of each of these parameters is discussed in details in chapter 5.

4.3.2.2 Choice of the classifier

4.3.2.2.1. What is the problem?

Hyperspectral remote sensing data has high spectral resolution with about 1000 bands spanning across the light spectrum from visible to infrared bands. It is difficult to reduce these bands to a smaller number of bands which have nearly the same amount of information as the original spectrum. The choice of appropriate bands which are useful for the phytoplankton specimen classification objective (choice of the classifier) is important for classification accuracy.

4.3.2.2.2. How to solve the problem?

It is difficult to decide which spectral feature can be used to discriminate between the specimens since the positions and the intensities of the spectral features vary differently

from one specimen to another (see Figs. 4.3 and 4.4). The best classifier(s) should be the one(s) for which the position of the peak does not vary significantly from one specie to another to be able to compare the variation in peak intensity from one species to another and thus discriminate between species. In this research the absorption peaks, reflectance peaks, and inflection points

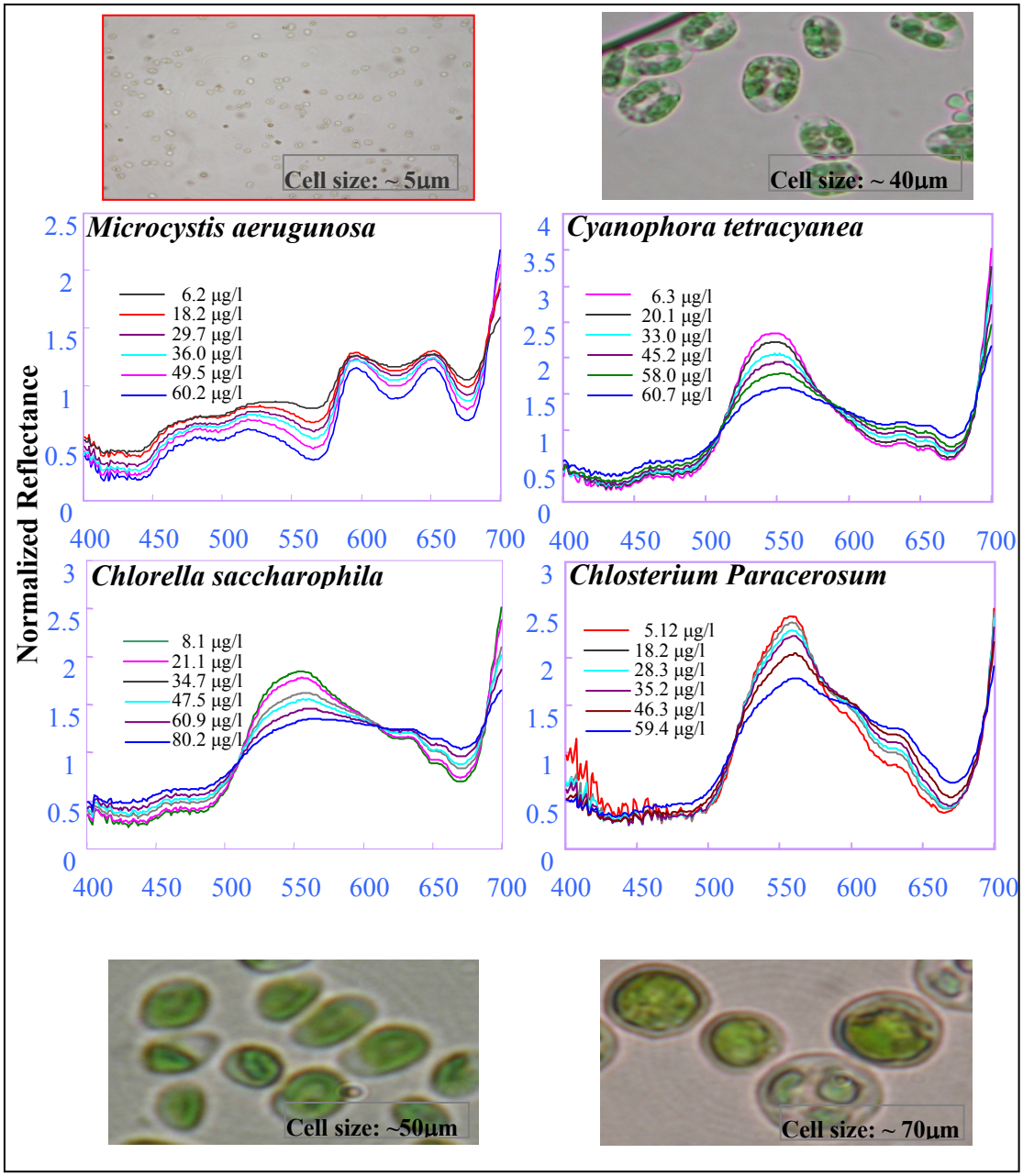

Fig. 4.3. Spectral data set for 4 phytoplankton specimens to be classified

Regression analysis between chlorophyll densities data and reflectance data was carried out to select the wavelengths of interest for the classification of the 4 specimens. First, the spectral features of interest were compared to find which of them have a good correlation coefficient within species and low correlation between species. It is found that the absorption peaks at 624nm and 724nm and the reflectance peak at 549nm can be used to classify the phytoplankton species. These "useful" absorption and reflectance peaks and their combinations which are used as classifiers are shown in Fig.

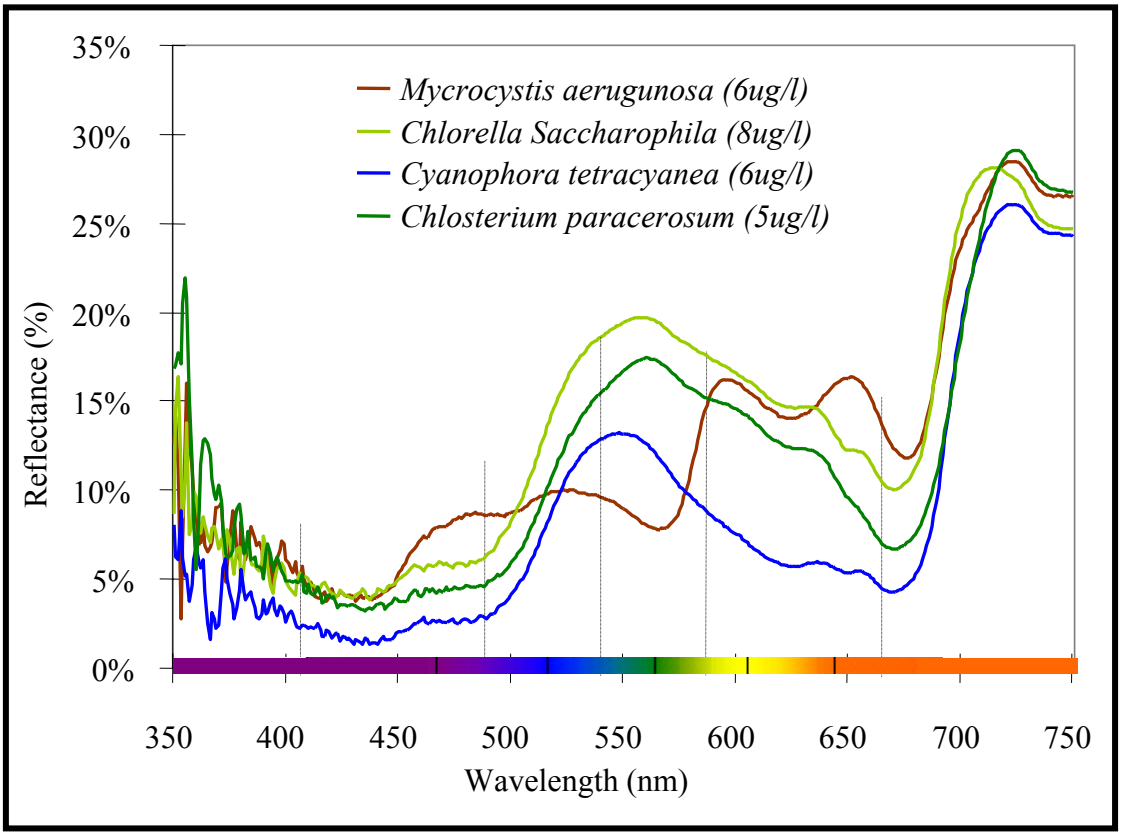

Fig.4.4. Specific wavelength to classify the 4 specimens of phytoplankton

4.3.2.2.1. Simple band classifiers

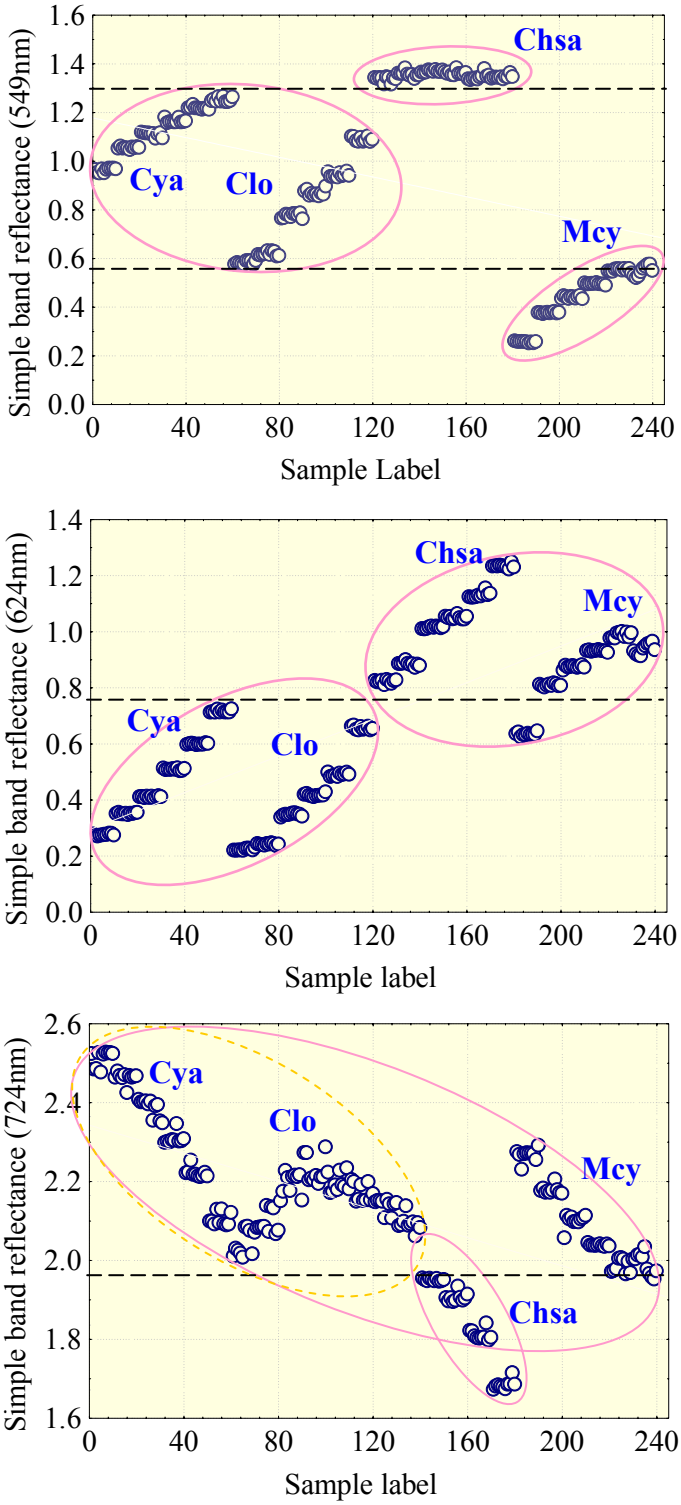

Fig. 4.5. Phytoplankton classification by using simple band classifiers

4.3.2.2.2. Band difference classifiers

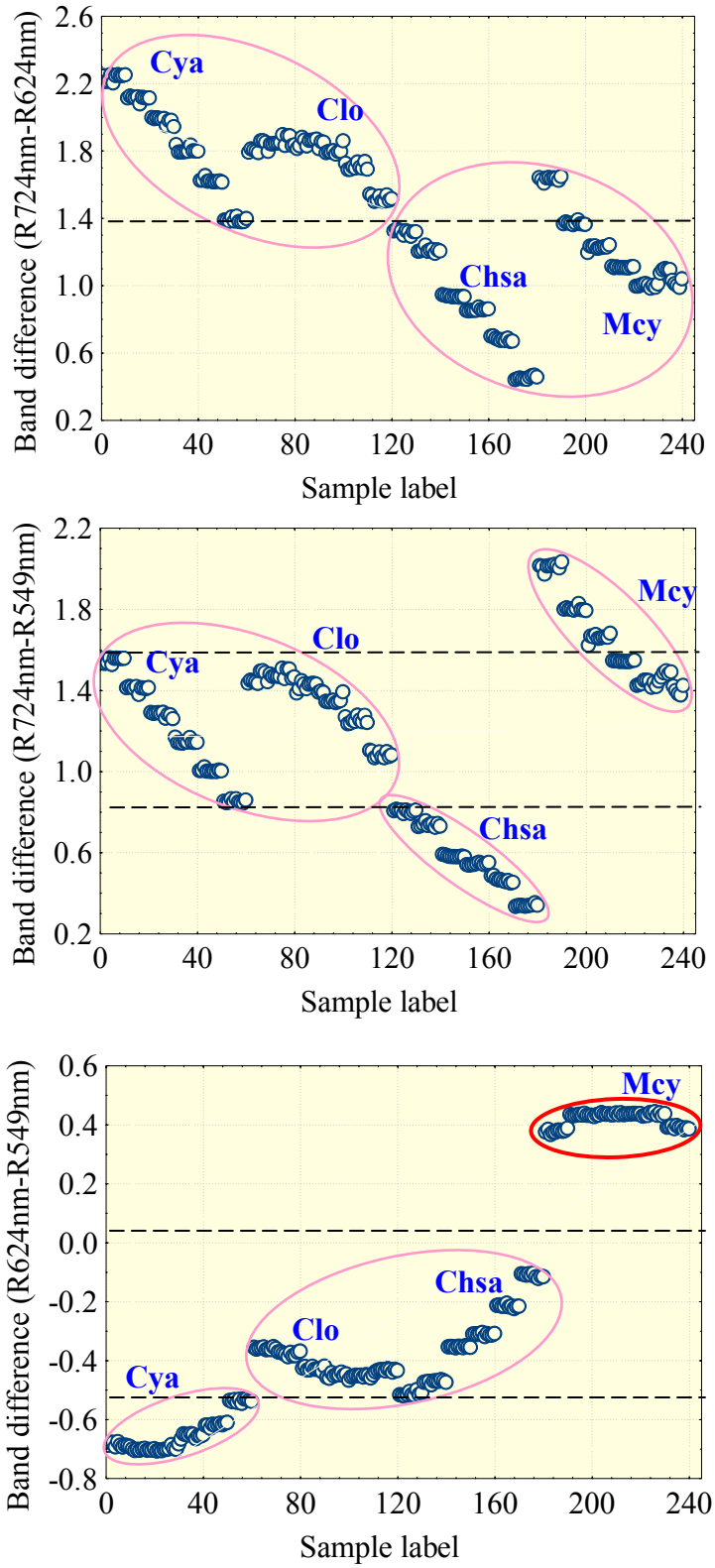

Fig. 4.6. Phytoplankton classification by using band difference classifiers

4.3.2.2.3 Band ratio classifiers

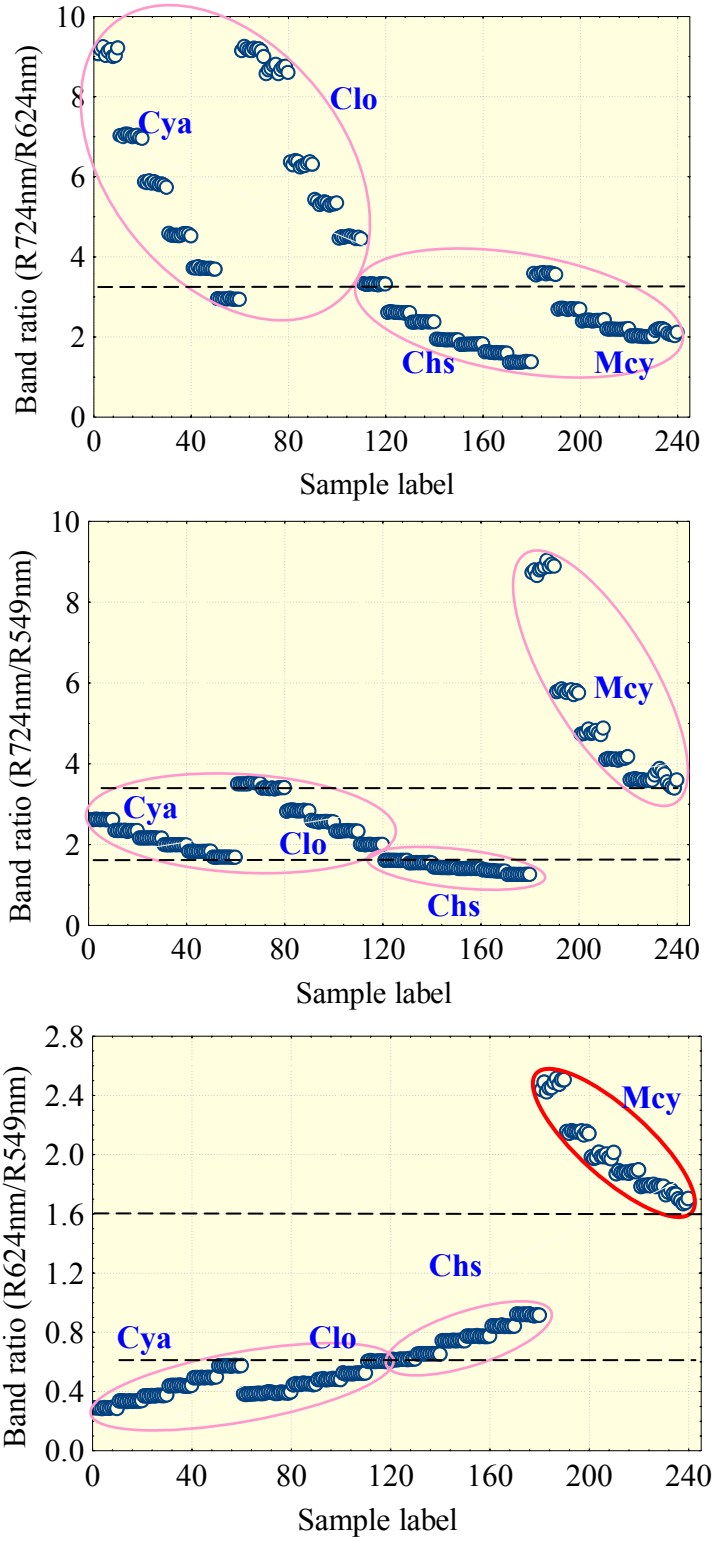

Fig. 4.7. Phytoplankton classification by using band ratio classifiers

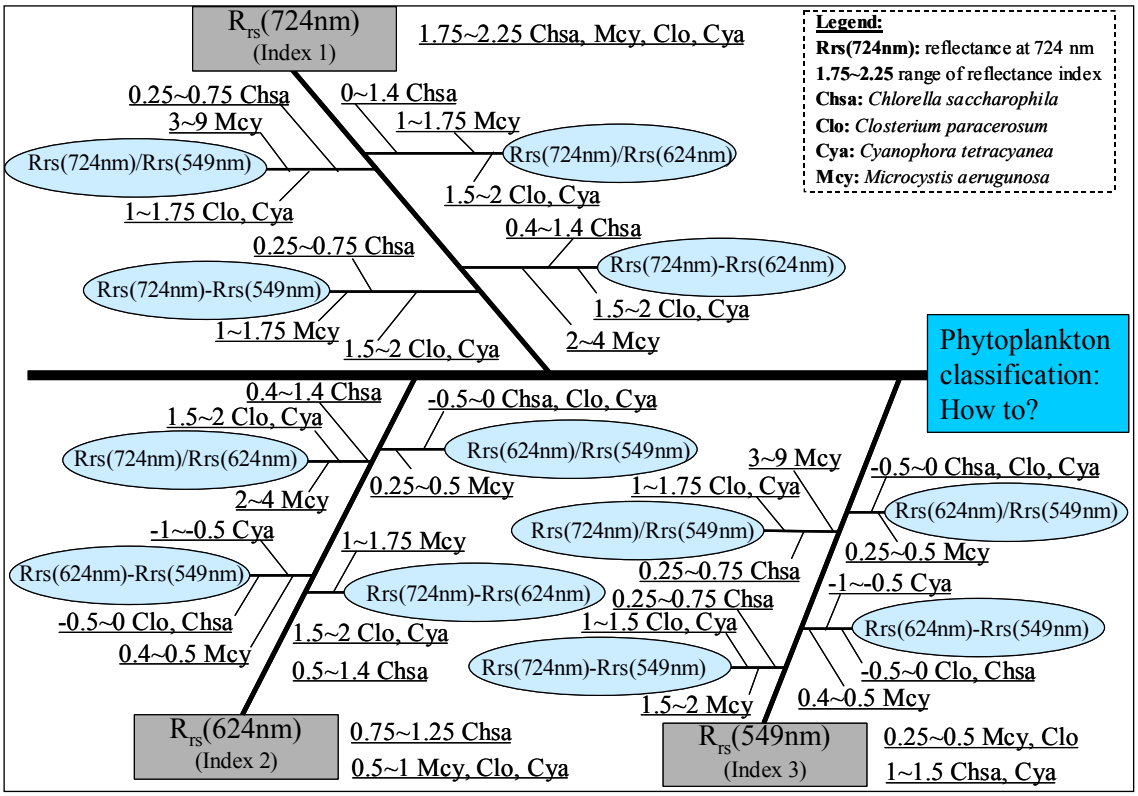

Fig. 4.8. Classification by using a combination of indexes

Chapter 5

Chlorophyll density estimation

The amount of chlorophyll in a water sample is used as a measure of the phytoplankton biomass. The magnitude of algae biomass can significantly affect the water quality. The use of the measurement of chlorophyll as an indicator of water quality is described in the Section 10200 A of *Standard Methods for the Examination of Water and Wastewater* (ASTM). This study tries to find out the way of chlorophyll density estimation by using the hyperspectral remote sensing technology.

5.1 Description of the problems affecting the chlorophyll density estimation accuracy

Regression analysis (see Appendix C) was carried out to propose models for estimation of chlorophyll density from remote sensing reflectance data. However a high divergence is found in the spectral data owing to large amount of noise in the spectral measurements.

The factors that affect the chlorophyll density estimation accuracy by using high spectral resolution spectrometer are discussed in this chapter. The influential factors (see Fig. 5.1) including the spectral measurement errors, the in-situ chlorophyll measurement errors, and the interference of the other water column constituents on the accuracy of chlorophyll density measurement are discussed in details in this chapter.

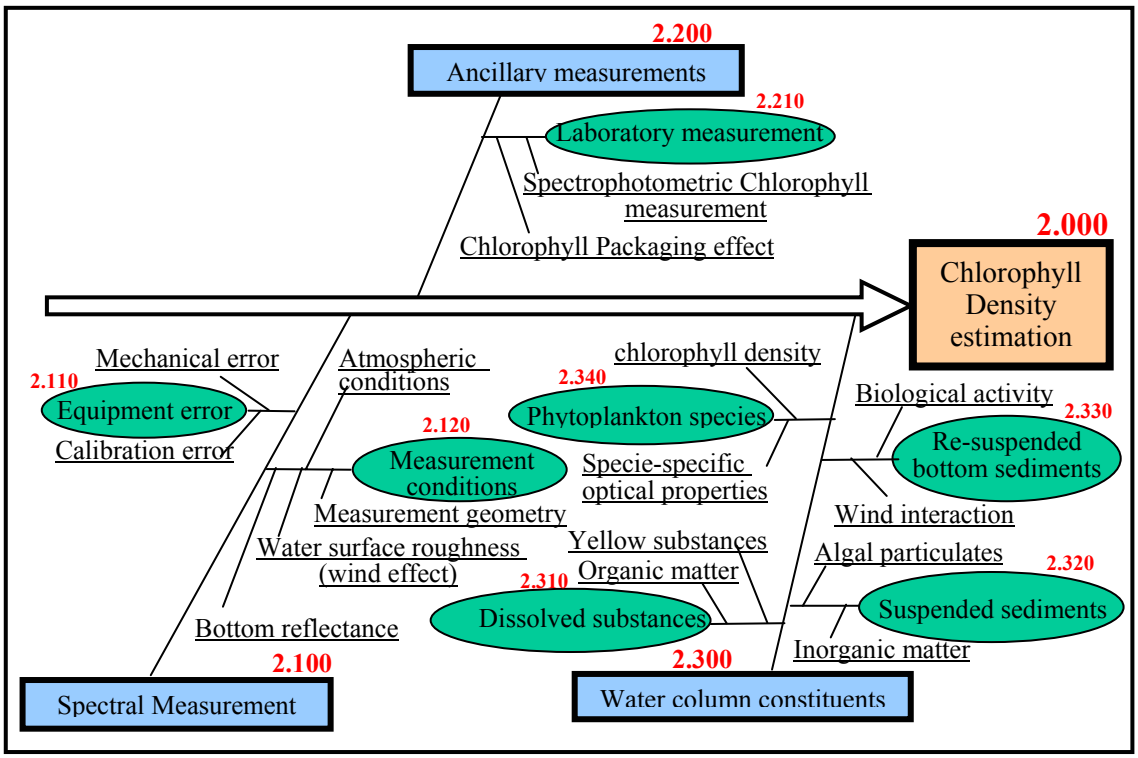

Fig. 5.1. Factors affecting the chlorophyll density estimation accuracy

5.2 Spectral measurement error

Spectral measurement errors include two types of errors: (i) errors introduced by the measurement conditions, and (ii) errors introduced by the equipment itself.

5.2.1 Measurement condition

The measurement conditions include (i) the atmospheric influence on the remote sensing data, (ii) the respective influences of the illumination source (sun, halogen lamps, etc,) and the viewing zenith angle of the sensor (spectrometer) on the spectral data. These influences are grouped under the “measurement geometry”, (iii) the water

surface roughness owing to the interaction between the water surface and the wind, which result in the effect of surface scattering on the remote sensing data, and (iv) the bottom influence on the spectral data, which is another kind of surface scattering.

5.2.1.1 Atmospheric conditions

5.2.1.1.1. What is the problem?

The most important atmospheric effect which affects the remotely sensed spectral data is gaseous and aerosol components of the atmosphere. The atmospheric effect originates in (i) the gaseous absorption of the solar light directly transmitted into the atmosphere, (ii) the gaseous scattering of the component of transmitted light reaching the sensor (Rayleigh scattering), and (iii) the aerosol scattering of the component of transmitted light reaching the sensor (Mie scattering).

In this study using the hyperspectral spectroradiometer this effect is not significant since the distance from the sensor to the measured target is very small. However this effect is discussed for complete review of phenomena that affect the accuracy of remotely sensed data.

5.2.1.1.2. Why is the problem important?

Systematic noises are generated by the Rayleigh and Mie scattered components of the light which interact with the atmosphere. These components can reach the sensor and therefore they can reduce the signal to noise ratio. As a result the spectral measurement may show increased amplitude of the target reflectance in the visible range of the light spectrum, especially in the shorter wavelengths like in blue band. Depending on the atmospheric properties at the time of spectral measurement time series images of the

target may not be comparable and unnecessary estimation errors can occur due to un-proper handling of the atmospheric effect.

5.2.1.1.3. How to solve the problem?

In controlled laboratory experiments the atmospheric effect is not significant since the distance from the sensor to the target is generally small. In the field conditions however (using satellite imagery or spectral data collected using hyperspectral spectroradiometer mounted onboard an airplane) the atmospheric effect is to be considered and data should be properly corrected.

Many methods, empirical and physically based, have been developed during the last decades to deal with the atmospheric effect.

Empirical methods can be divided into (i) interactive methods where certain test areas have to be identified, like “flat field” and an “empirical line fit” method is applied to correct for atmospheric effect (Kruse, 1988), and (ii) non-interactive empirical methods use statistical techniques like the “dark-object substraction” method (Shavez, 1975, and an improved version, Chavez, 1988)

Physically based methods like ATCOR (Richter, 1996, Richter, 2002), ATREM/TAFKAA (Goa and Davis, 1997, Gao et al., 2000), ENVI/FLAASH (Research Systems, Inc), or ACORN (Analytical Imaging and Geophysics, LLC), will use radiative transfer models, like 6S model (Vermonte et al., 1997) or MODTRAN (Berk et al., 1998).

The radiative transfer models require the knowledge of a set of parameters (atmosphere type/concentration profile of gases, aerosol type and concentrations, flight and ground elevations, illumination and observation zenith angles) whereas the geometric parameters can be determined from satellite flight data record, the atmospheric

parameters are not immediately accessible to the user. In the case of imaging spectrometer with adequate spectral channels, aerosol and water vapor concentrations may be estimated from the data itself.

The correction of atmospheric effect is one step in the spectral data post-processing, which consists of 4 steps

1. Radiometric calibration to convert DN to at-sensor radiance, which is a radiometric quantity measured in $W/m^2/sr/nm$

2. Atmospheric correction to substract the path radiance, i.e. the straight light from the atmosphere and to correct the adjacency effect, i.e. the outshining of the target by nearby bright objects (Dave, 1980)

3. Correction of the anisotropic reflection properties of the target, i.e. the bi-directional effect discussed in previous section.

4. Reflectance calibration to substract the spectral effect of solar illumination by dividing through the incoming irradiation.

5.2.1.2 Measurement geometry

5.2.1.2.1. What is the problem?

The combined effect of illumination and observation zenith angles on the remotely sensed data is called the bi-directional effect. The bi-directional reflectance affects the remotely sensed data in three ways: (i) through the so-called “hot spot”, (ii) through shadow casting (“surface scattering”) and (iii) through multiple scattering between structure elements of the target.

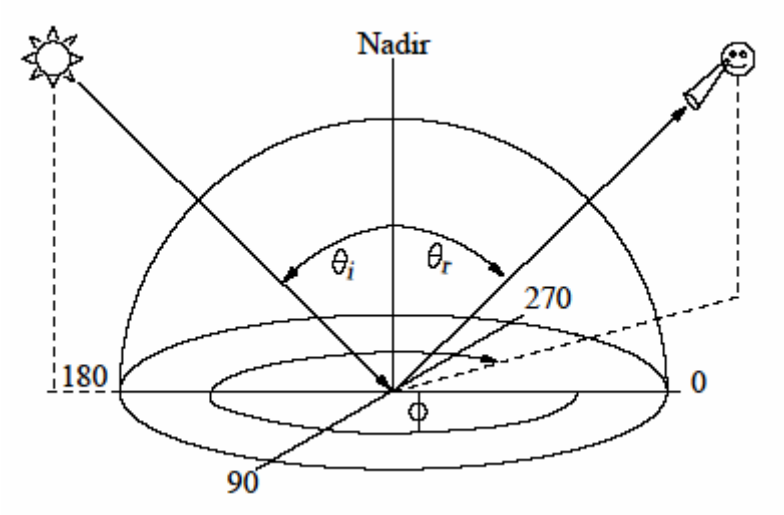

Note: θi incident solar zenith angle, θr reflected observation zenith angle, φ observation azimuth angle

Fig. 5.2 Geometric system for illumination and observation of remotely sensed target

(i) The most prominent effect of the bi-directional reflectance is the "hot spot", which is a bright reflected image of the illumination source (sun or halogen lamp…). In cases where the "hot spot" is placed in the field of view of the sensor the magnitude of the signal increases within the visible range of the light spectrum.

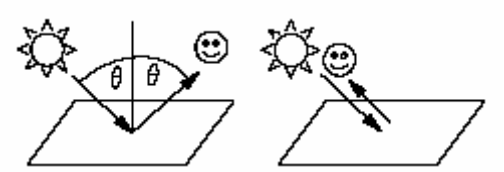

(ii) Apart from the "hot spot", the bi-directional effect is caused by shadow casting. The amount of cast shadow increases with increasing solar (illumination) zenith angle and can be considered maximum at dusk and dawn when the zenith angle approaches 90 degrees. The amount of cast shadow contributing to the target reflectance not only

depends on the illumination zenith angle but also it depends on the position (zenith angle of the sensor). In case where the sun (illumination source) is behind the sensor (ie sensor and illumination source are pointing in the same direction with comparable zenith angles) the cast shadow is hidden by the object itself, while with the sun in opposite direction the shadow is darkening the target (assuming no "hot spot" in the field of view of the sensor). The shadow casting effect is often referred to as "geometric" or "surface" scattering.

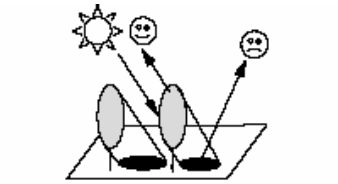

(iii) Another source of bi-directional effect is the multiple scattering between the structure elements of the target (irregularities of waves or vegetation at the water surface and visible bottom). This kind of scattering is called "volume scattering".

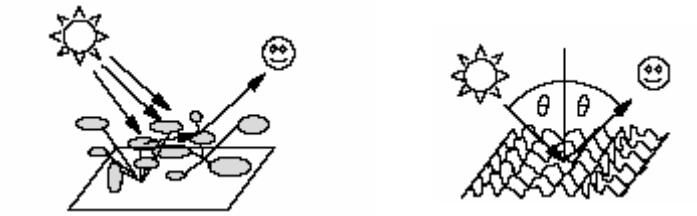

5.2.1.2.2. Why is the problem important?

Since the amount of the bi-directional effect contributing to the spectral measurement of the target is directly proportional to the distributions of both the illumination and the observation zenith angles, data collected for comparable targets at different locations may not be comparable and hence estimation models using such data may return

erroneous results. Therefore, it is important to understand and to correct the effect of both the illumination zenith angle and the observation zenith angle on the spectral data recorded by the sensor.

5.2.1.2.3. How to solve the problem?

In controlled conditions (laboratory experiments) it is possible to avoid at least the specular reflection and the hot spot by properly setting up the experimental apparatus.

In field conditions it is often not possible to avoid both the specular and hot spots. In any case the volume scattering will depend on the target surface characteristics and therefore may not be avoided.

To solve the problem then, it is needed to analyze the raw spectral data and try to identify the effects of these phenomena in particular regions of the spectrum (i.e. identify the spectral signatures of the phenomena) and correct their respective effects on the raw spectral data using appropriate correction coefficients.

In this study, experiment was carried out in the laboratory to measure the spectral reflectance data for a set of illumination and viewing zenith angles. The experimental data is used to identify and to evaluate the effect of zenith angles on the reflectance data. Many cases were examined by setting the sensor at zenith angles of 0, 10, 15 and 20 degrees and for each position of the sensor the illumination zenith angle was set at 0, 15, 30 and 45 degrees. The experimental results are summarized in figures 5.3 and 5.4.

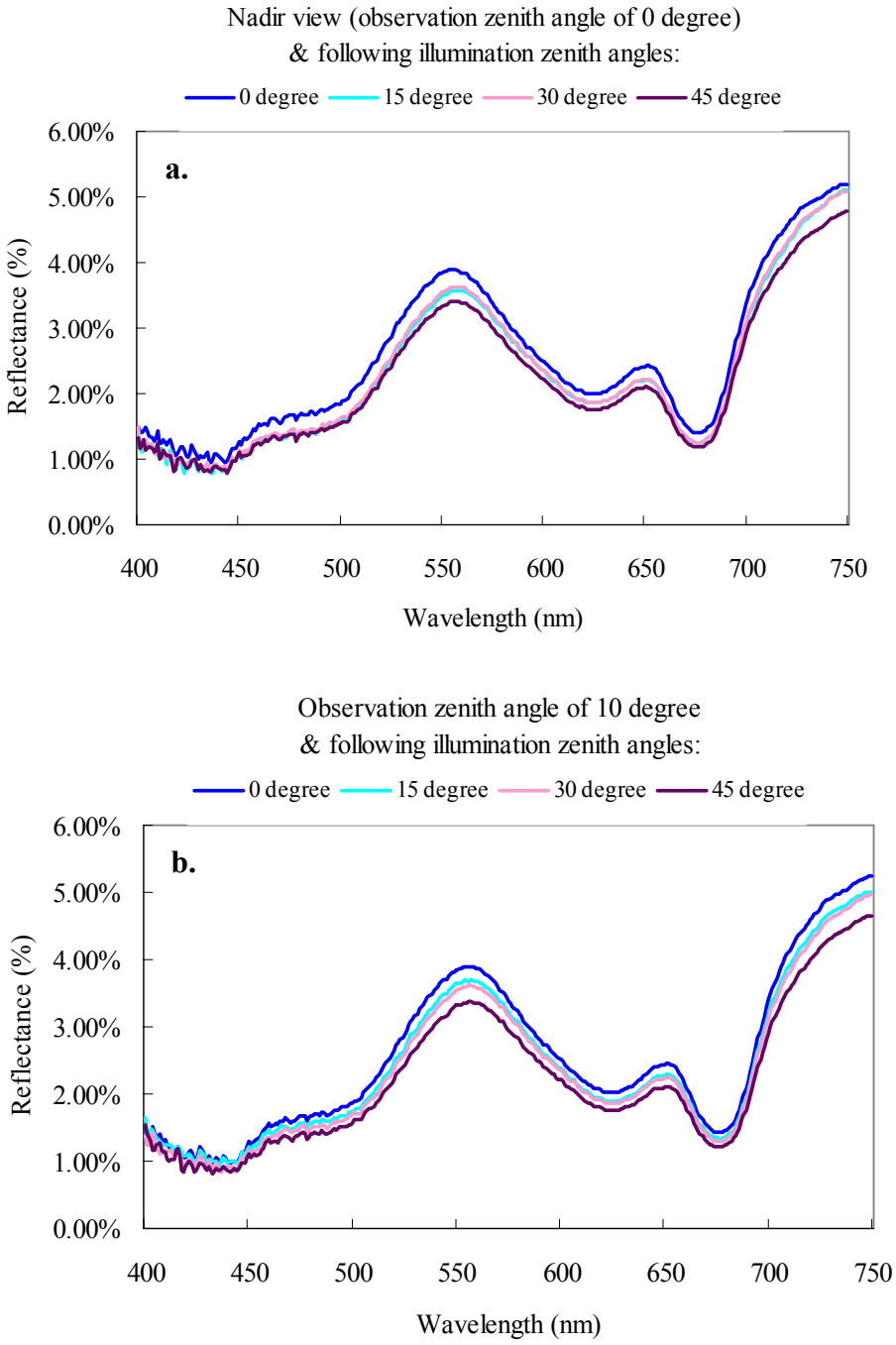

Fig. 5.3 Spectral reflectance of water sample observed with fixed zenith angles of **(a.)** 0 degree, and **(b.)** 10 degrees, and varying illumination zenith angle

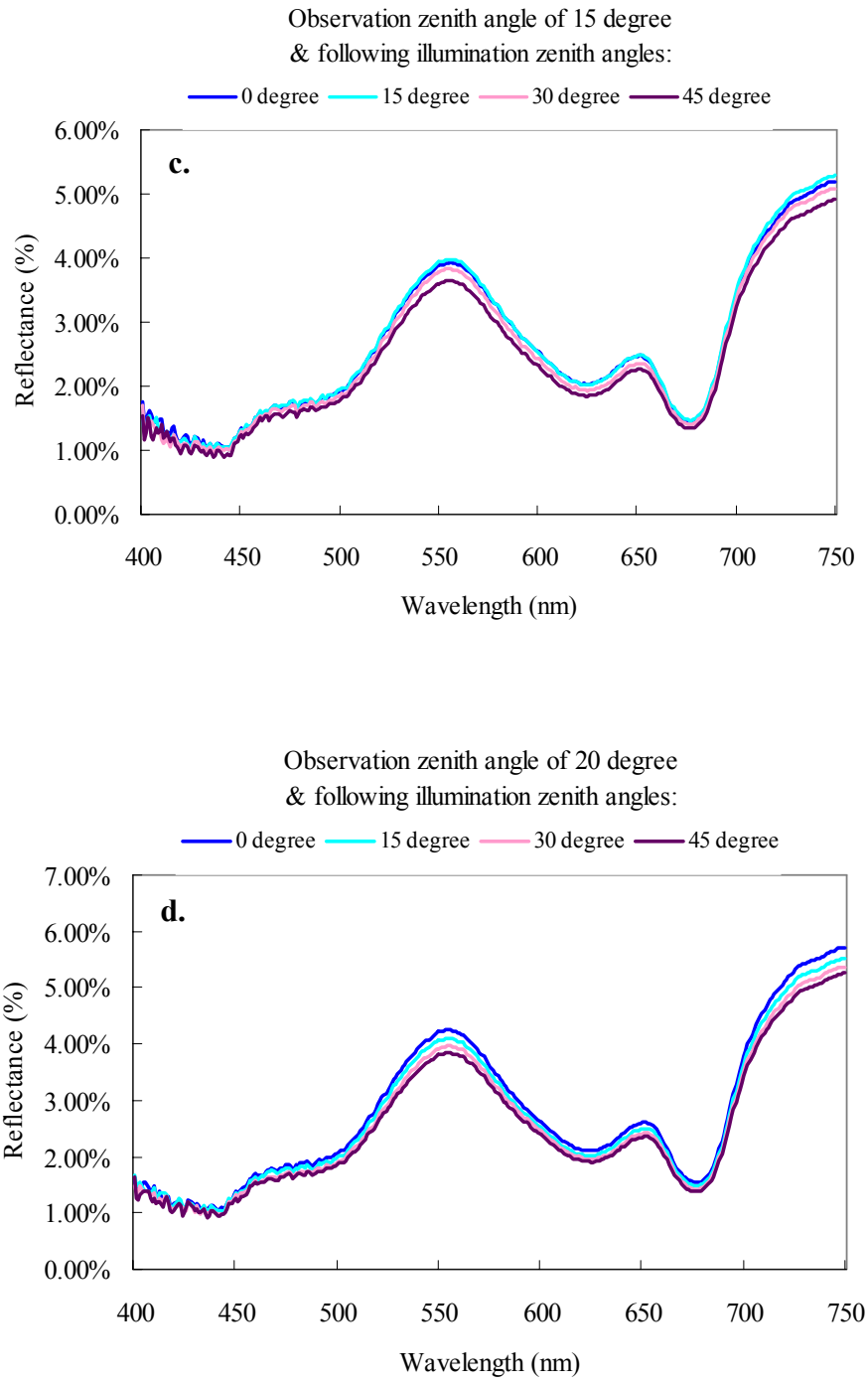

Fig. 5.4 Spectral reflectance of water sample observed with fixed zenith angles of **(c.)** 15 degrees, and **(d.)** 20 degrees and varying illumination zenith angle

All figures show that for a fixed observation zenith angle the reflectance of the target decreases with increasing illumination zenith angle. The decrease in reflectance is observed throughout the visible spectrum 400nm-720nm. However the gap in reflectance is not identical over the visible band. A mean decrease of 0.1% to 0.2% is observed in the Violet and the Blue band between 400 nm and 520 nm. Larger gaps are observed throughout the green band between 530nm and 570nm and in the red band between 710nm and 750nm. Both bands show a mean value of 0.5%. This decreasing pattern of the reflectance can be explained by the following factors:

(i) the flux of irradiation intensity per unit surface area of the water surface decreases with increasing illumination zenith angle.

(ii) With increasing illumination zenith angle the amount of the shadow area which is cast by the experiment tank walls increases. The shadow area can cover about the half of the water surface the experimental batch has small dimensions 60cmx30cmx30cm

(iii) the hot spot and specular reflection are outside the field of view of the sensor

5.2.1.2.4. findings

1. The effect of illumination and viewing zenith angle on the spectral reflectance is wavelength dependant.

2. It is found that for a fixed observation zenith angle if the illumination zenith angle is increased from 0 to 45 degrees, the intensity of the water surface reflectance is decreased by 0.2% in the violet and the blue bands (400-520nm) and a mean decrease of 0.5% through the green and the red band. These can be used to correct the raw spectral data with respect to change in illumination and observation zenith angles.

3. For any observation zenith angle between 0 and 20 degrees the decrease in reflectance with increasing illumination zenith angle seem identical. Therefore the

change in reflectance intensity should be attributable to the relative difference in zenith angles between the sensor and illumination source, which is called the bi-directional reflectance effect.

3. This decreasing pattern seem to occur owing to a mean decrease of irradiation flux with increasing illumination zenith angle, introduction of shadow in the field of view of the sensor by neighboring objects with increasing illumination zenith angle and weakened effect of specular reflection with increasing illumination zenith angle.

5.2.1.3. Water surface roughness (wind effect)

5.2.1.3.1. What is the problem?

Optically shallow waters are by nature highly dynamic environments that experience a variety of processes, which alter their optical properties. For the application of hyperspectral remote sensing of optically shallow waters, it is important to understand the effects some of these processes have on the optical properties of the bottom boundary layer. Waves and tides, for example, re-suspend sediments in varying degrees depending on topology, sediment characteristics, and the strength of the forcing mechanism. To a hyperspectral sensor, the apparent reflectance of the bottom will change dramatically depending on these bottom boundary conditions. Although the interactions of waves and tides with bottom sediments have been studied and modeled, their effects on the optical properties of the bottom boundary-layer and hence on the remote-sensing reflectance has rarely, if ever, been systematically studied.

5.2.1.3.2. Why is the problem important?

As pointed out by Philpot [1989] and Maritorena et al. [1994], bathymetric mapping with passive multispectral imagery is a non-unique modeling problem. That is, for

example, the same remote sensing reflectance can result from two different bottom depths although the bottom albedos differ accordingly. Similarly, an apparent change in the bottom albedo caused by a nepheloid layer will result in errors in bottom depth estimation from the remote sensing reflectance data. However, these errors can be anticipated, and possibly corrected, if adequate information of re-suspension events in the target area can be obtained and fed into an appropriate optical model.

5.2.1.3.3. How to solve the problem?

This effect has not been studied experimentally in this study. The following approach is proposed and is exclusively theortical. This is a common method followed in study of resuspension phenomena using the remote sensing technology. For reference see for example Philpot (1989) and Maritorena et al. (1994).

Optical modeling will consist of four major components: 1) developing optical-property models for re-suspended sediments and associated optically-active matter, 2) forward numerical modeling for solving the radiative transfer equation, 3) developing empirically-based coupled hydrodynamic-optical models for bottom-boundary layer effects, and 4) developing semi-analytical models for remote sensing of optically shallow waters that includes the optical effects of the bottom boundary layer and suspended sediments in the water column.

Modeling component (1) would be easy to carry out and simply requires the appropriate data on re-suspension phenomenon and on the wind velocity, then relate the intensity of re-suspension to corresponding velocities. Component (2) would require software like Hydrolight. Achieving component (3) will rely heavily on the quantity and quality of the data. However these kinds of model maybe strongly site specific. Modeling

component (4) is also likely to be site specific to some degree and its general applicability will no doubt depend on how comprehensive a data set we will be.

5.2.1.4. Bottom reflectance

5.2.1.4.1. What is the problem?

Light radiation, which is reflected from the bottom influences the water color if water is shallow. The effect varies with the water depth, the clarity of water, the type of substances present in the water column, and the type of bottom.

5.2.1.4.2. Why is the problem important?

In the natural condition even in cases in which the water quality is the same over a given water body there is great chance that the bottom depth and type may vary. In this case the spectral data will show different measurements for comparable water quality. It is therefore necessary to correct the spectral data from the influence of the bottom contribution to the total signal recorded.

5.2.1.4.3. How to solve the problem?

A laboratory testing is carried out to understand and attempt to solve the problem of bottom reflectance. In this study a stochastic Monte Carlo approach is used to estimate the contribution of the bottom to the water leaving radiance which is recorded by the sensor.

5.2.1.4.4. Findings

The Monte Carlo approach is used to estimate the contribution of the bottom to the water leaving radiance which is recorded at sensor, using 3 different groups of sample spectra which are collected both in optically deep and optically shallow water bodies. It is found that:

- In highly turbid water “group 1 samples”: the contribution of the bottom substrate to the total water leaving radiance recorded at sensor was about 4% and 0% for samples S1-INL1, and S2-CPD1 respectively. The bottom influence on the total signal which is recorded at sensor is negligible or can even be totally absent in the highly turbid water columns.

- In moderately turbid “group 2 samples”: the bottom contributes to about 6.8% and 9.3% of the total signal recorded at sensor for samples S3-PPD1 and S3-PPD2 respectively. However, the significance of this bottom contribution is limited only to the green waveband domain of the light spectrum especially when the physical depth is greater than 1 m as shown in Fig. 5.5. This case may not be a major problem for bio-optical chlorophyll estimation modeling.

    - In low turbidity samples, on the contrary, this case is a major problem for chlorophyll density estimation. In all the testing samples of “group 3” the noise contributed by the bottom substrates amounts to 20% or more of the total signal which is recorded by the spectrometer.

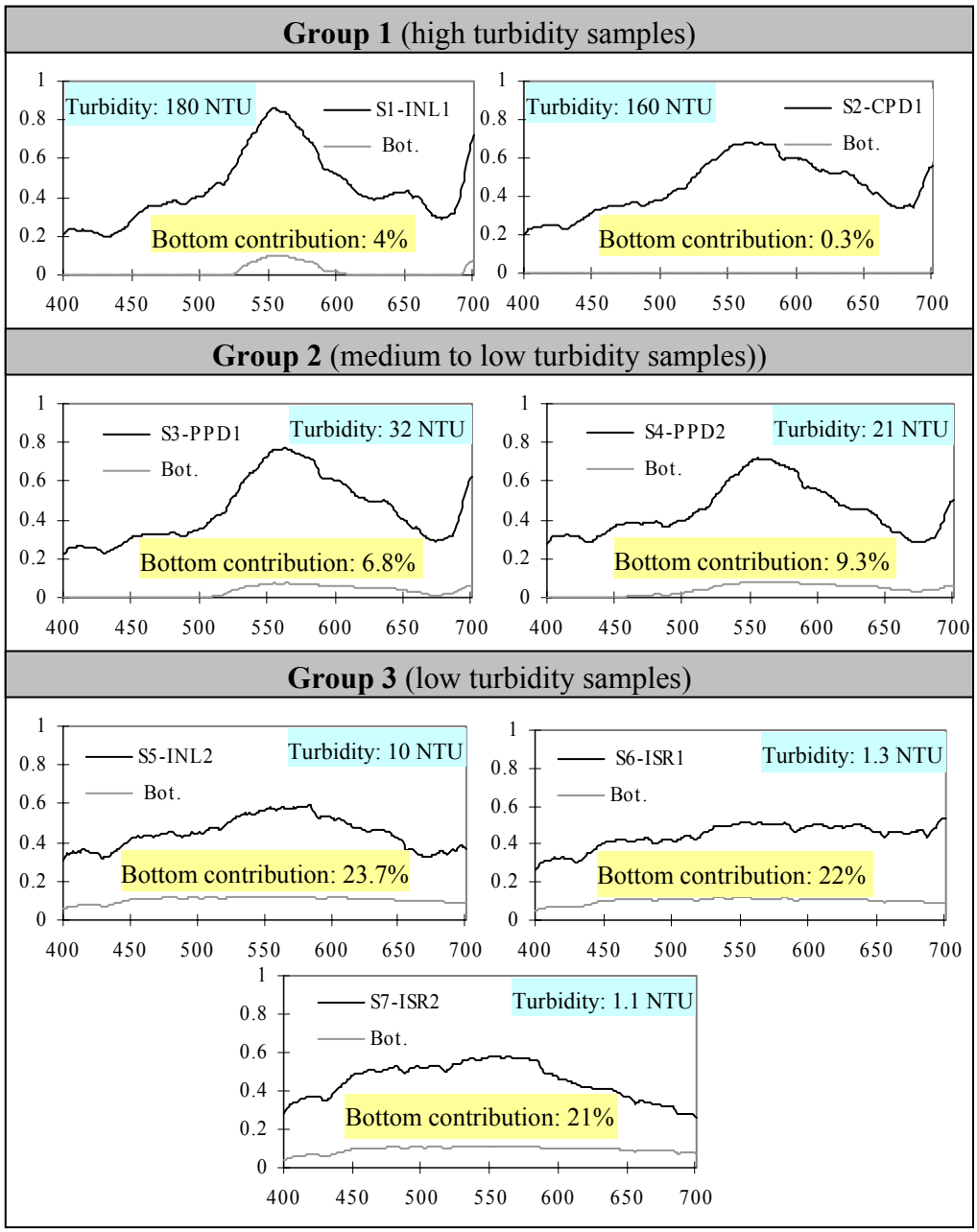

Fig. 5.5. Results of Monte Carlo simulations showing the contribution of the bottom, represented in solid gray lines, to the total water leaving radiance recorded at sensor, shown in solid black lines.

The question is "how accurately the Monte Carlo algorithm developed here un-mixes the contributions of the bottom and the water column radiance components of the testing samples?" The findings clearly suggest the potential positive outcome that could

be expected if a more extensive testing with different kinds of bottom substrates were to be carried out.

5.2.2. Equipment error

The error due to equipment can be classified into 2 types: (i) the calibration error, and (ii) the light source un-stability error.

5.2.2.1. Calibration error

Reliable spectrometric data depends, to perhaps the greatest extent, upon accurate calibration of the instrument, which is used to collect the data (FieldSpec Pro, 2002).

5.2.2.2. Light source un-stability

For the spectral measurements that are carried out in the laboratory, it is important to assure the light source stability. When using halogen lamp it is found (Nakamoto, 2006) that the light intensity has a strong time dependency in the first few hours of warming. The intensity stabilizes thereafter and appear again few hours later owing to high temperature. This light source un-stability introduces fluctuations in the spectral data or can produce spectral artifacts that are signal-like noises.

For outdoors illumination commonly solar illumination light un-stability may occur owing to atmospheric absorption especially in cloudy and humid conditions.

In both cases indoors and outdoors applications one countermeasure is to collect a measurement of the white reference panel once for each measurement of the specimen or the target and to use the ratio of the target spectrum to the white reference spectrum. This kind of countermeasure can eliminate the systematic noises.

5.3. Chlorophyll density measurement error

5.3.1. Extractive method error

The classical method of determining the quantity of chlorophyll at a particular site is to collect a fairly large water sample and analyze it in the laboratory. The procedure involves filtration of the sample to concentrate the chlorophyll containing organisms, mechanical rupturing of the collected cells, and extraction of the chlorophyll from the disrupted cells into the organic solvent, acetone. The extract is then analyzed by spectro-photometry. The accuracy of the method depends on the sample solution matrix and the calculation equations used (Lorenzen & Jeffrey, 1980; Write *et al*., 1997). As a matter of fact, each equation returns a different chlorophyll value. An alternative estimation method is simply to report the amount of total chlorophyll pigments (Golterman & Clymo, 1971), that is, the estimate of all chlorophyll pigments and degradation products resident in a given water sample.

5.3.2. In-situ measurement error

5.3.2.1. What is the problem?

The YSI 6600 chlorophyll sensor was used in this study for real-time estimation of chlorophyll simultaneously with the spectral measurement. This kind of optical measurement using YSI 6600 water quality logger is based on an alternative method for the measurement of chlorophyll density, which overcomes the disadvantages described above, albeit with the potential loss of accuracy. In this procedure, chlorophyll is determined in-vivo, i.e., without disrupting the cells as in the extractive analysis. The YSI 6600 chlorophyll sensor is designed for these in-vivo applications and its use

allows the facile collection of large quantities of chlorophyll data in either spot sampling or continuous monitoring applications. It is important to remember, however, that the results of in-vivo analysis will not be as accurate as those from extractive analysis procedure.

5.3.2.2. How to solve the problem?

The limitations of the in-vivo method are outlined below and should be carefully considered before making chlorophyll determinations with your YSI sonde and sensor. Some of the sources of inaccuracy can be minimized by combining the data from the YSI 6600 with data from extractive analysis of a few samples acquired during a sampling or monitoring study. However, the in-vivo studies will never replace the standard procedure. Rather, the estimates of chlorophyll concentration from the easy-to-use YSI chlorophyll system are designed to complement the more accurate (but more difficult to obtain) results from more traditional methods of chlorophyll determination.

5.3.2.3. Review of the limitations of in-vivo measurement method using YSI 6600 instrument and setting directions to solve the problems.

One key characteristic of chlorophyll is that it fluoresces, that is, when irradiated with light of a particular wavelength, it emits light of a higher wavelength (or lower energy). The ability of chlorophyll to fluoresce is the basis for YSI 6600 chlorophyll measurement system. This instrument induces chlorophyll fluorescence by shining a beam of light of the proper wavelength into the sample, and then measuring the higher wavelength light which is emitted as a result of the fluorescence process. The YSI 6600 chlorophyll estimation system uses a light emitting diode (LED) as the source of the irradiating light that has a peak wavelength of approximately 470 nm. LEDs with

this specification produce radiation in the visible region of the spectrum with the light appearing blue to the eye. On irradiation with this blue light, chlorophyll resident in whole cells emits light in the 650-700 nm region of the spectrum. To quantify the fluorescence, the system detector is usually a photodiode of high sensitivity that is screened by an optical filter that restricts the detected light. The filter prevents the 470 nm exciting light from being detected when it is backscattered off of particles in the water. Without the filter, or in case of trouble with the filter, turbid water would appear to contain fluorescent phytoplankton, even though none were present.

5.3.2.3.1. Effect of temperature on readings

While this study did not consider the temperature effect on the chlorophyll measurement using YSI 6600 instrument, the effect of temperature on the chlorophyll sensor itself is very small according to YSI user guide, YSI experiments have indicated that instead of temperature-instrument type dependence, it is rather the fluorescence of phytoplankton suspension that shows significant temperature dependence.

For example the experiment carried out by the YSI technicians and described in details in the YSI 6600 user guide showed that the apparent chlorophyll content of laboratory test samples of algae increased from 185 to 226 µg/L when the temperature was dropped from 21 °C to 1 °C even though no change in phytoplankton content took place. In the absence of compensation, this effect would obviously result in errors in field chlorophyll readings if the site temperature were significantly different from the calibration temperature. This temperature error can be reduced by employing a chlorophyll temperature compensation routine which in principle is taken into account and carried out automatically by the "Chl tempco" code which is in the sonde software under the Advanced Sensor menu.

From the YSI study, it appears that entry of a value of 1 to 2 % per degree C is appropriate to partially account for changes in the fluorescence of environmental phytoplankton with temperature. This value can be estimated in the above example as follows:

Change in Temperature = 21–1 = 20 °C

Change in Fluorescence = 226-185 = 41 µg/L

% Change in Fluorescence = (41/185) x 100 = 22.1

Chl Factor = 22.1/20 = 1.11 % per degree °C

However the use of this empirically derived compensation does not guarantee accurate field readings since each species of phytoplankton is likely to be unique with regard to the temperature dependence of its fluorescence.

Direction to solve the problem

Changes in fluorescence with temperature are a key limitation of the in-vivo measurement method (see below), which can only be reduced, not eliminated, by this compensation. In this study it is thought and proposed that the best way to minimize errors is to calibrate with phytoplankton standards of known chlorophyll content that are as close as possible in temperature to that of the environmental water under investigation.

5.3.2.3.2. Effect of turbidity on chlorophyll readings

As described above, the filters in front of the photodiode in the YSI 6025 chlorophyll probe prevent most of the 470 nm light which is used to excite the chlorophyll molecules from reaching the detector after being backscattered off of non-fluorescent particles (turbidity) in environmental water. However, the filter system is not perfect

and a minor interference on chlorophyll readings from suspended solids may result. Laboratory experiments indicate that a suspension of typical soil measured with a YSI 6026 sensor will have a turbidity interference characterized by a factor of about 0.03 µg/L per NTU. For example, the turbidity of the water must be above 100 NTU to produce an apparent chlorophyll reading equal to 3 µg/L. In very cloudy water, the user may wish to use the independently-determined turbidity value and the above compensation factor to correct measured chlorophyll values using, for example, a spreadsheet.

5.3.2.3.3. Interferences from other fluorescent species

The analytical methods described in *Standard Methods* for chlorophyll involve disruption of the living organisms present in suspension, followed by extraction of molecular chlorophyll into a homogeneous solution in an organic solvent. Acidification of the extract helps to minimize the interferences caused by a number of other, non-chlorophyll species. In addition, readings can be taken at various wavelengths on a spectrophotometer or a laboratory fluorometer to differentiate between the various forms of chlorophyll (a, b, c) and pheophytin a.

In contrast to this fairly controlled situation, sensors operate under heterogeneous conditions where the sensor will measure, at least to some degree, everything which fluoresces in the region of the spectrum above 630 nm when irradiated with 470 nm light. Therefore, the sensor is really quantifying overall fluorescence under these optical conditions, rather than chlorophyll specifically. While it is probable that most of the fluorescence is due to suspended plant and algal matter and that much of the fluorescence from this biomass is due to chlorophyll, it is impossible to exclude interferences from other fluorescent species using the approach described above. Note

that *in-vivo* measurement using the YSI cannot differentiate between the different forms of chlorophyll.

5.4 Water column constituents

The water column constituents (see Fig 5.3.1) influence the water reflectance and therefore interfere with the chlorophyll quantification by using remote sensing technology. Water column constituents can be grouped into the following: (i) the phytoplankton species (ii) the dissolved organic matter (iii) the suspended inorganic sediments, and (iv) the re-suspended bottom sediments.

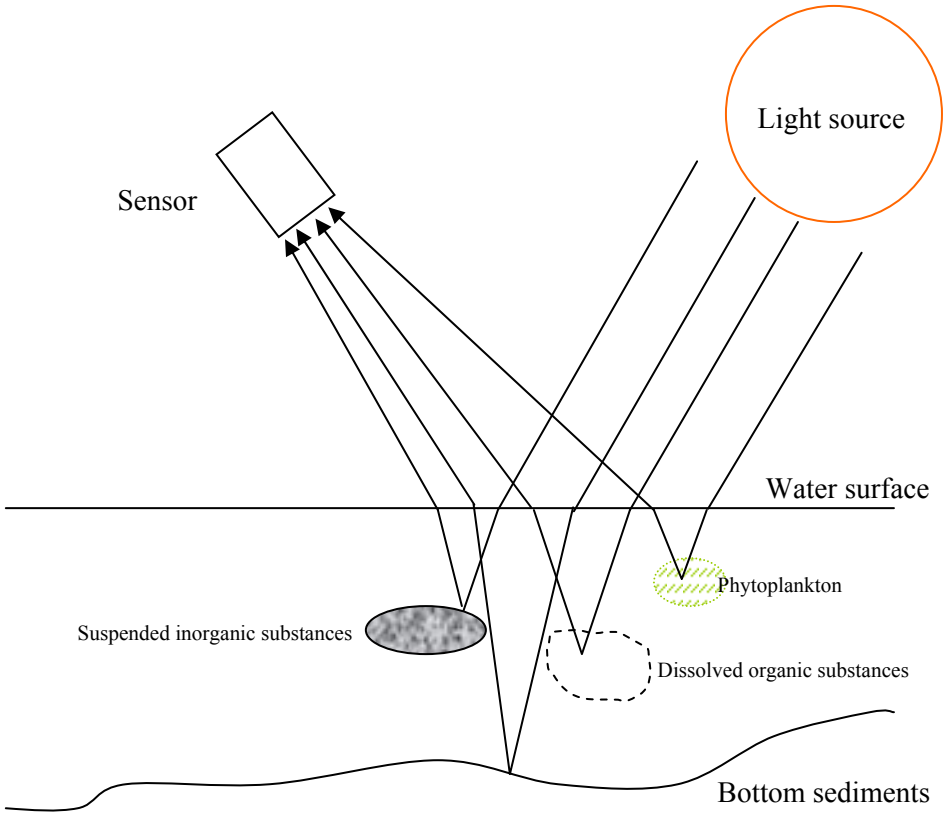

Fig. 5.6. Factors that influence the water reflectance which is measured by the sensor

5.4.1. The Phytoplankton Component

The phytoplankton are ubiquitous, microscopic, free-floating organisms which are found in the illuminated surface layers of the water column. They are the single-celled plants that form the base of the aquatic food web, and they are an important component of the global carbon cycle. According to current estimates, the global carbon fixation by oceanic phytoplankton roughly matches terrestrial carbon fixation over an annual scale. Thousands of phytoplankton species, with characteristic sizes, shapes and physiological properties, are known to exist in the aquatic environment, and their species composition and concentration can change with time and space. The concentration of the main phytoplankton pigment, chlorophyll-a, is often taken as an index of phytoplankton biomass. However, it is important to recognize that chlorophyll-a is accompanied by a number of auxiliary pigments in the phytoplankton cells (pigment analyses using High Performance Liquid Chromatography, HPLC, technique show the presence of fifteen or so pigments in a typical phytoplankton sample). The pigment composition of a water sample can vary with the community structure of the phytoplankton population in the sample, as well as with the physiological state of the cells (*e.g.*, photoadaptation and nutritional status). If a single group of substances were to be identified as being the most important agent responsible for variations in the optical properties of aquatic environments, then it would be phytoplankton. But even in the most pristine of aquatic environments, these organisms co-exist with other microscopic organisms such as zooplankton, heterotrophic bacteria and viruses. Non-living degradation products of these organisms would also be present in the milieu as detritus. For practical experimental reasons when we quantify the optical properties of phytoplankton from natural aquatic environments, the contributions from such other microscopic particles are often not

distinguished from those of phytoplankton. For example, the size spectra of several of these organisms overlap, making it difficult, if not impossible, to separate them by filtration. Furthermore, in analyses of optical data from the natural environment, it is often a major problem to distinguish the phytoplankton signal from those of other substances that covary with it. Therefore, in the remote-sensing context, the "phytoplankton component" incorporates other microscopic organisms as well, unless otherwise stated. This is in recognition of the fact that, from an optical point of view, the highly-pigmented phytoplankton typically dominate the signal from microscopic organisms.

5.4.2. Suspended inorganic sediments

The suspended inorganic sediments include all inorganic particulate material that is not included in the phytoplankton component. In shallow lakes and inland water bodies, wave and current action can bring bottom sediments into suspension, modifying significantly the watercolor. Shallow lakes and reservoirs waters influenced by the outflow of rivers, and areas of large tidal excursions are examples of regions where one might anticipate particulate material in suspension to play an important role in determining the optical properties of the water column. Unlike that of the phytoplankton component, their influence is confined typically to certain lakes and inland water bodies. It is important to recognize that the term "suspended material" does not apply to a single type of material, but to a whole family of materials with their own individual characteristics. For example, reflective white sands, when brought into suspension, will have a very different influence on watercolor from, say, red clay in suspension in the

water column. They may also include suspended particles of other origin, such as continental dust deposited on the water by winds or volcanic deposits.

5.4.3. Yellow substances

Yellow substances, variously called “gelbstoff”, “colored, dissolved organic matter” (CDOM) or “gilvin”, are a group of organic, dissolved substances, consisting of humic and fulvic acids. They may have a local origin, for example from the degradation of phytoplankton cells and other organic particles, or they may be advected to a locality from a distant source. For example, rivers that flow through heavily-wooded regions and over organic-rich soils accumulate a load of yellow substances along their flow path. Localities where yellow substances from distant sources accumulate may have much higher concentrations than regions where only locally-derived yellow substances are present. Yellow substances are known to undergo photodegradation, such that locally-derived yellow substances are likely to accumulate more at depth than in the surface layers of water bodies. The absorption properties of yellow substances are also known to be somewhat variable. Absorption spectra of the so-called non-pigmented, “detrital” particulate material resemble the absorption spectra of yellow substances very closely. Hence, for practical reasons in remote sensing, the detrital component is often combined with the yellow-substances component. This study recommends to follow this practice, even though there are arguments for including the yellow substances in the phytoplankton component or the suspended-material component.

5.4.4. Bottom sediments re-suspension

In addition to these three types of substances present in the water column, light reflected off the bottom of a water body can also influence ocean color, provided the water is sufficiently shallow, and the water sufficiently clear. Again, the influence of the bottom on the watercolor can vary with the depth of the water body, the clarity of the water, the type of substances present in the water, and the type of bottom. The bottom may be rocky or sandy, and may or may not be covered, partially or fully, by a variety of benthic organisms (*e.g.*, algae, molluscs). All of these factors will influence the manner in which bottom effects are manifested in the color of the water, as seen by a remote sensor.

It is recognized that these three categories of substances listed above, and perhaps the bottom characteristics, can influence watercolor. Typically, the estimation of chlorophyll density is done by calibrating changes in watercolor against changes in the concentration of chlorophyll-a in the surface layers of the lake or reservoir. Simple algorithms designed for such applications function best if substances other than phytoplankton are either insignificant, or correlated with phytoplankton.

However, we also recognize that such algorithms have a higher probability of failure in waters in which particulate matter (other than the phytoplankton component) and yellow substances or bottom effects exert an important influence. Furthermore, it would be useful to know how, when and where these algorithms may fail, and how we can improve the performance of water-color algorithms, and extend their domain of applicability.

Chapter 6

Findings

6.1 Phytoplankton species classification

6.1.1 Effect of the phytoplankton species on the hyperspectral data

- The variation of the intensities of spectral absorption peaks chlorophyll and accessory pigments in four species of phytoplankton is researched. It is found that:

- The absorption peak at 488nm (R488) is consistently found for all the species and its intensity is not significantly different from one species to another.

- The reflectance peak at 538 nm (R538) is weak for *Microcystis aerugunosa* due to strong absorption in the blue and the green spectral range between 540nm and 590nm by the pigment phicobilin which is the characteristic accessory pigment of *Microcystis aerugunosa*.

- In the case of *Chlorella saccharophila* the peak is not consistently found at 538 nm but it is shifted towards longer wavelengths at about 560 nm because the presence of strong reflectance peak of chlorophyll-b pigment at about 560 nm. The peak intensity is decreased because of strong absorption in the red band and the blue band.

- *Cyanophora tetracyanea* has a strong reflectance peak at 550 nm owing to overlap of the chlorophyll-a and the chlorophyll b reflectance spectra.
- This research takes advantage of this type of characteristics to attempt to classify the phytoplankton species.

6.1.2 Classification results

- Potentially harmful phytoplankton specimen "*Mycrocystis aerugunosa"* could be discriminated and classified into a separate group of phytoplankton by using simple classifiers. This is an important finding to help manage the eutrophication in shallow lakes and reservoirs by using hyperspectral remote sensing technology.

- However the classification of other phytoplankton specimens "*Chlorella saccharophyla*", "*Closterium paracerosum*", and "*Cyanophora tetracyanea*" that have similar spectral shape was not possible.

6.2 Chlorophyll density estimation

The selected regression models for estimation of chlorophyll density are shown in Appendix C. It was found that the estimation errors could be reduced when considering the probability density within 50% of spectral data distribution (Appendix D)

6.2.1 For regression model 1: R538nm/R488nm

It is found that the chlorophyll density estimation could be improved as in the following table:

Class of chlorophyll concentration	Range of accuracy for full data distribution	Range of accuracy for 50 % distribution
5 µg/l	± 11 µg/l	**± 3 µg/l**
10 µg/l	± 13 µg/l	**± 3 µg/l**
15 µg/l	± 10 µg/l	**± 4 µg/l**
20 µg/l	± 12 µg/l	**± 3 µg/l**
25 µg/l	± 8 µg/l	**± 3 µg/l**
50 µg/l	± 20 µg/l	**± 8 µg/l**
100 µg/l	± 50 µg/l	**± 16 µg/l**

These results mean that if the water sample is measured 45 times there is 50% probability to achieve measurements accuracies shown summarized in this table. The model prediction mean accuracy is about ± 3 µg/l for estimated chlorophyll concentrations ranging from 5 to 20 μ g/l. Minimal accuracy was found for chlorophyll concentration about 5 μ g/l. This model is good for estimation of chlorophyll in water columns with concentrations lower than 20 μ g/l.

6.2.2 For regression model 2: R581nm/R463nm

It is found that the chlorophyll density estimation could be improved as in the following table:

Class of chlorophyll concentration	Range of accuracy for full data distribution	Range of accuracy for 50% data distribution
5 µg/l	± 20 µg/l	**± 10 µg/l**
10 µg/l	± 15 µg/l	**± 7 µg/l**
15 µg/l	± 12 µg/l	**± 5 µg/l**
20 µg/l	± 20 µg/l	**± 7 µg/l**
25 µg/l	± 20 µg/l	**± 5 µg/l**
50 µg/l	± 10 µg/l	**± 6 µg/l**
100 µg/l	± 32 µg/l	**± 9µg/l**

These results mean that if the water sample is measured 45 times there is 50% probability to achieve measurements accuracies shown summarized in this table. The model prediction accuracy increases with increasing chlorophyll concentration because the data collected from water columns with high chlorophyll concentrations are less effected by scattering from the bottom and therefore have less random noise than their low concentrations counterparts. A mean accuracy of ± 7 µg/l can be achieved for chlorophyll concentrations 50 μ g/l up. Minimal accuracy was found for chlorophyll concentration between 5 to 10 μ g/l. This model is good for estimation of chlorophyll in water columns with concentrations higher than 50 μ g/l. The model is not recommended for chlorophyll concentrations less than 10 μ g/l

6.2.3 For regression model 3: R644nm/R463nm

It is found that the chlorophyll density estimation could be improved as in the following table:

Classe of chlorophyll concentration	Range of error for full data distribution	Range of error for 50% data distribution
5 µg/l	± 28 µg/l	**± 6 µg/l**
10 µg/l	± 25 µg/l	**± 9 µg/l**
15 µg/l	± 35 µg/l	**± 8 µg/l**
20 µg/l	± 20 µg/l	**± 8 µg/l**
25 µg/l	± 15 µg/l	**± 9 µg/l**
50 µg/l	± 10 µg/l	**± 7 µg/l**
100 µg/l	± 15 µg/l	**± 9 µg/l**

These results mean that if the water sample is measured 45 times there is 50% probability to achieve measurements accuracies shown summarized in this table. The model prediction accuracy increases with increasing chlorophyll concentration because the data collected from water columns with high chlorophyll concentrations are less effected by scattering from the bottom and therefore have less random noise than their low concentrations counterparts. A mean accuracy of 80% can be achieved for chlorophyll concentrations 50 μ g/l up. The prediction accuracy of this model is decreased because of its weak slope. Minimal accuracy was found for chlorophyll concentration about 10 μ g/l. This model is good for estimation of chlorophyll in water

columns with concentrations higher than 50 μ g/l. The model is not recommended for chlorophyll concentrations less than 10 μ g/l

6.2.4. For regression model 4: R654nm/R463nm

It is found that the chlorophyll density estimation could be improved as in the following table:

Classe of chlorophyll concentration	Range of error for full data distribution	Range of error for 50% data distribution
5 µg/l	± 30 µg/l	**± 10 µg/l**
10 µg/l	± 30 µg/l	**± 9 µg/l**
15 µg/l	± 45 µg/l	**± 10 µg/l**
20 µg/l	± 25 µg/l	**± 9 µg/l**
25 µg/l	± 20 µg/l	**± 5 µg/l**
50 µg/l	± 20 µg/l	**± 8 µg/l**
100 µg/l	± 28 µg/l	**± 9 µg/l**

These results mean that if the water sample is measured 45 times there is 50% probability to achieve measurements accuracies shown summarized in this table. The model prediction mean accuracy is about ± 9µg/l for estimated chlorophyll concentrations ranging from 20 to 100 μ g/l. Minimal accuracy was found for chlorophyll concentration about 5 μ g/l. This model is good for estimation of

chlorophyll in water columns with concentrations higher than 20 μ g/l and is not recommended for estimation of chlorophyll concentrations lower than 20μg/l.

6.3 Effects of instrumentation error and measurement conditions error on the classification and estimation of phytoplankton

6.3.1 Effect of the zenith angles of the hyperspectral Sensor and the illumination source on the remotely sensed hyperspectral data

In this research it is found that:

- The effect of illumination and viewing zenith angle on the spectral reflectance is wavelength dependant.

- It is found that for a fixed observation zenith angle if the illumination zenith angle is increased from 0 to 45 degrees, the intensity of the water surface reflectance is decreased by 0.2% in the violet and the blue bands (400-520nm) and a mean decrease of 0.5% through the green and the red band. These can be used to correct the raw spectral data with respect to change in illumination and observation zenith angles.

- For any observation zenith angle between 0 and 20 degrees the decrease in reflectance with increasing illumination zenith angle seem identical. Therefore the change in reflectance intensity should be attributable to the relative difference in zenith angles between the sensor and illumination source which in practice is called the bi-directional relectance effect.

- This decreasing pattern seem to occur owing to a mean decrease of irradiation flux with increasing illumination zenith angle, introduction of shadow in the field of view of the sensor by neighboring objects with increasing illumination zenith angle and weakened effect of specular reflection with increasing illumination zenith angle.

6.3.2 Effect of the water depth on the remote sensing data.

- It is found that when the radiation propagates within the water column it interacts with the water molecules as well as the dissolved and the suspended sediments contained in the water column. The combined effect of absorption and scattering which is called attenuation results in the progressive decrease in the radiation intensity as it propagates. Then the radiation intensity depends on the water depth and it decreases with increasing water depth.

- Remote sensing reflectance spectra vary largely over the Red band between 620 and 750 nm and in the blue band between 400 nm and 500 nm. The spectra are characterized by (i) minimal values in the blue region (400-500nm) owing to the combined effect of absorption by phytoplankton pigments, and other dissolved substances (ii) a peak in the green region (about 550 nm) owing to minimal values of total absorption by phytoplankton, in this region the scattering by phytoplankton is dominant that is why the phytoplankton appears green (iii) a minimum in the red band (about 675nm) owing to chlorophyll absorption (iv) a local maximum in the range 690-715nm owing to minimum in total absorption by phytoplankton and dissolved substances (v) lower

values in the NIR region (about 750nm) owing to high absorption by pure water, specifically in this region the remote sensing reflectance varied from 9 to 6% respectively for 10cm depth and 30cm depth.

- Among all the 5 features explained above only the NIR feature seems to have a good correlation with water depth (correlation coefficient of r = 0.8). Even though we cannot ignore uncertainties and spectral noises which are introduced by different factors affecting measurement accuracy the mean variation observed was about 4% decrease in reflectance for 20cm increase in water depth.

- All other features seem to be influenced by the combined effect of (i) phytoplankton absorption (ii) scattering by phytoplankton walls and (iii) variation in water depth.

6.3.3 Effect of the bottom type on the remotely sensed data

The Monte Carlo approach is used to estimate the contribution of the bottom to the water leaving radiance which is recorded at sensor, using 3 different groups of sample spectra which are collected both in optically deep and optically shallow water bodies. It is found that:

- In highly turbid water "group 1 samples": the contribution of the bottom substrate to the total water leaving radiance recorded at sensor was about 4% and 0% for samples S1-INL1, and S2-CPD1 respectively. The bottom influence on the total signal which is

recorded at sensor is negligible or can even be totally absent in the highly turbid water columns.

- In moderately turbid "group 2 samples": the bottom contributes to about 6.8% and 9.3% of the total signal recorded at sensor for samples S3-PPD1 and S3-PPD2 respectively. However, the significance of this bottom contribution is limited only to the green waveband domain of the light spectrum especially when the physical depth is greater than 1 m as shown in Fig. 5.6. This case may not be a major problem for bio-optical chlorophyll estimation modeling.

- In low turbidity samples, on the contrary, this case is a major problem for chlorophyll density estimation. In all the testing samples of "group 3" the noise contributed by the bottom substrates amounts to 20% or more of the total signal which is recorded by the spectrometer.

The question is "how accurately the Monte Carlo algorithm developed here un-mixes the contributions of the bottom and the water column radiance components of the testing samples?" The findings clearly suggest the potential positive outcome that could be expected if a more extensive testing with different kinds of bottom substrates were to be carried out.

6.4. Major problems to be encountered in field remote sensing

- The raw spectral data is affected by large amount of noise which is generated by (i) the equipment error including the calibration and un-stability of the light source (ii) the measurement conditions including spectral contamination from sunlight and skylight,

atmospheric conditions, measurement geometry, water surface roughness and bottom reflectance effect

- For the phytoplankton classification, besides the raw data error some additional problems include (i) how to obtain spectral data from pure phytoplankton species and use this information for accurate classification (ii) How to choose the classifier to obtain good discrimination between the species?

- For the chlorophyll density estimation additional problems include (i) the ancillary data measurement error and (ii) the influence from water column constituents such as dissolved substances, suspended sediments, difference in the species in phytoplankton community, and bottom sediments re-suspension problem

6.5. Major findings

Major findins in this research include:

(1) Potentially harmful phytoplankton specimen "*Mycrocystis aerugunosa"* could be discriminated and classified into a separate group of phytoplankton by using simple classifiers. This is an important finding to help manage the eutrophication in shallow lakes and reservoirs by using hyperspectral remote sensing technology. However remaining problems include (i) how to obtain spectral data from pure phytoplankton species and use this information for accurate classification (ii) How to choose the classifier to obtain good discrimination between the species?

(2) The accuracies of classification and chlorophyll density estimation were not enough to support the eutrophication monitoring objectives owing to large amount of error in the raw spectral data. Important problems to be solved include: (i) the ancillary data measurement error and (ii) the influence from water column constituents such as dissolved substances, suspended sediments, difference in the species in phytoplankton community, and bottom sediments re-suspension problem.

Chapter 7

Conclusion and Recommendations

7.1 Conclusions

This research suggests the potential possibility of phytoplankton classification and chlorophyll density estimation by using the hyperspectral remote sensing technology with a limited accuracy.

The classification objective is partially achieved, harmful phytoplankton specimen "*Microcystis aerugunosa*" could be discriminated from other phytoplankton specimens. However, other phytoplankton specimens such as "*Cyanophora tetracyanea"*, "*Chlorella saccharophila"*, and "*Closterium paracerosum"* which have similar spectral characteristics could not be clearly classified by using hyperspectral spectrometer.
The accuracies of specimen classification and their chlorophyll density estimation are still not enough to support the eutrophication monitoring objectives owing to large amount of error in the raw spectral data.

At this stage of the research, the major problems which affect the accuracies of phytoplankton classification and chlorophyll density estimation are delineated and directions are set to solve the problems.

Unless the problems affecting the phytoplankton classification accuracy, the problems affecting the chlorophyll density estimation accuracy and the problem of up-scaling the findings to field remote sensing are solved together, the remote sensing technology will not fit the necessary accuracy for routine use in monitoring of the eutrophication in the shallow lakes and reservoirs.

7.2 Recommendations

7.2.1. Recommendations for future studies

In the future studies it is recommended to:

1) Evaluate the effect of the variation in sun intensity on the spectral data accuracy

2) Evaluate the skylight effect on the spectral data measurement accuracy

3) Evaluate the packaging effect of chlorophyll pigment on the accuracy of chlorophyll density estimation

4) Study the specie-specific variation of chlorophyll density

5) Study the specie-specific variation of optical properties such as the specific absorption and the scattering

6) Evaluate the interference of the water column constituents such as suspended sediments, dissolved organic matter, and yellow substances, on the accuracy of chlorophyll density estimation

7) Evaluate the wind interaction effect resulting in: (i) bottom sediments re-suspension, and (ii) water surface roughness, on the spectral data measurement accuracy

8) Evaluate the bottom effect on the spectral data measurement accuracy

9) Evaluate the costs of tertiary wastewater treatment and the cost of eutrophication monitoring by using hyperspectral remote sensing technology

7.2.2 Recommendation for capacity building in the developing countries

How can this study contribute to capacity building in the developing countries?
This study involves important aspects of eutrophication control using eco-engineering techniques, which are known to be environmentally friendly and cost effective and easy to apply. remote sensing is only a tool to help manage eutrophication at large scale. About 80% time and efforts were spent on eco-engineering aspect whereby important skills are learnt including (1) water and phytoplankton sampling techniques in freshwater systems, (2) phytoplankton identification and cell counting by using light microscope (3) chlorophyll extraction and its density estimation in laboratory (4) phytoplankton culturing techniques and in-situ measurement of chlorophyll to estimate algae biomass.

These techniques can be used for eutrophication monitoring and control without special requirement as needed by the remote sensing technology which is for the time being difficult to apply in the developing countries.

Japan International Cooperation Agency (JICA) capacity building program has a good framework. JICA has a long tradition of organizing specialized training courses and on the job training, both in developed and developing countries for the purpose of capacity building.

These training programs promote formal linkage and experience sharing among agencies in touch with water resources and environmental management in arid region. The eco-engineering aspect of this study can be used within the framework of JICA cooperation network.

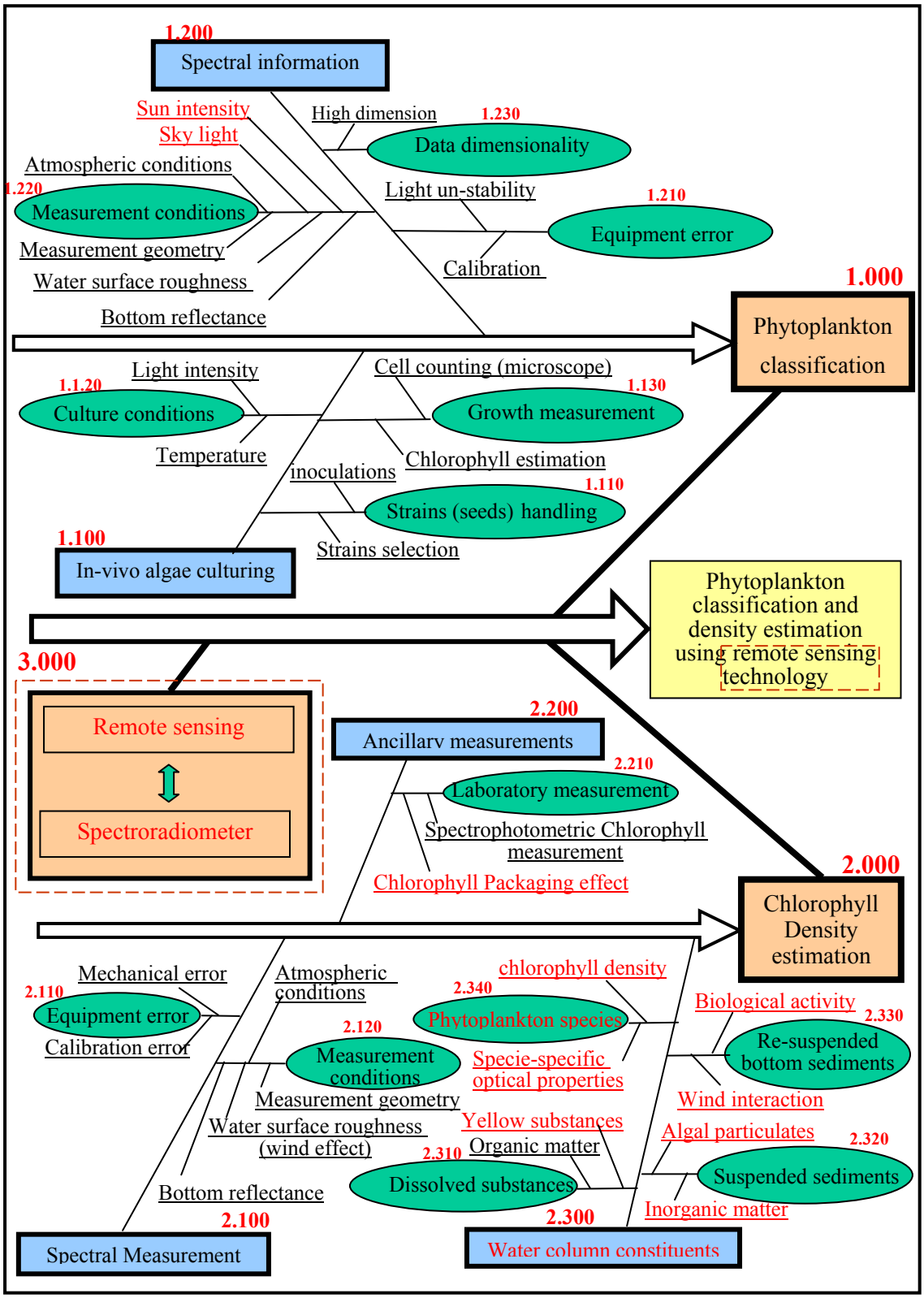

Fig. 7.1 Problems to be researched in future study

References

Alberotanza L., 1986, *'The Use of Remote Sensors to Investigate Optical and Biological Characteristics of Lagoon Waters: Monitoring to Detect Changes in Water Quality Series'*, Proceedings of Budapest Symposium, IAHS Publ. 157.

Arar, E.J., 1994, '*Evaluation of a new fluorometric technique that uses highly selective interference filters for measuring chlorophyll a in the presence of chlorophyll b and pheopigments*.' USEPA Summary Report.

Axler, R.P., and Owen, C.J., 1994, '*Measuring chlorophyll and pheophytin: Whom should you believe?'* Lake and Reserv. Manage. 8(2): 143-151.

Baker, K.S., 1983, '*Chlorophyll determinations with filter fluorometer: Lamp/filter combination can minimize error'*. Limnol. Oceanogr. 28(5): 1037-1040.

Barale V., and Bergamasco A., 1984, *'Nimbus 7 CZCS images as inputs in circulation modelling of the North Adriatic Sea',* : 1st Congresso, Gruppo Nazionale per la Fisica dell'Atmosfera e dell'Oceano, Rome, Italy, June 19--22, 1984. Nuovo Cimento C, Serie 1, 8 C, 621-630.

Bidigare, R.R., Morrow, J.H., and Kiefer, D.A., 1989, '*Derivative Analysis of Spectral Absorption by Photosynthetic Pigments in the Western Sargasso Sea'*. Journal of Marine Research, 47: 323-341.

Bidigare, R.R., Ondrusek, M.E., Morrow, J.H. and Kiefer, D.A., 1990, '*In-vivo absorption properties of algal pigments'*. SPIE Ocean Optics X, 1302: 290-302.

Butler, W. L., Hopkins, D. W., 1970, '*Higher Derivative Analysis of Complex Absorption Spectra'*, Photochemistry and Photobiology, 12:439-450.

Carlson, R.E., 1977, '*A trophic state index for lakes*.' Limnology and Oceanography. 22:361-369

Carlson, Robert E., 1991, '*Expanding the Trophic State Concept to Identify Non-Nutrient Limited Lakes and Reservoirs'*. Enhancing the States' Lake Management Programs, p. 59-71.

Cullen, J.J., A.M. Ciotti, R.F. Davis, M.R. Lewis, 1997, *'Optical detection and assessment of algal blooms'*. Limnol. Oceanogr. 42(5): 1223-1239.

Doerffer ,R., and Fischer, J., 1994, *'Concentrations of chlorophyll, suspended matter, and gelbstoff in case II waters derived from satellite coastal zone color scanner data with inverse modeling methods'*, J. Geophys. Res. 99, 7457-7466,

Evans, C.A., J.E. O'Reilly,1983, '*A Handbook for the Measurement of Chlorophyll a in Netplankton and Nannoplankton'*. Biomass Handbook No.9. N.O.A.A

Fairchild, J.F., Ruessler, D.S., and Carlson. A.R., 1998, '*Comparative sensitivity of five species of macrophytes and six species of algae to atrazine, metribuzin, alachlor, and metolachlor'*. Environ Toxicol Chem. 17(9): 1830-1834.

Goulder, R., 1969, '*Interactions between the rates of production of a freshwater macrophyte and phytoplankton in a pond*'. Oikos, 20, 300-309.

Holligan, P.M., 1983, '*Satellite Studies on the Distribution of Chlorophyll and Dinoflagellate Blooms in the Western English Channel'*. Cont. Shelf Res. 2(2-3):81-96.

Holm-Hansen O., Lorenzen, C.J., Holmes, R.W., Strickland. J.D., 1965, '*Fluorometric Determination of Chlorophyll.'* J. Cons. Int. Explor. 30: 3-15.

Kiefer, D. A., Chamberlin, W. S., and Booth. C. R., 1989, '*Natural fluorescence of chlorophyll a: relationship to photosynthesis and chlorophyll concentration in the western South Pacific gyre'*. Limnology and Oceanography, 34: 868-881.

Kishino, M. Ishizaka J., Satoh H., Kusaka K., Saitoh S., Miyoi T., and Kawasaki, K., 1996, '*Optical characteristics of seawater in the North Pacific Ocean*.' SPIE Ocean Optics XIII, 2963: 173-178. (MER-2020, 2040)

Kishino, M., Booth, C.R., Okami, N., 1984, '*Underwater radiant energy absorbed by phytoplankton, detritus, dissolved organic matter and pure water'*. Limnology and Oceanography, 29(2): 340-349.

Kiyosawa, H.,. Ishizaka, J Takahashi M. Ishikawa K., 1995, '*Methods of Estimating Biomass Structure of Pelagic Plankton Community - Methods for Northwest Pacific Carbon Cycle Study'* J.NIRE, 4(1): 87-103 (in Japanese with English abstract).

Lorenzen, C.J., 1970, Surface chlorophyll as an index of the depth, chlorophyll content, and primary productivity of the euphotic layer. Limnol. Oceanogr. 15:479-480.

Marra, J., Dickey T., Chamberlin W., Ho C., Granata T., Kiefer, D., Langdon C, Smith R., Baker, K., Bidigare, R. and Hamilton M., 1992, *'The estimation of seasonal primary production from moored optical sensors in the Sargasso Sea*'. Journal of Geophysical Research 97: 7399-7412.

Mayer, P., R. Cuhel, N. Nyholm., 1997, '*A simple in vitro fluorescence method for biomass measurements in algal growth inhibition tests*'. Water Research 13(10):2525-2531.

Mjelde, M. and Faafeng, B.A., 1997, *'Ceratophyllum demersum hampers phytoplankton development in some small Nowegian lakes over a wide range of phosphorous level and geographic latitude,'* in E. Jeppesen, M. Sondergaard, and K. Chrostoffersen (eds.) The restructuring role of submerged macrophytes in lakes, Springer Verlag, New York.

Moore, L. and K. Thornton, 1988, *'Lake and Reservoir Restoration Guidance Manual.'* USEPA. EPA 440/5-88-002.

Olson, R.J., A.M. Chekalyuk, H.M. Sosik, 1996, *'Phytoplankton photosynthetic characteristics from fluorescence induction assays of individual cells'*. Limnol. Oceanogr. 41(6): 1253-1263.

Paasche, E., 1973, *'Silicon and the ecology of marine plankton diatoms. I: Thalassiosira pseudonana (Cyclotella nana) grown in a chemostat with silicate as limiting nutrient.'* Marine Biology 19(2):117-126.

Reed, R.E., Kirkpatrik G.J., Kamykowski, D., 1996, *'Short-period photophysiological responses of Thalassiosira pseudonana during photoacclimation to near-surface irradiance'*. SPIE Ocean Optics XIII, 2963: 514-519.

ReVelle, P., C. ReVelle, 1988, '*The Environment: Issues and Choices for Society*.' 3rd. ed. Jones and Bartlett Publishers. Boston. 749pp.

Richerson, P.J., Li, X., Meillier, L.M., 1998, *'Algal Biomass Monitoring Manual: Determination of algal biomass using a field fluorometric method in Clear Lake, California'*. Prepared by UCD-CLERC.

Scheffer, M., 1998, '*Ecology of shallow lakes*'. Kluwer Academic Publishers, Netherlands. pp. 357.

Scheffer, M., Rinaldi, S., Gragnani, A., Mur, L.R. and Van Nes, E.H., 1997, '*On the dominance of filamentous cyanobacteria in shallow turbid lakes*'. Ecology, 78: 272-282.

Smith, W. H., Jr., L. A. Codispoti, D. M. Nelson, T. Manley, E. J. Buskey, H. J. Niebauer and G. F. Cota, 1991, *'Importance of Phaeocystis blooms in the high-latitude ocean carbon cycle'*. Nature 352(6335):514-516.

Smith, W. O., Jr. and D. M. Nelson, 1990, *'Phytoplankton growth and new production in the Weddell Sea marginal ice zone in the austral spring and autumn'*. Limnol. Oceanogr. 35:809-821.

Stramski D, Sciandra A, Claustre H (2002) *Variations in the optical properties of the marine diatom Thalassiosira pseudonana induced by various sources of growth limitation*. Limnol. Oceanogr. 47:00-00

U.S. Environmental Protection Agency, 1999, *'California Scientists Develop Water Monitoring System.'* Nonpoint Source News-Notes, 58:16-17.

US Environmental Protection Agency, 1998, '*National Strategy for the development of regional nutrient criteria.*' EPA-822-R-98-002.

US Environmental Protection Agency, 2000, '*National Water Quality Inventory: 1998 Report to Congress*.' www.epa.gov/305b/98report Last updated October 5 2000.

Vyhnalek, V., Z. Fisar, A. Fisarova, J. Komarkova, 1993, *'In-vivo fluorescence of chlorophyll a: estimation of phytoplankton biomass and activity in Rimov Resevoir(Czech Republic).'* Wat. Sci. Tech. 28: 29-33.

Welschmeyer, N.A, 1994, *'Fluorometric analysis of chlorophyll a in the presence of chlorophyll b and pheopigments'*. Limnol. Oceanogr. 39(8): 1985-1992.

Yentsch, C.S. and D.W. Menzel, 1963, *'A method for the determination of phytoplankton chlorophyll and pheophytin by fluorescence.'* Deep-Sea Res. 10: 221-231.

Appendices

Appendix A: Regression models for chlorophyll estimation showing the diversion of the band ratio data relative to the total slope of the regression line along with the confidence interval of estimation

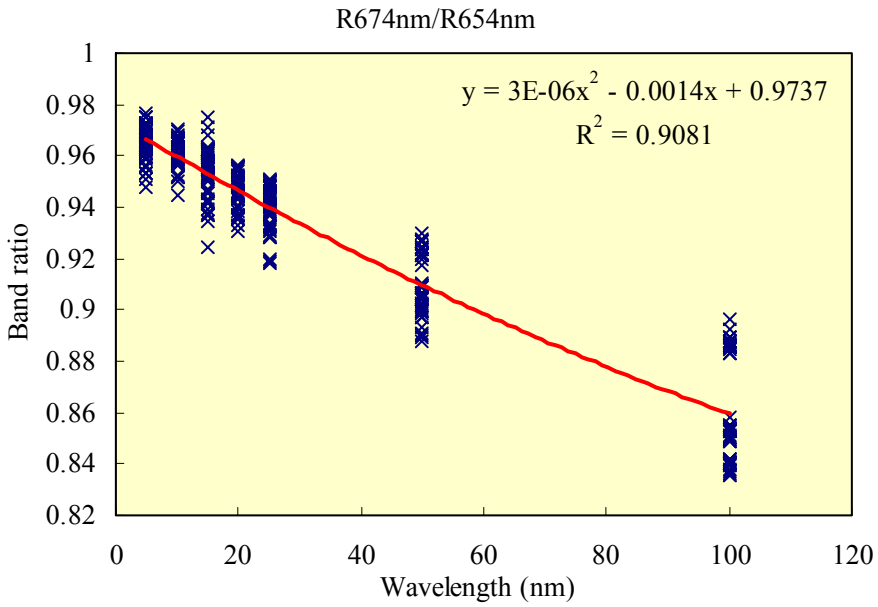

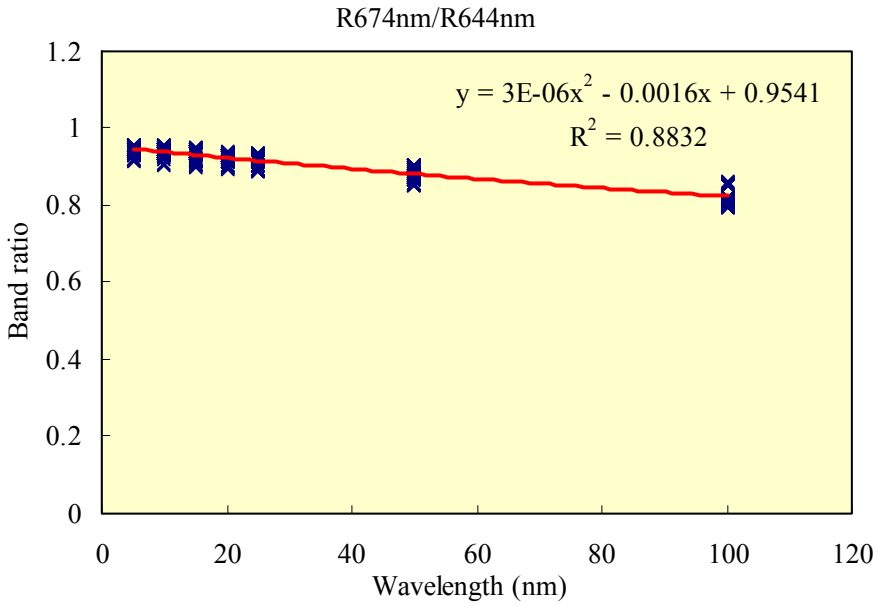

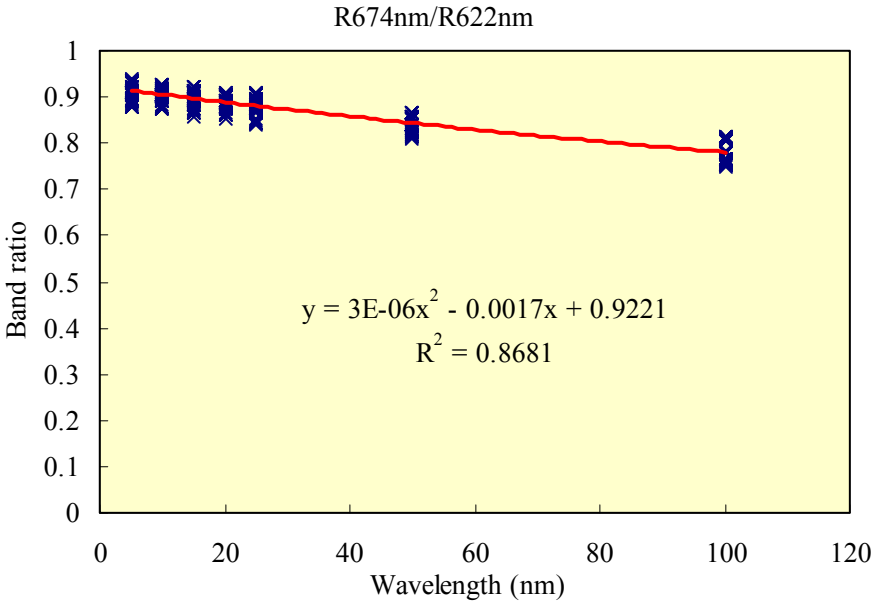
R674nm/R622nm
Band ratio
Wavelength (nm)
y = 3E-06x2 - 0.0017x + 0.9221
R2 = 0.8681
0
0.1
0.2
0.3
0.4
0.5
0.6
0.7
0.8
0.9
1
0
20
40
60
80
100
120

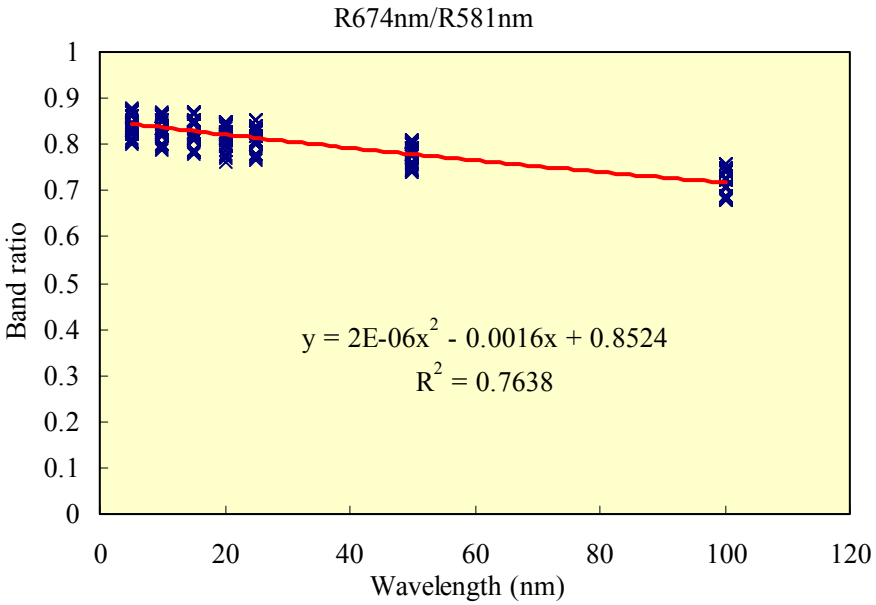
R674nm/R581nm
Band ratio
Wavelength (nm)
y = 2E-06x2 - 0.0016x + 0.8524
R2 = 0.7638
0
0.1
0.2
0.3
0.4
0.5
0.6
0.7
0.8
0.9
1
0
20
40
60
80
100
120

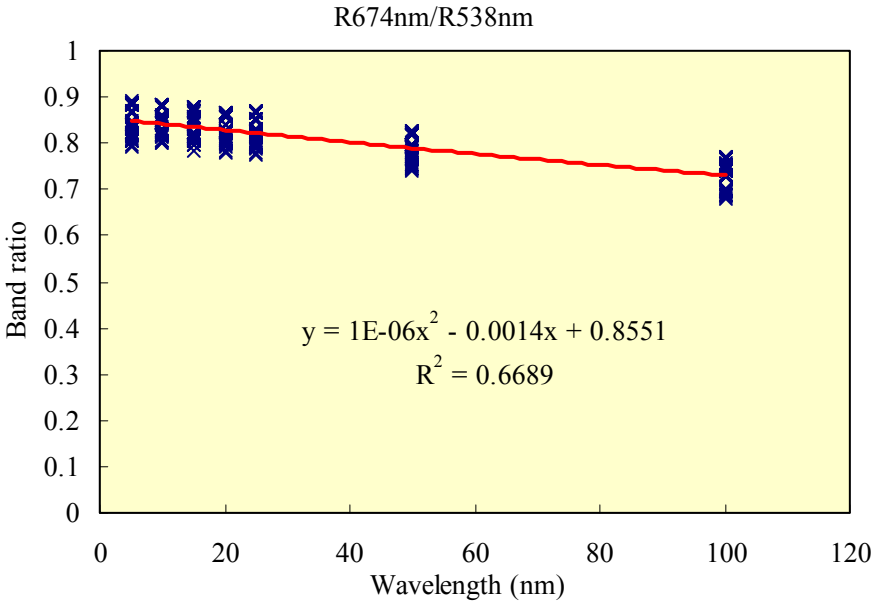
R674nm/R538nm
Band ratio
Wavelength (nm)
y = 1E-06x2 - 0.0014x + 0.8551
R2 = 0.6689
0
0.1
0.2
0.3
0.4
0.5
0.6
0.7
0.8
0.9
1
0
20
40
60
80
100
120

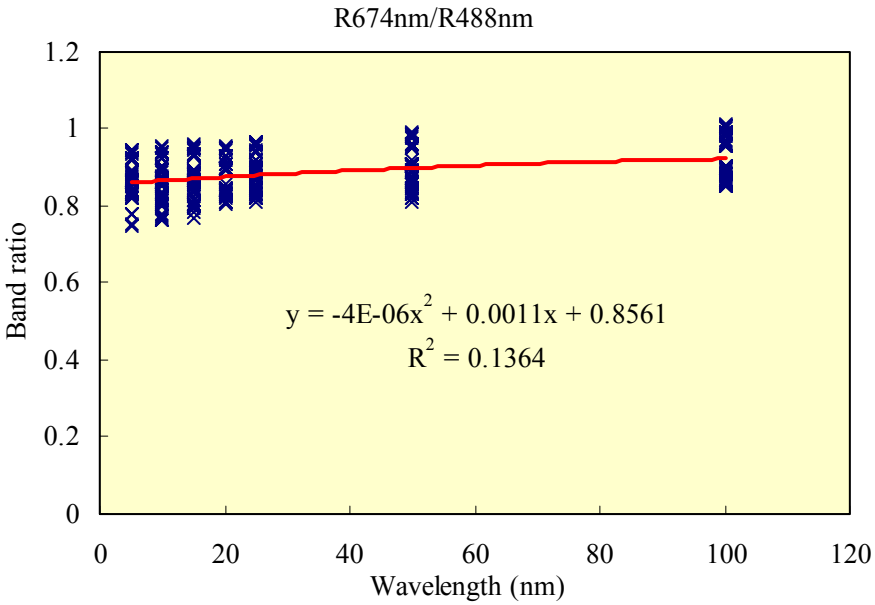
R674nm/R488nm
Band ratio
Wavelength (nm)
y = -4E-06x2 + 0.0011x + 0.8561
R2 = 0.1364
0
0.2
0.4
0.6
0.8
1
1.2
0
20
40
60
80
100
120

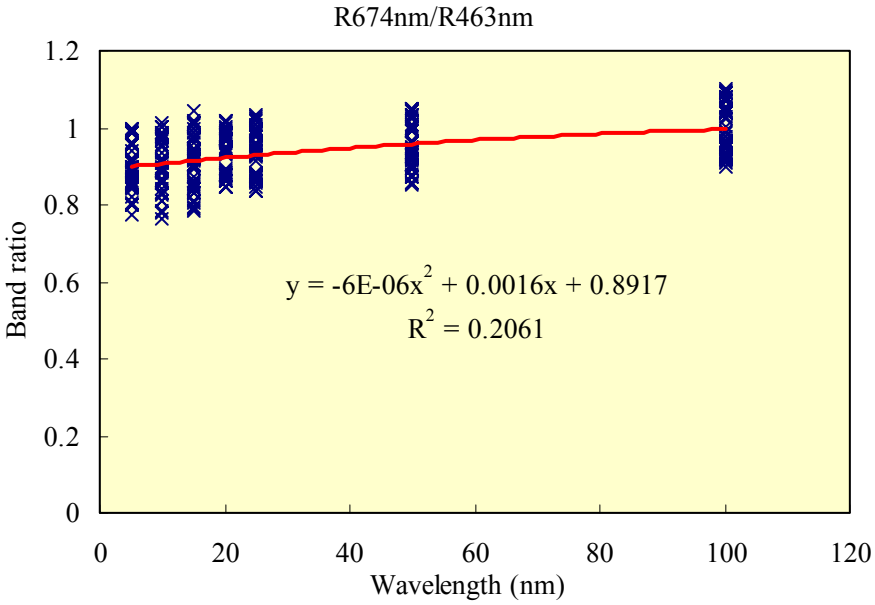
R674nm/R463nm
Band ratio
Wavelength (nm)
y = -6E-06x2 + 0.0016x + 0.8917
R2 = 0.2061
0
0.2
0.4
0.6
0.8
1
1.2
0
20
40
60
80
100
120

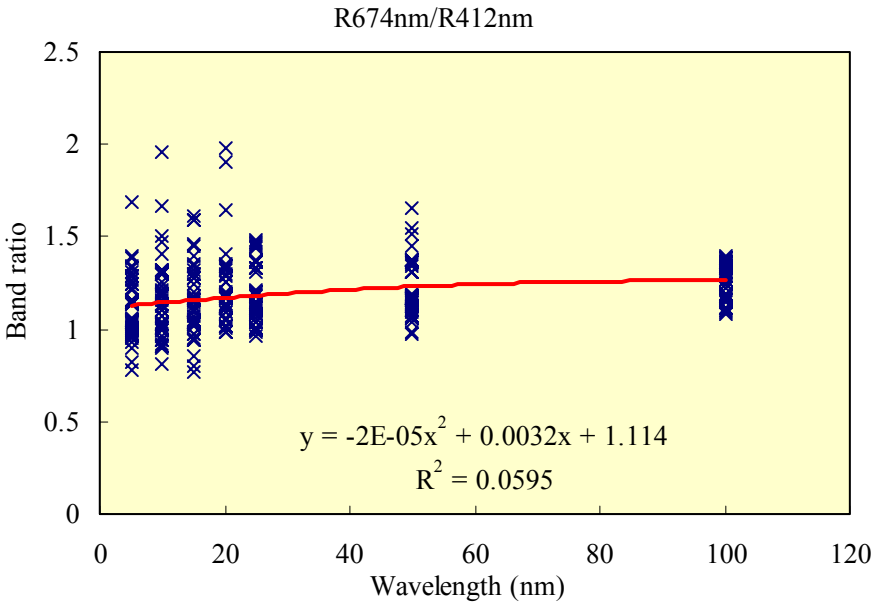
R674nm/R412nm
Band ratio
Wavelength (nm)
y = -2E-05x2 + 0.0032x + 1.114
R2 = 0.0595
0
0.5
1
1.5
2
2.5
0
20
40
60
80
100
120

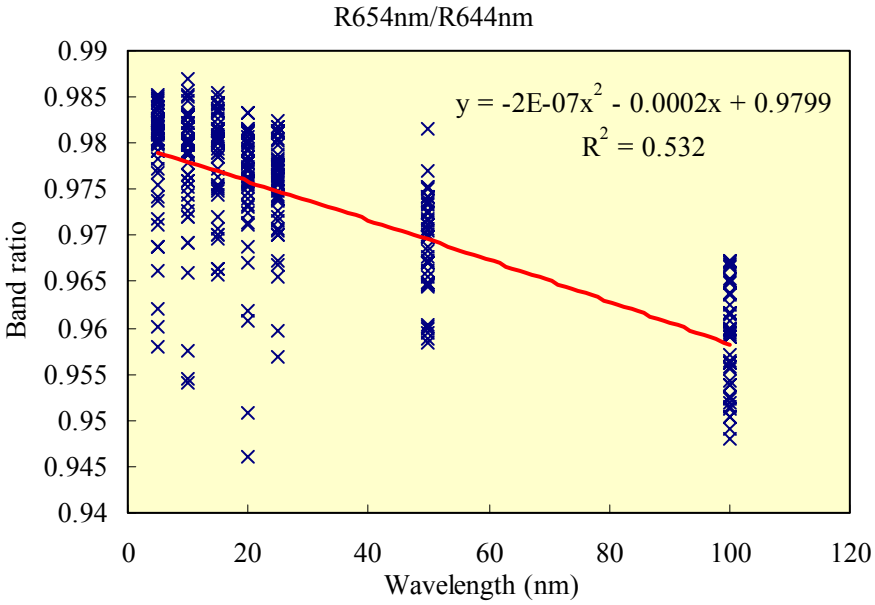
R654nm/R644nm
y = -2E-07x^2 - 0.0002x + 0.9799
R^2 = 0.532
Band ratio
Wavelength (nm)
0.99
0.985
0.98
0.975
0.97
0.965
0.96
0.955
0.95
0.945
0.94
0
20
40
60
80
100
120

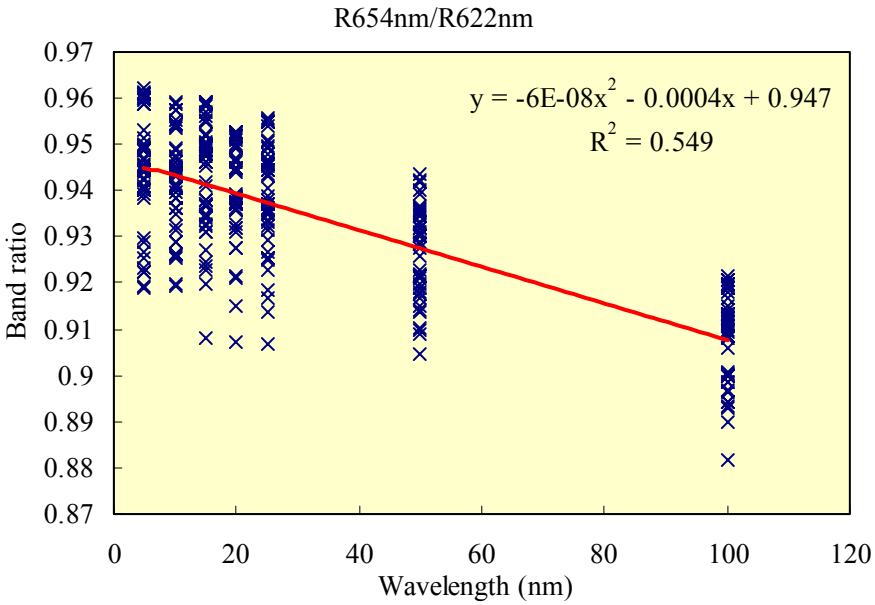
R654nm/R622nm
y = -6E-08x^2 - 0.0004x + 0.947
R^2 = 0.549
Band ratio
Wavelength (nm)
0.97
0.96
0.95
0.94
0.93
0.92
0.91
0.9
0.89
0.88
0.87
0
20
40
60
80
100
120

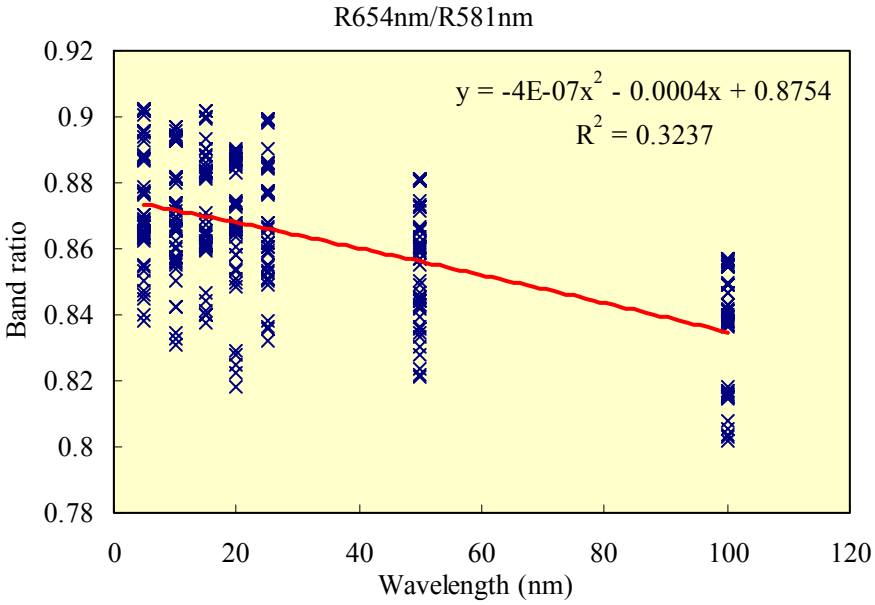
R654nm/R581nm
y = -4E-07x2 - 0.0004x + 0.8754
R2 = 0.3237
Band ratio
Wavelength (nm)
0.92
0.9
0.88
0.86
0.84
0.82
0.8
0.78
0
20
40
60
80
100
120

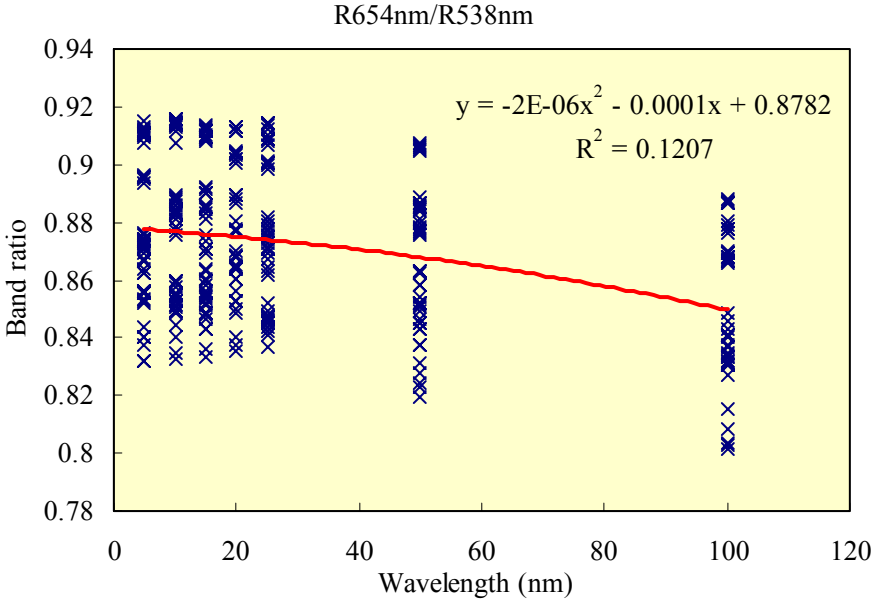
R654nm/R538nm
y = -2E-06x2 - 0.0001x + 0.8782
R2 = 0.1207
Band ratio
Wavelength (nm)
0.94
0.92
0.9
0.88
0.86
0.84
0.82
0.8
0.78
0
20
40
60
80
100
120

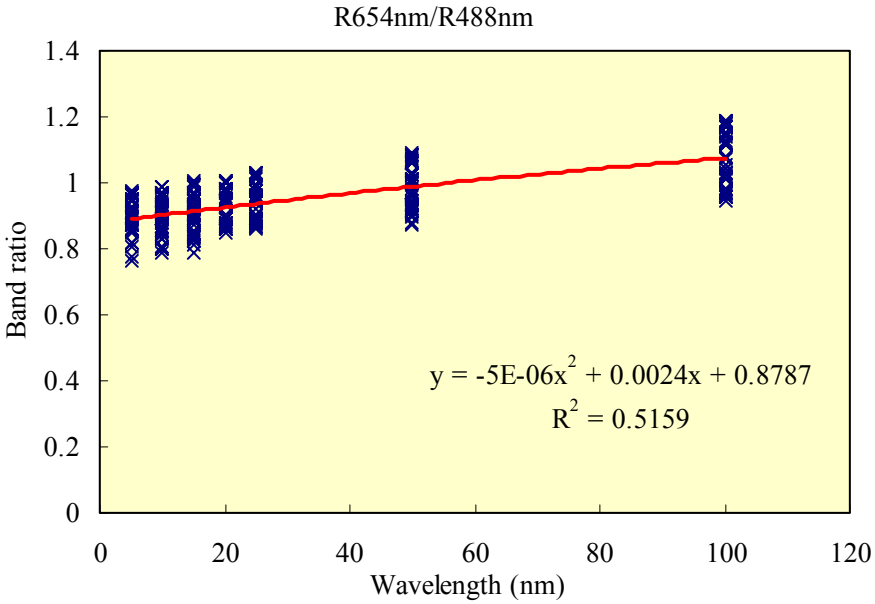
R654nm/R488nm
Band ratio
Wavelength (nm)
y = -5E-06x2 + 0.0024x + 0.8787
R2 = 0.5159
0
0.2
0.4
0.6
0.8
1
1.2
1.4
0
20
40
60
80
100
120

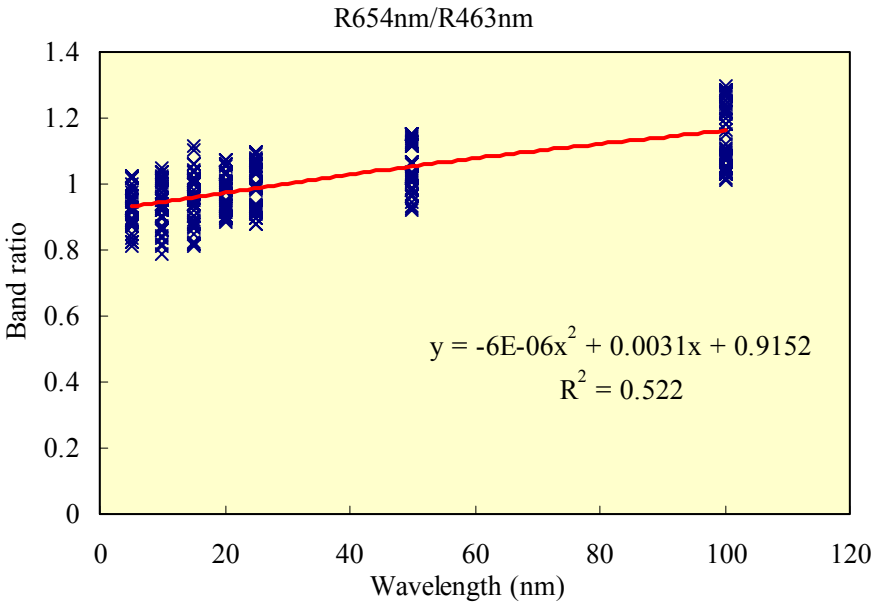
R654nm/R463nm
Band ratio
Wavelength (nm)
y = -6E-06x2 + 0.0031x + 0.9152
R2 = 0.522
0
0.2
0.4
0.6
0.8
1
1.2
1.4
0
20
40
60
80
100
120

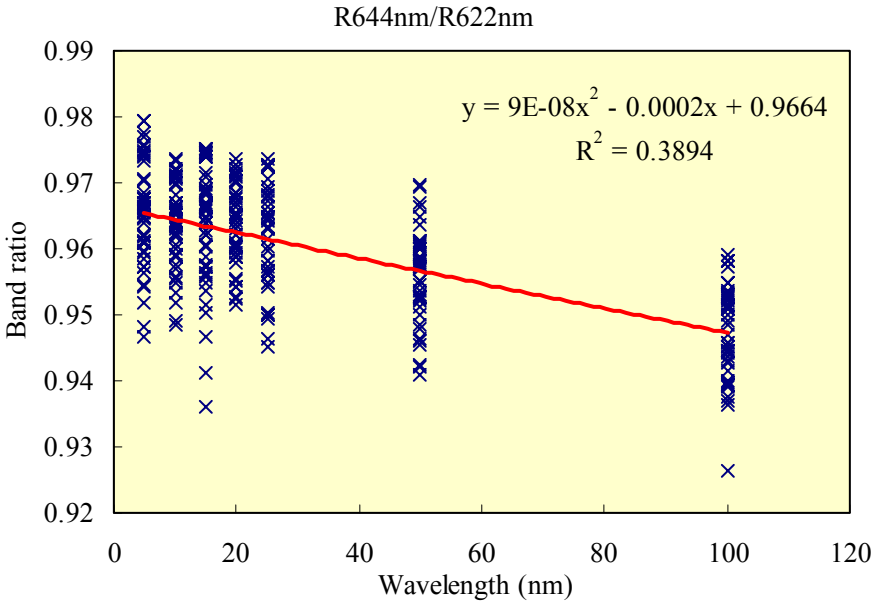
R644nm/R622nm
y = 9E-08x2 - 0.0002x + 0.9664
R2 = 0.3894
Band ratio
Wavelength (nm)
0.99
0.98
0.97
0.96
0.95
0.94
0.93
0.92
0
20
40
60
80
100
120

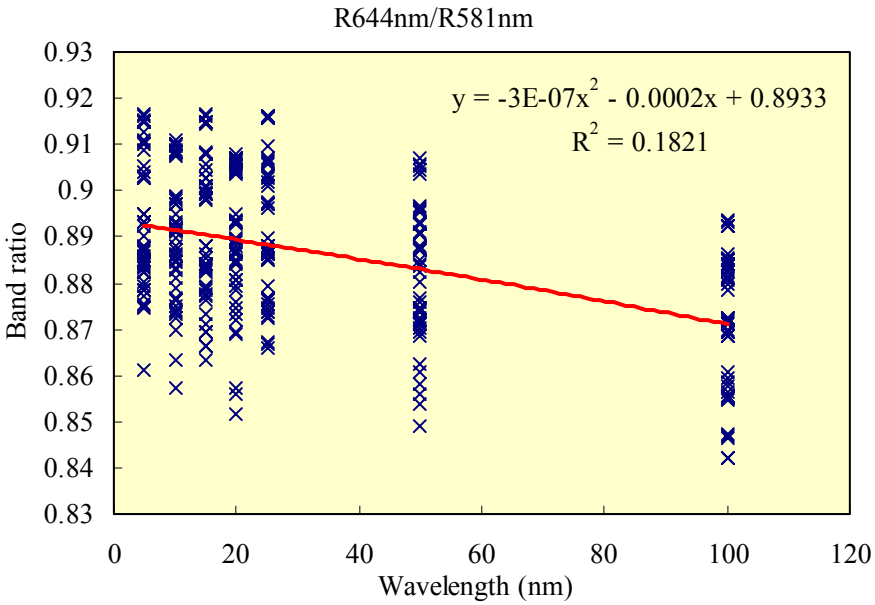
R644nm/R581nm
y = -3E-07x2 - 0.0002x + 0.8933
R2 = 0.1821
Band ratio
Wavelength (nm)
0.93
0.92
0.91
0.9
0.89
0.88
0.87
0.86
0.85
0.84
0.83
0
20
40
60
80
100
120

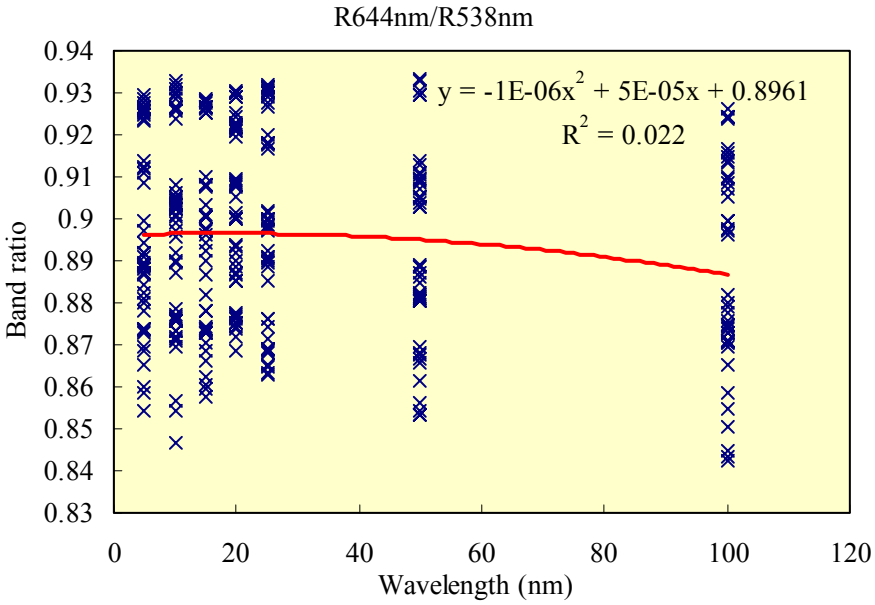
R644nm/R538nm
y = -1E-06x2 + 5E-05x + 0.8961
R2 = 0.022
Band ratio
Wavelength (nm)
0.94
0.93
0.92
0.91
0.9
0.89
0.88
0.87
0.86
0.85
0.84
0.83
0
20
40
60
80
100
120

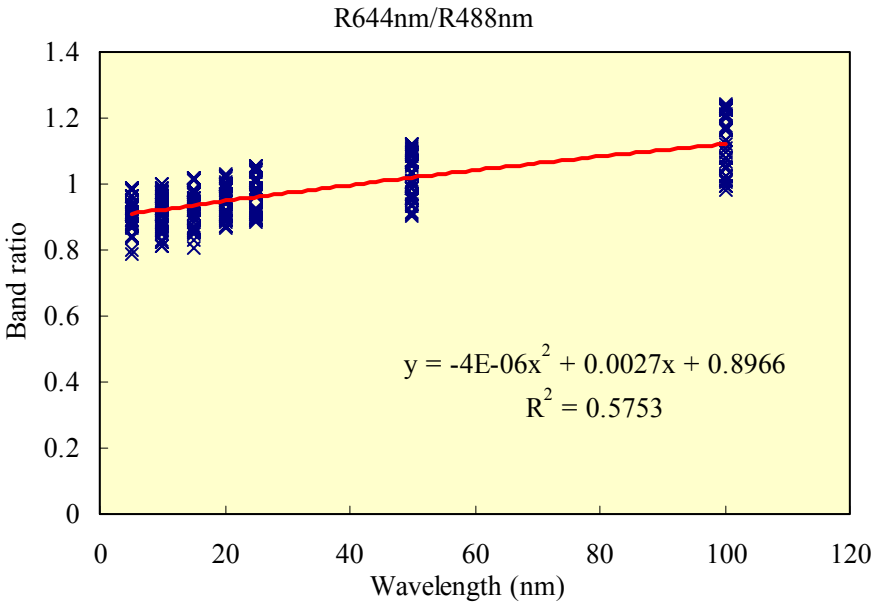
R644nm/R488nm
y = -4E-06x2 + 0.0027x + 0.8966
R2 = 0.5753
Band ratio
Wavelength (nm)
1.4
1.2
1
0.8
0.6
0.4
0.2
0
0
20
40
60
80
100
120

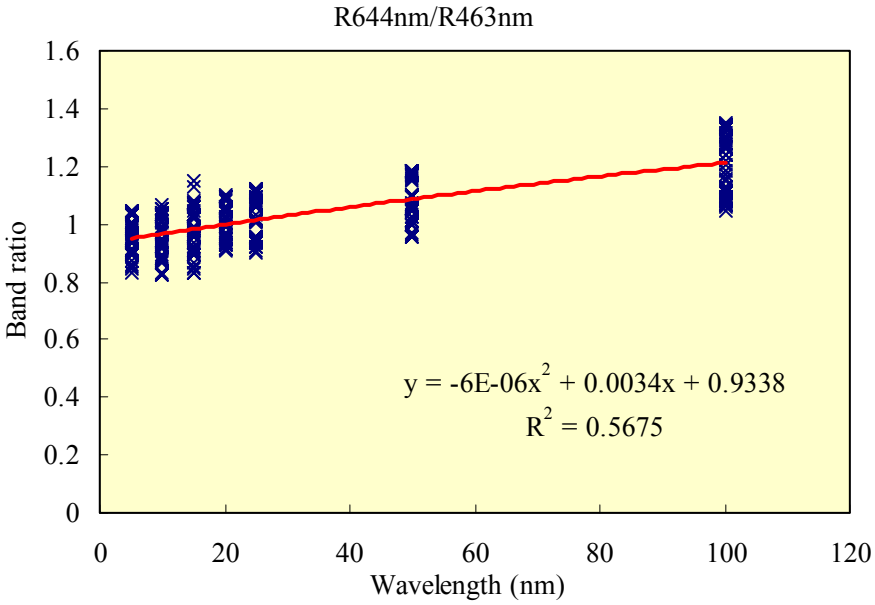
R644nm/R463nm
Band ratio
Wavelength (nm)
y = -6E-06x2 + 0.0034x + 0.9338
R2 = 0.5675
0
0.2
0.4
0.6
0.8
1
1.2
1.4
1.6
0
20
40
60
80
100
120

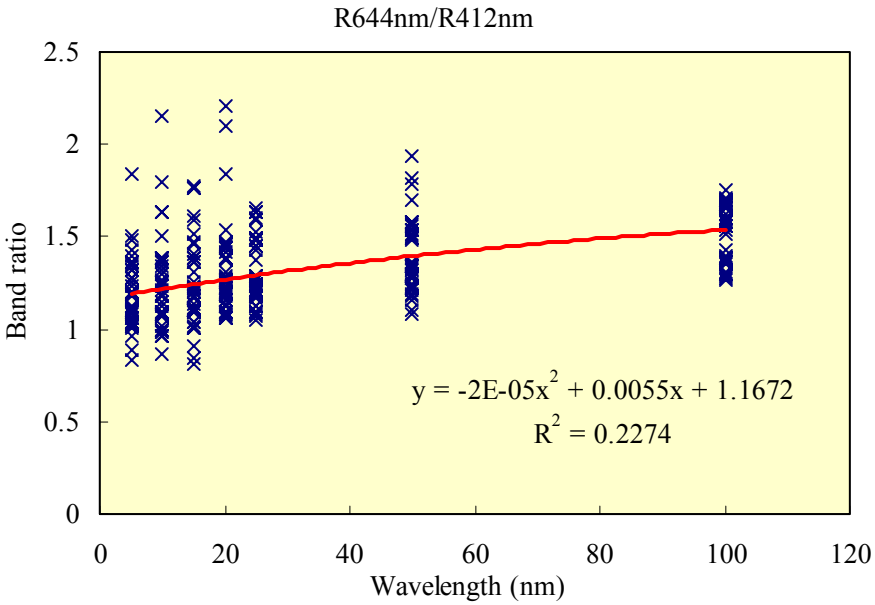
R644nm/R412nm
Band ratio
Wavelength (nm)
y = -2E-05x2 + 0.0055x + 1.1672
R2 = 0.2274
0
0.5
1
1.5
2
2.5
0
20
40
60
80
100
120

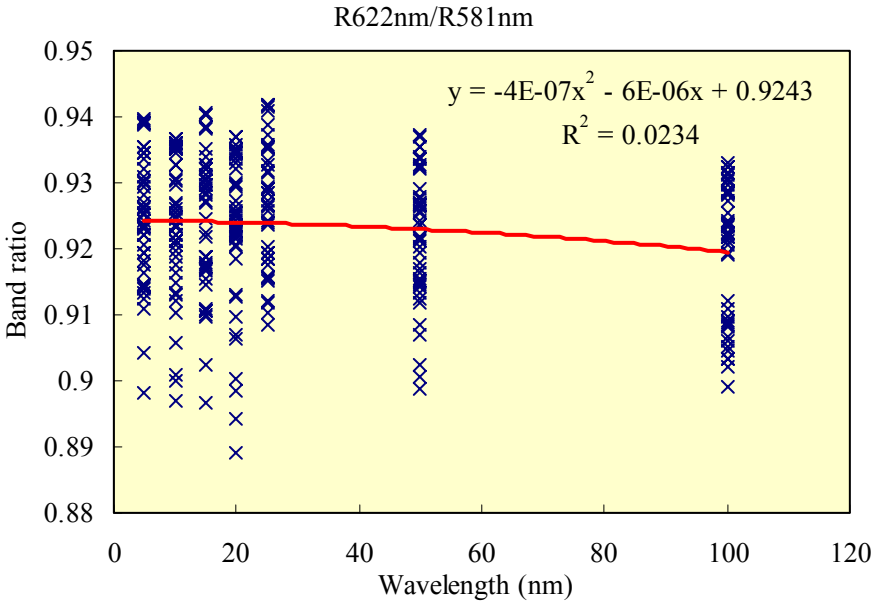
R622nm/R581nm
y = -4E-07x2 - 6E-06x + 0.9243
R2 = 0.0234
Band ratio
0.95
0.94
0.93
0.92
0.91
0.9
0.89
0.88
0
20
40
60
80
100
120
Wavelength (nm)

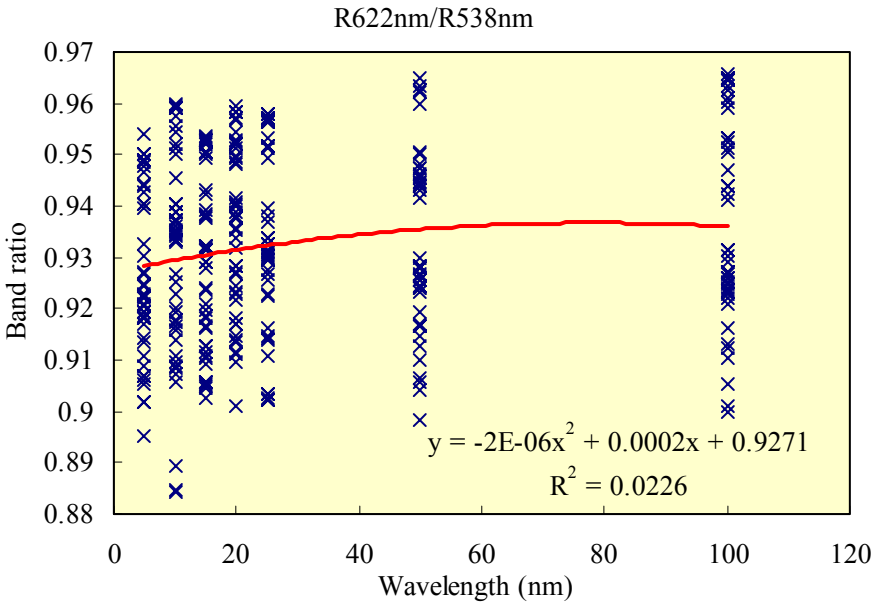
R622nm/R538nm
y = -2E-06x2 + 0.0002x + 0.9271
R2 = 0.0226
Band ratio
0.97
0.96
0.95
0.94
0.93
0.92
0.91
0.9
0.89
0.88
0
20
40
60
80
100
120
Wavelength (nm)

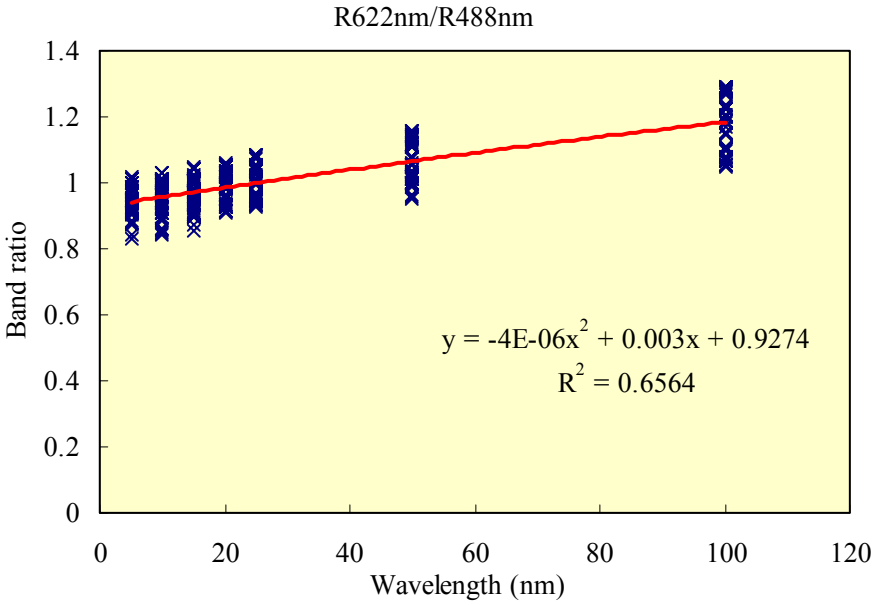
R622nm/R488nm
Band ratio
Wavelength (nm)
y = -4E-06x2 + 0.003x + 0.9274
R2 = 0.6564
0
0.2
0.4
0.6
0.8
1
1.2
1.4
0
20
40
60
80
100
120

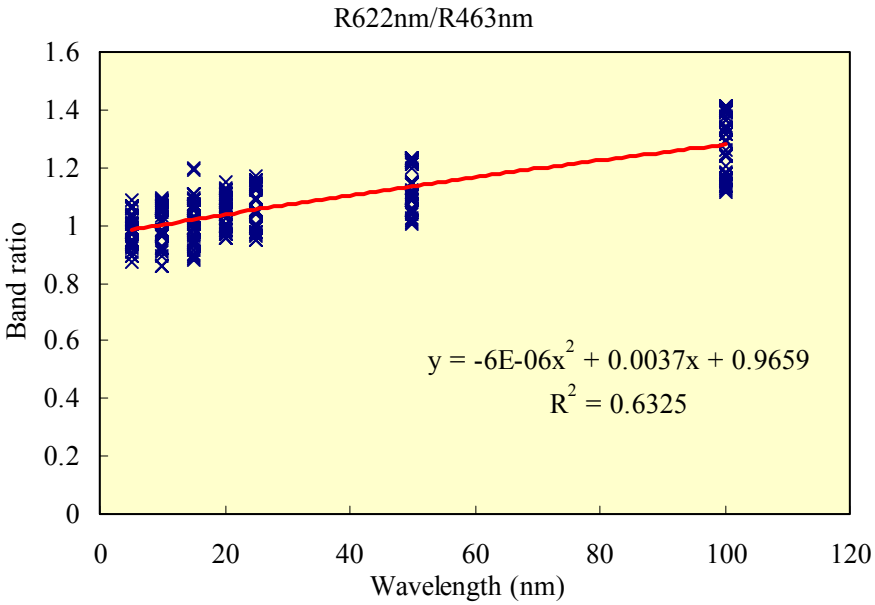
R622nm/R463nm
Band ratio
Wavelength (nm)
y = -6E-06x2 + 0.0037x + 0.9659
R2 = 0.6325
0
0.2
0.4
0.6
0.8
1
1.2
1.4
1.6
0
20
40
60
80
100
120

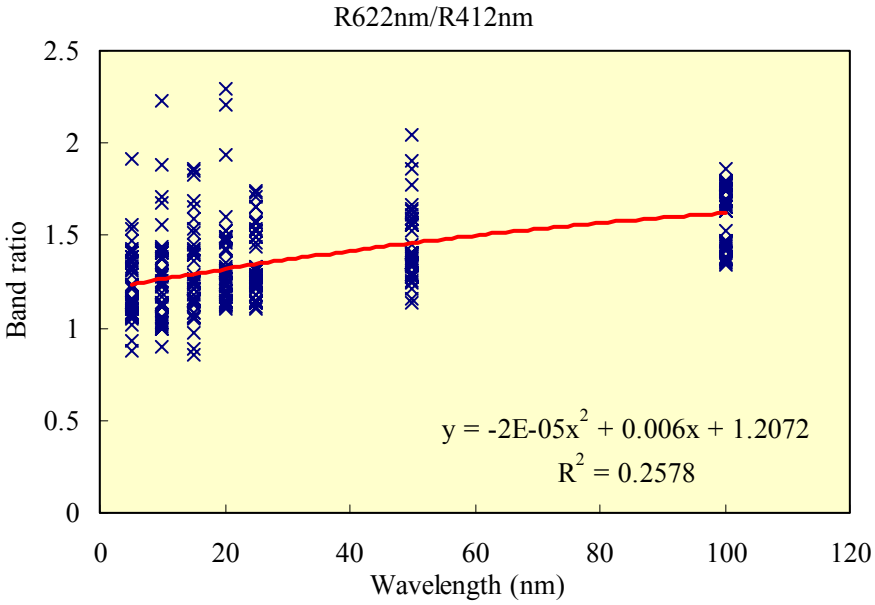
R622nm/R412nm
Band ratio
Wavelength (nm)
y = -2E-05x2 + 0.006x + 1.2072
R2 = 0.2578
0
0.5
1
1.5
2
2.5
0
20
40
60
80
100
120

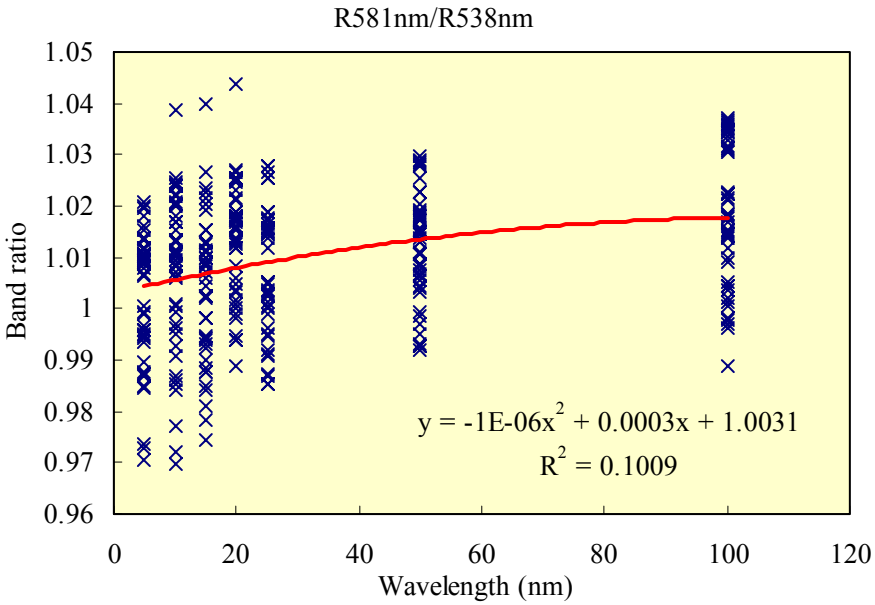
R581nm/R538nm
Band ratio
Wavelength (nm)
y = -1E-06x2 + 0.0003x + 1.0031
R2 = 0.1009
0.96
0.97
0.98
0.99
1
1.01
1.02
1.03
1.04
1.05
0
20
40
60
80
100
120

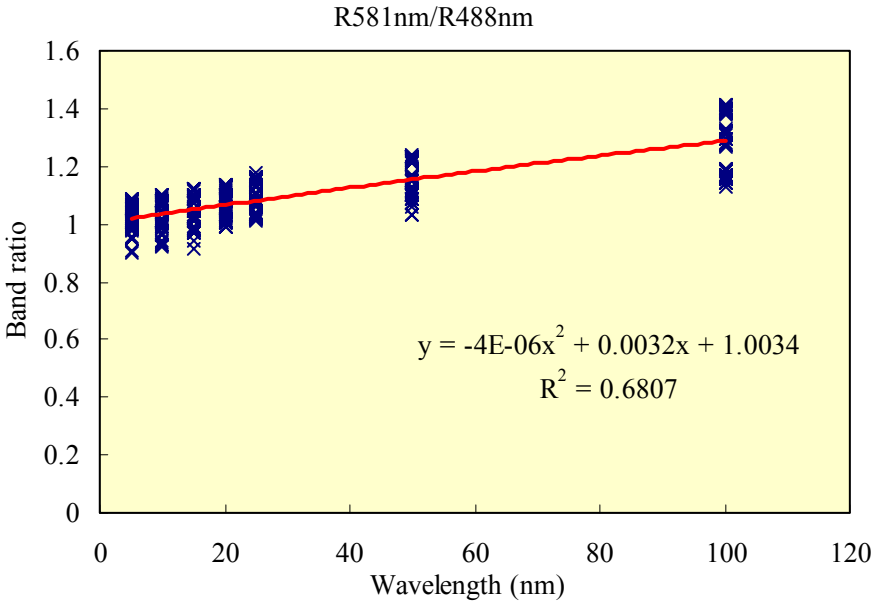
R581nm/R488nm
Band ratio
Wavelength (nm)
y = -4E-06x2 + 0.0032x + 1.0034
R2 = 0.6807
0
0.2
0.4
0.6
0.8
1
1.2
1.4
1.6
0
20
40
60
80
100
120

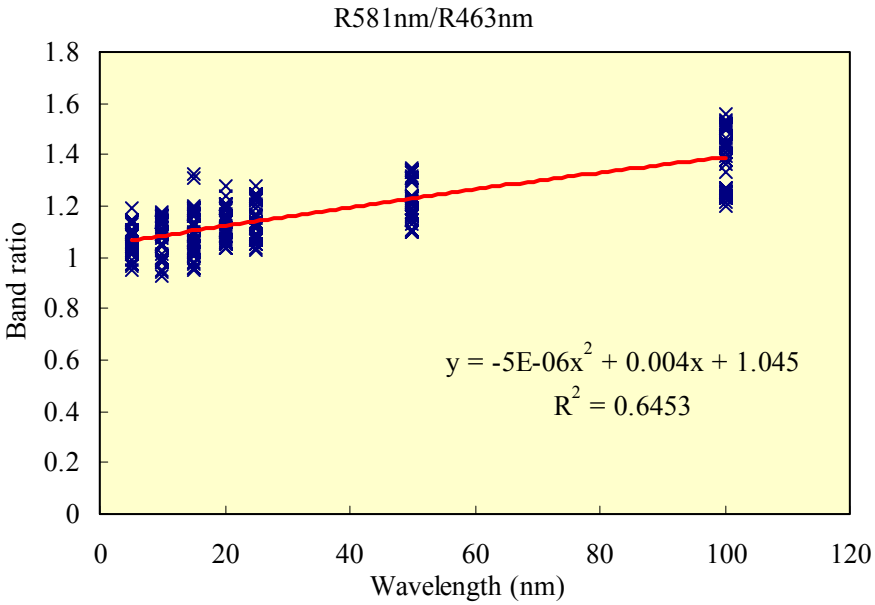
R581nm/R463nm
Band ratio
Wavelength (nm)
y = -5E-06x2 + 0.004x + 1.045
R2 = 0.6453
0
0.2
0.4
0.6
0.8
1
1.2
1.4
1.6
1.8
0
20
40
60
80
100
120

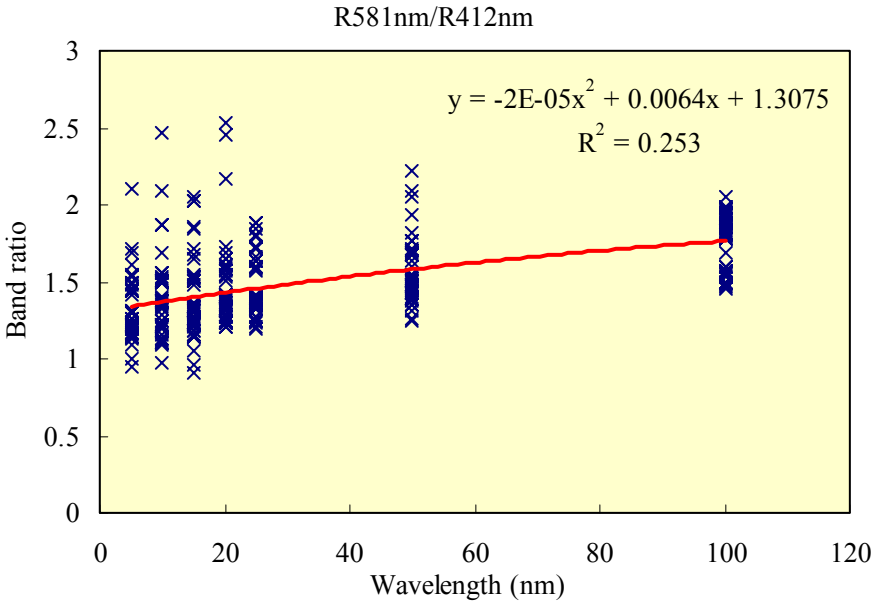
R581nm/R412nm
y = -2E-05x2 + 0.0064x + 1.3075
R2 = 0.253
Band ratio
Wavelength (nm)
0
0.5
1
1.5
2
2.5
3
0
20
40
60
80
100
120

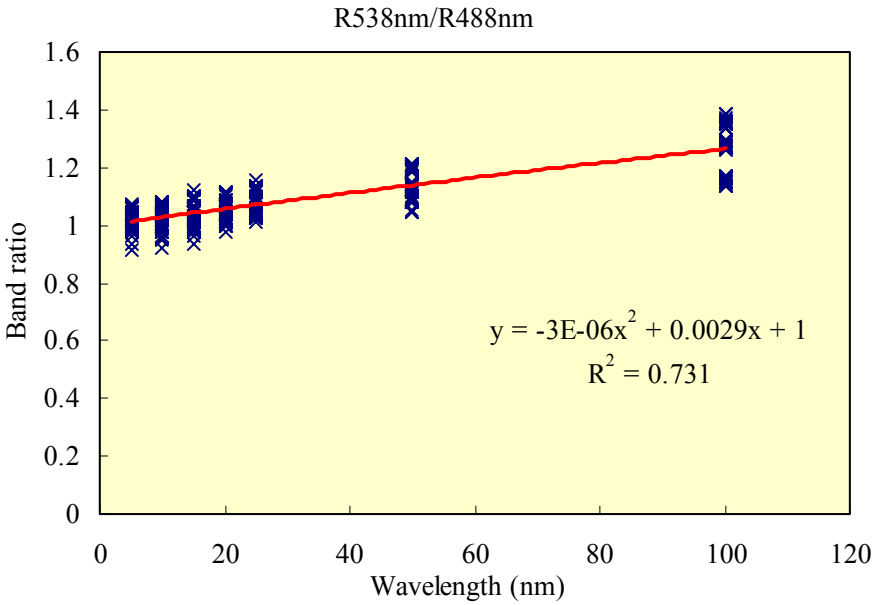
R538nm/R488nm
y = -3E-06x2 + 0.0029x + 1
R2 = 0.731
Band ratio
Wavelength (nm)
0
0.2
0.4
0.6
0.8
1
1.2
1.4
1.6
0
20
40
60
80
100
120

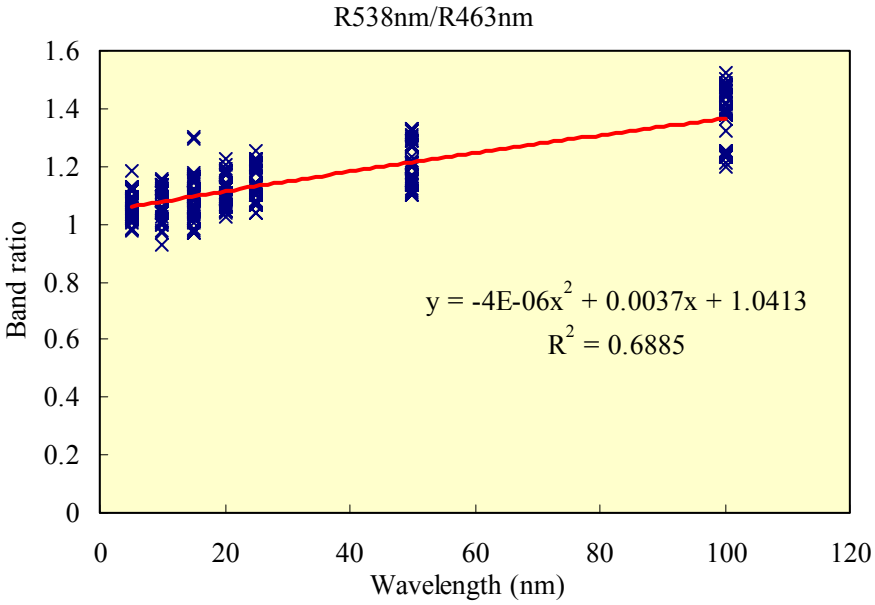
R538nm/R463nm
Band ratio
Wavelength (nm)
y = -4E-06x2 + 0.0037x + 1.0413
R2 = 0.6885
0
0.2
0.4
0.6
0.8
1
1.2
1.4
1.6
0
20
40
60
80
100
120

Appendix B: Mathematical equations used to develop Monte Carlo algorithm

Rational of Monte Carlo Modeling:

Monte Carlo modeling has been previously used in various research fields involving light transport, to deal with complex interactions between light photons and matter. Jerome et al. (1969), studied the neutron transport problems using Monte Carlo method; Witt (1977), and Yusef-Zadeh et al. (1984) modelled the light scattering in interstellar dust; Govaerts et al. (1998) have used the Monte Carlo approach to model the light scattering in three dimensional heterogeneous media. Monte Carlo method is routinely used in the field of hydrologic optics to model various characteristics of the radiative transfer within the water column. However the method is very complicated and may not be easy to apply in the field condition because:

(i) the method uses empirically derived scattering phase functions and water column attenuation coefficients to account for the absorption and scattering events which are undergone by the radiation beam as it propagates.

(ii) the method requires to estimate the light intensity at infinitesimal discrete depth therefore to calculate the light intensity along a path of 1m depth requires many calculations

(iii) For each infinitesimal step at least 10000 random numbers should be generated to get realistic result.

The mathematical basis of Monte Carlo method can be found in Cashew et al. (1959), Zeremba (1968), Kalos et al. (1986), and Lux et al. (1991). Following Lux et al. (1991),

the Monte Carlo method can be defined as any application where a stochastic model is constructed in which the expected value of a certain random variable (or a combination of several variables) is equivalent to the value of a physical quantity to be determined. This expected value is then estimated by the average of multiple independent samples representing the ramdom value introduced above.

5.2.3. Description of the method

Following Preisendorfer (1976), the optical properties of the water column can be grouped into two classes: (i) the inherent optical properties including the extinction coefficient (sum of absorption and scattering coefficients), and the volume scattering phase function; and (ii) the apparent optical properties including the irradiance attenuation, which depends on the radiance but also on the inherent optical properties. Consequently, irradiance propagation in a given water body depends on all the optical properties which are distributed in the water column. In order to compute the irradiance incident on top of the bottom substrate, and the contribution of the bottom to the radiance reflectance recorded at sensor, two steps were proposed as shown in Fig. 5.1.

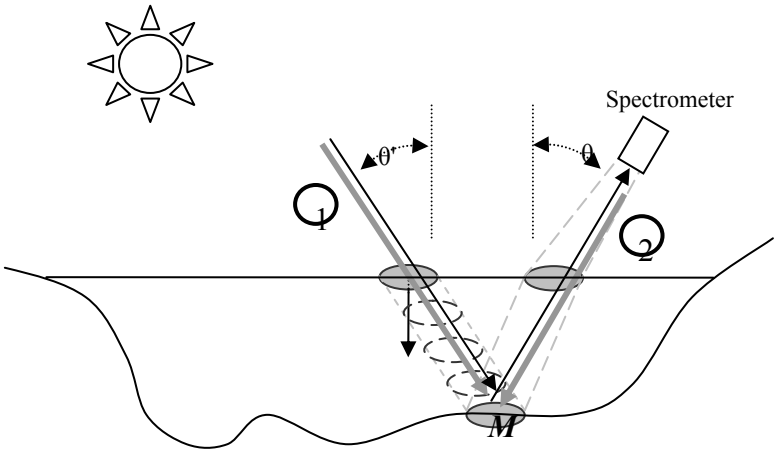

Note: 1: downwelling irradiance attenuation by the water column and its constitutive substances, 2: upwelling radiance reflected by the combined effect of the bottom substate and the water column.

Fig. 5.1 A physical model of irradiance propagation through a natural water body.

5.2.3.1. Expression of the downwelling radiance reaching the bottom (Step 1)

Let an infinitesimal light beam propagate through a water column in the downwelling direction (θ_d, ϕ_d), where θ_d and ϕ_d stand as the zenith and the azimuth angle of the light source respectively. At any position X=(x,y,z) relative to a Cartesian coordinate system, with origin at the incident point on top of the water column, the infinitesimal

variation of the radiance due to the combined effect of attenuation and scattering along the infinitesimal path dr is given by the radiative transfer equation shown in annex:

This equation can be discretized into equation 5.10.

$$L(z_i,\lambda)\cos 30 = -c(\lambda)\sum_{i=1}^{N} L(z_{i-1},\lambda)\Delta z_i + \sum_{i=1}^{N} L(z_{i-1},\lambda,\xi)\Delta z_i$$

(5.10)

The attenuation spectra $c(\lambda)$ (see Fig. 5.3) were derived from the Reflectance spectra of the testing samples using the inversion model developed by Ibrahim et al., (2005) presented as follows:

$$c(\lambda) = [-0.014 + 2.058 * R_{rs}(551)] * \left[\frac{c_w(710) * R_{rs}(710)}{b_p(710) * R_{rs}(\lambda)} - 1 \right]$$

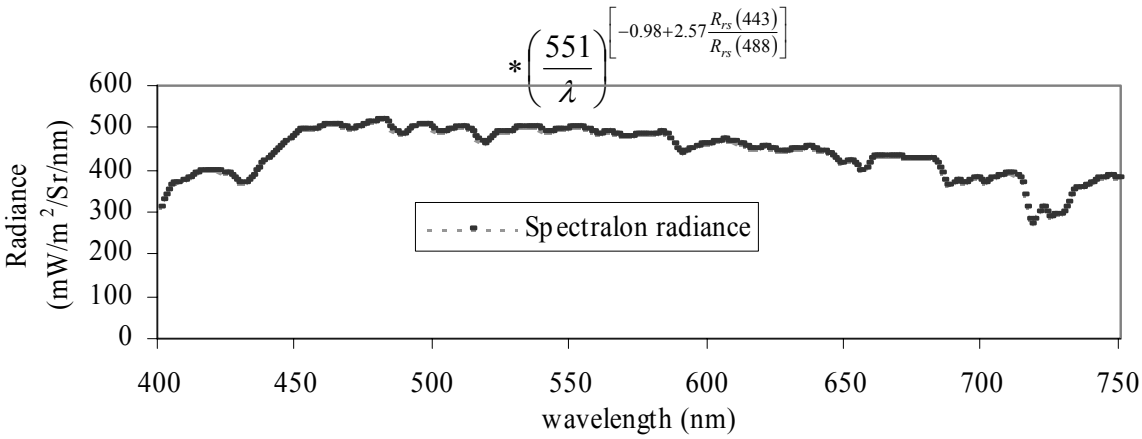

Note: The illumination zenith angle was set to 30°; the sensor was nadir pointing.

Fig. 5.2 The radiance of the white reference panel (Spectralon) collected under sunlight

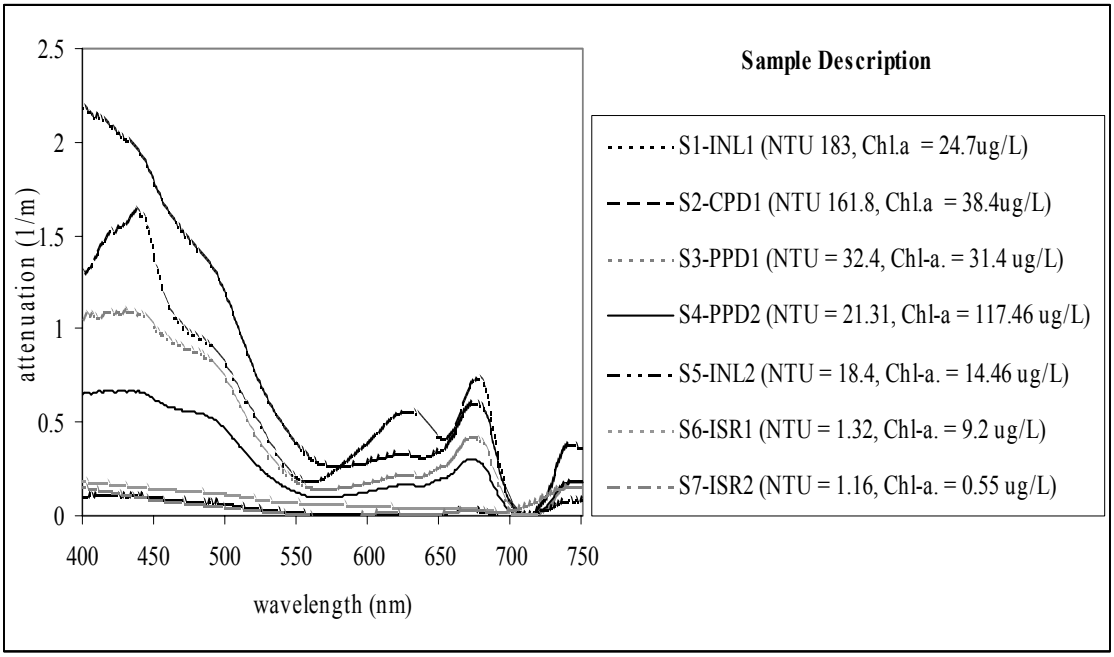

Fig. 5.3. Attenuation coefficients spectra of the testing samples

5.2.1.2. Estimation of the Reflectance recorded at sensor

By definition, Reflectance is the ratio of the upwelling radiance to the downwelling irradiance both expressed just above the water surface; that is:

$$R_{rs}\left(0^{+},\lambda,\theta_{u}\right)=L_{u}\left(0^{+},\lambda,\theta_{u},\phi_{u}\right)/E_{d}\left(0^{+},\lambda,\theta_{d},\phi_{d}\right) \qquad (5.12)$$

From this equation, the upwelling radiance just above the water surface can be written as a function of the downwelling irradiance just above the water surface and the Reflectance. The radiance of the white panel (spectralon) is used in this study to approximate the downwelling radiance $E_{d}\left(0^{+},\lambda,\theta_{d},\phi_{d}\right)$; detailed description can be found in FieldSpec-Pro user guide (2002), which is also available to download on the ASD website.

The spectra of $L(0^+,\lambda,\theta_u,\phi_u)$ could be derived using the Reflectance data shown in Fig. 3.5.

5.2.1.1.3. Expression of the bottom contribution to the water leaving radiance recorded at sensor

To find the contribution of the point M located on the lambertian bottom (see Fig. 5.4), the expression of the radiance contributed by this point at sensor level needs to be written.

Let us suppose $L(M,\psi)$ and $L(M,\psi')$ are the radiances which are received by the point M at bottom respectively, from the light source in an elementary solid angle $d\omega$ (step 1), and from the sensor along the reverse path in the elementary solid angle $d\omega'$ (step 2).

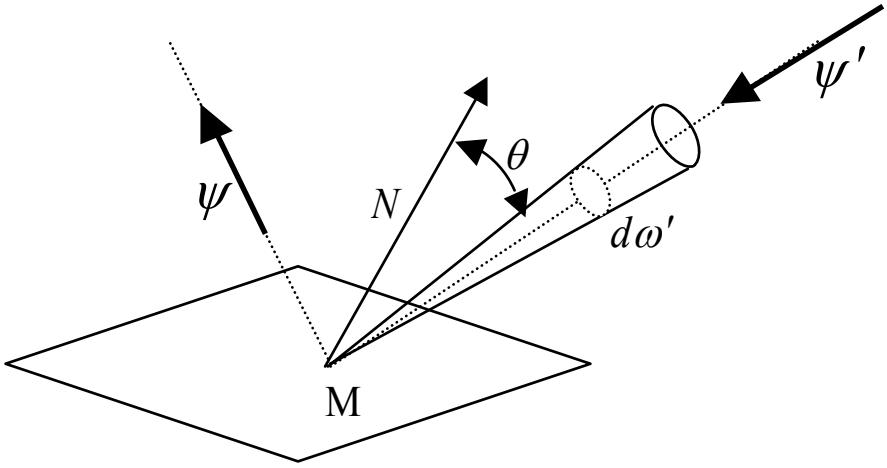

Fig. 5.4. Illustration of the BRDF of an ideal lambertian surface.

If $\rho_{bd}(M,\psi,\psi')$ is the bi-directional reflectance distribution function (BRDF) associated with the incident direction "ψ"and the reflected direction "ψ'", the contribution of the point M located on the lambertian bottom to the signal received by the sensor is:

$$L(M,\psi)=\int_{\psi'}\rho_{bd}(M,\psi,\psi')L(M,\psi')\cos\theta d\omega'$$

To solve this equation it need to sample a random direction "ξ" with density proportional to $\rho_{bd}(M,\theta,\phi,\theta',\phi')\cos\theta$, which allows finding the following estimator:

$$L(M,\psi) \approx R(M,\psi)L(M,\xi) \tag{5.15}$$

Since the bottom is assumed to be a lambertian surface, the random direction ξ will always be the ideal reflection direction (Shirley, 1991).

The density of the random directions "ξ" can be generated by considering $\rho_{bd}(M,\theta,\phi,\theta',\phi')\cos\theta$ as a width-two weighting function that is non-zero for a random pair $(x,y) \in [-1,1]^2$:

$$w(x,y) = (1-|x|)(1-|y|)$$

Random numbers are generated with a density equal to "w" by applying a transformation to the uniform random pair $(\xi_1,\xi_2) \in [0,1]^2$. The transformed random pair is $(t(\xi_1),t(\xi_2))$, where the transformation function is:

$$t(u) = \begin{cases} -0.5+\sqrt{2u} & if \quad u < 0.5 \qquad (5.17) \\ 1.5-\sqrt{2(1-u)} & if \quad u \geq 0.5 \qquad (5.18) \end{cases}$$

quation 5.15, in this case is rewritten as:

$$L(M,\psi) \approx R(M,\psi)L(M,\xi) \tag{5.19}$$

where, the reflectivity factor $R(M,\psi)$ is written as:

$$R(M,\psi) = \int_{\psi'} \rho_{bd}(M,\psi,\psi')\cos\theta d\omega \tag{2.20}$$

Equation 5.19 is used to compute the contribution of the bottom radiance to the water leaving radiance recorded at sensor. The results of the Monte Carlo simulations are shown in Fig. 5.16.

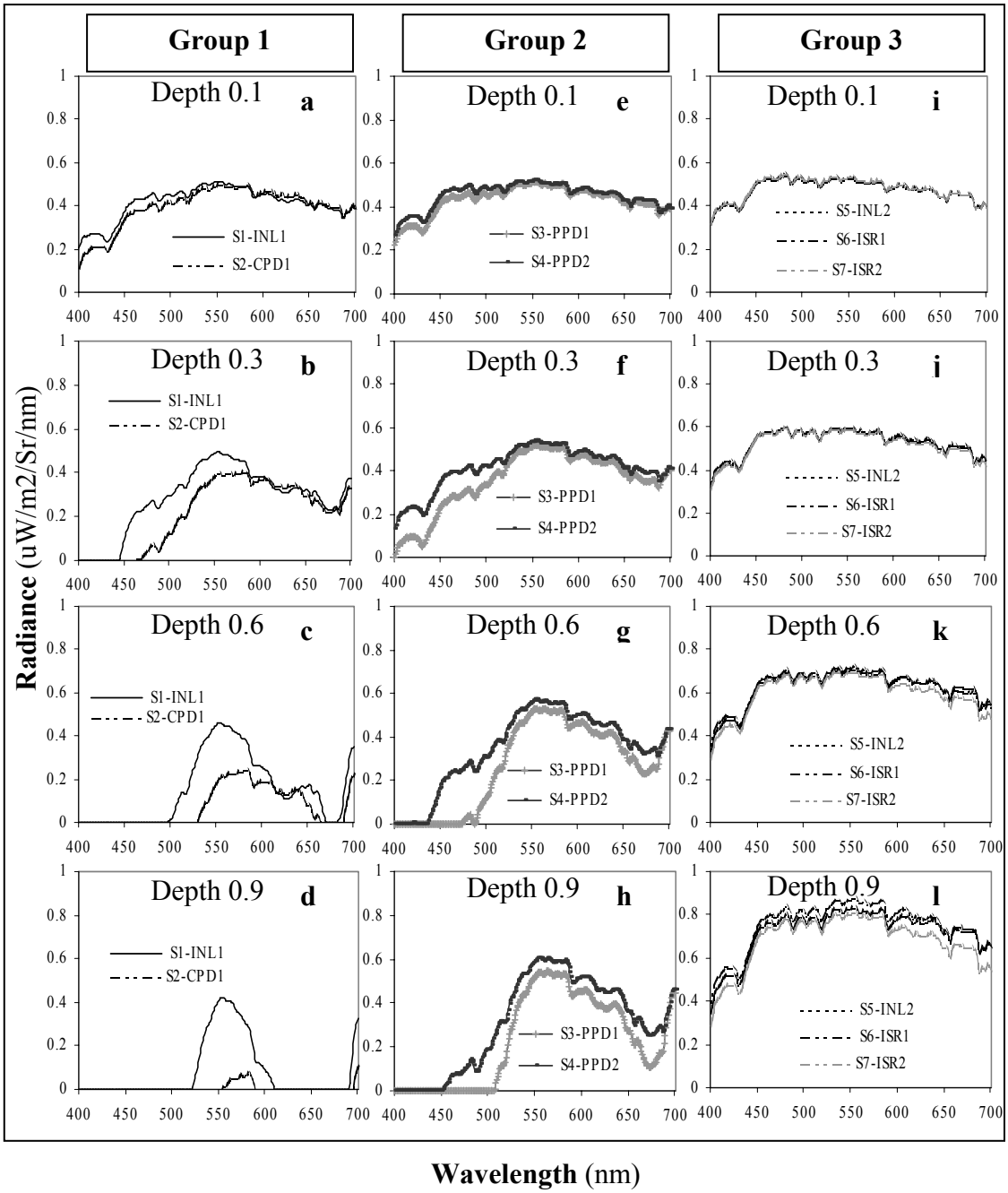

Fig. 5.5. The simulated downwelling radiance at selected water depths for the 3 groups of testing samples: 0.1m (a, e, I); 0.3m (b, f, j); 0.6m (c, g, k); and 0.9m (d, h, l)

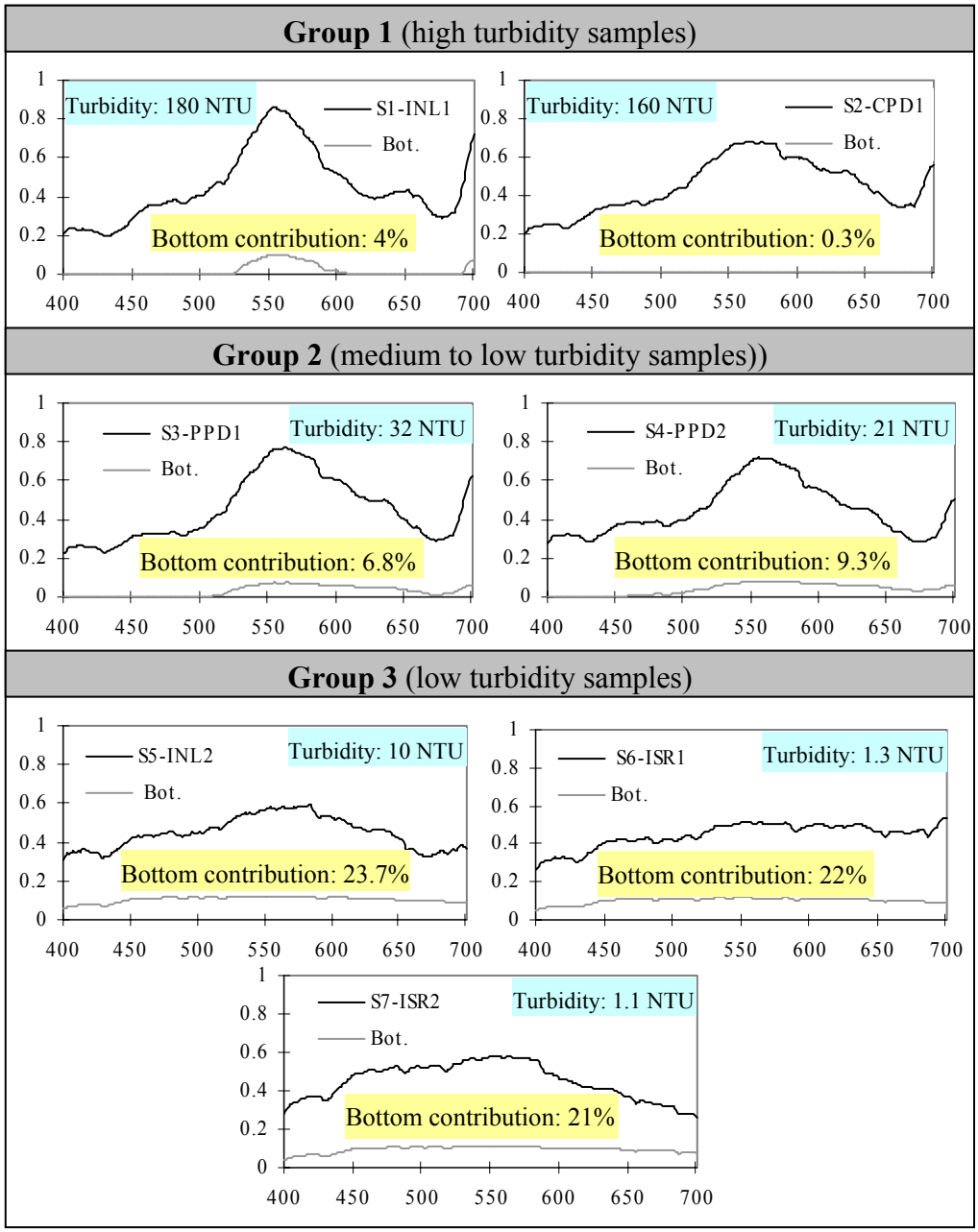

Fig. 5.6. Results of Monte Carlo simulations showing the contribution of the bottom, represented in solid grey lines, to the total water leaving radiance recorded at sensor, shown in solid black lines.

Radiative transfer equation

$$dL(X,\lambda,\theta,\phi)/dr = -c(X,\lambda)L(X,\lambda,\theta,\phi) + \int_0^{4\pi} \beta(X,\lambda,\theta_d,\phi_d,\theta',\phi')L(X,\lambda,\theta',\phi')d\omega' \quad \text{Eq.2}$$

Explicite form of the radiative transfer equation

$$\cos\theta\, dL(z,\lambda)/dz = -c(z,\lambda)L(z,\lambda) + \int_0^{4\pi} \beta(z,\lambda,\theta,\phi,\theta',\phi')L(z,\lambda,\theta',\phi')\sin\theta' d\theta' d\phi' dz$$

Expression of the downwelling radiance term

$$L(z,\lambda)\cos\theta = -c(\lambda)\int_0^{z_M} L(z,\lambda)dz + \int_0^{2\pi}\int_0^{\frac{\pi}{2}}\int_0^{z_M} \beta(z,\lambda,\theta,\phi,\theta',\phi')L(z,\lambda,\theta',\phi')\sin\theta' d\theta' d\phi' dz \quad \text{Eq.4}$$

Henyey-Greenstein phase function

$$p(\cos\theta_s) = (1-g_\lambda^2)/2(1+g_\lambda^2 - 2g_\lambda\cos\theta_s)^{3/4} \quad \text{Eq.5}$$

Probability distribution function of the Henyey-Greenstein phase function as follows:

$$\int_\alpha^{\chi_1} p_{par}(\chi)d\chi = \int_\alpha^{\chi_1} (1-g_\lambda^2)/2(1+g_\lambda^2 - 2g_\lambda\chi)^{3/4} d\chi \quad \text{Eq.6}$$

$$\cos\theta_s = \begin{cases} \frac{1}{2g}\left[(1+2g^2) - \left[(1-g^2)/(1-g+2g\xi)\right]\right]^2 & ;\ g \neq 0 \quad \text{Eq.7} \\ 2\xi - 1 & ;g = 0 \quad \text{Eq.8} \end{cases}$$

Explicite form of the downwelling radiance

$$L(z,\lambda)\cos\theta = -c(\lambda)\int_0^{z_M} L(z,\lambda)dz$$

$$+\int_0^{2\pi}\int_0^{\frac{\pi}{2}}\int_0^{z_M}\cos\theta_s L(z,\lambda,\theta',\phi')\sin\theta' d\theta' d\phi' dz \qquad \text{Eq.9}$$

Expression of the downwelling radiance after random sampling of its propagation direction

$$L(z,\lambda)\cos\theta = -c(\lambda)\int_0^{z_M} L(z,\lambda)dz + \int_0^{z_M} L(z,\lambda,\xi)dz \qquad \text{Eq.10}$$

Discretized form of the downwelling radiance

$$L(z_i,\lambda)\cos 30 = -c(\lambda)\sum_{i=1}^{N} L(z_{i-1},\lambda)\Delta z_i + \sum_{i=1}^{N} L(z_{i-1},\lambda,\xi)\Delta z_i$$

Expression of the spectral attenuation by the water column at given wavelength

$$c(\lambda) = [-0.014 + 2.058 * R_{rs}(551)] * \left[\frac{c_w(710) * R_{rs}(710)}{b_p(710) * R_{rs}(\lambda)} - 1\right] * \left(\frac{551}{\lambda}\right)^{\left[-0.98+2.57\frac{R_{rs}(443)}{R_{rs}(488)}\right]} \qquad \text{Eq.12}$$

Expression of the bottom contribution to the water leaving radiance recorded at sensor

$$L(M,\psi) = \int_{\psi'} \rho_{bd}(M,\psi,\psi')L(M,\psi')\cos\theta d\omega' \qquad \text{Eq.13}$$

Explicit form of the bottom contribution to the water leaving radiance recorded at sensor

$$L(M,\theta,\phi) = \int_{\phi=0}^{2\pi}\int_{\theta=0}^{\frac{\pi}{2}} \rho_{bd}(M,\theta,\phi,\theta'\phi')L(M,\theta',\phi')\cos\theta\sin\theta d\phi \qquad \text{Eq.14}$$

Non-zero weighing function for the random pair (x, y)

$$w(x,y) = (1-|x|)(1-|y|) \qquad \text{Eq.16}$$

Transformation function of the random pair (x, y)

$$t(u)=\begin{cases}-0.5+\sqrt{2u} & if \quad u<0.5 \\ 1.5-\sqrt{2(1-u)} & if \quad u\geq 0.5\end{cases} \qquad \text{Eq.17} \quad \text{Eq.18}$$

Bottom contribution to the water leaving radiance recorded at sensor

$$L(M,\psi)\approx R(M,\psi)L(M,\xi) \qquad \text{Eq.19}$$

Where the reflectivity factor $R(M,\psi)$ is written as

$$R(M,\psi)=\int_{\psi'}\rho_{bd}(M,\psi,\psi')\cos\theta d\omega \qquad \text{Eq.20}$$

Appendix C: selected models which have the least divergence by comparing to the total slope of the model.

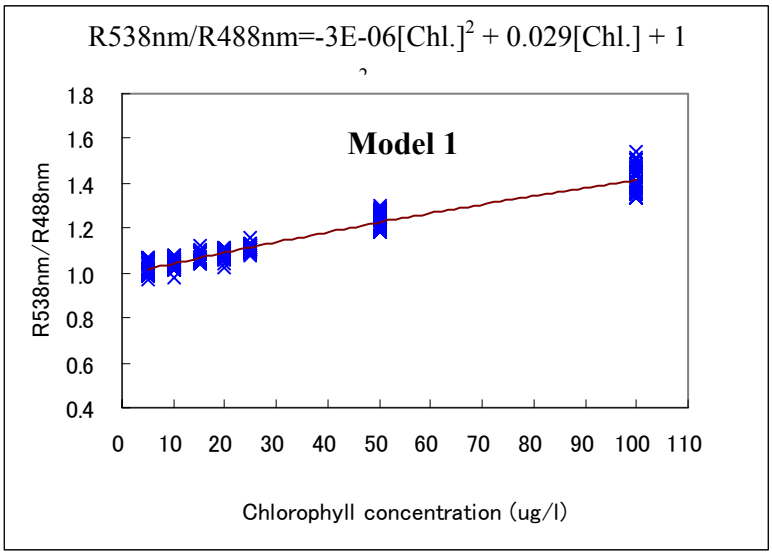

Fig. 4.13 Regression model for chlorophyll estimation using band ratio values R538nm/R488nm

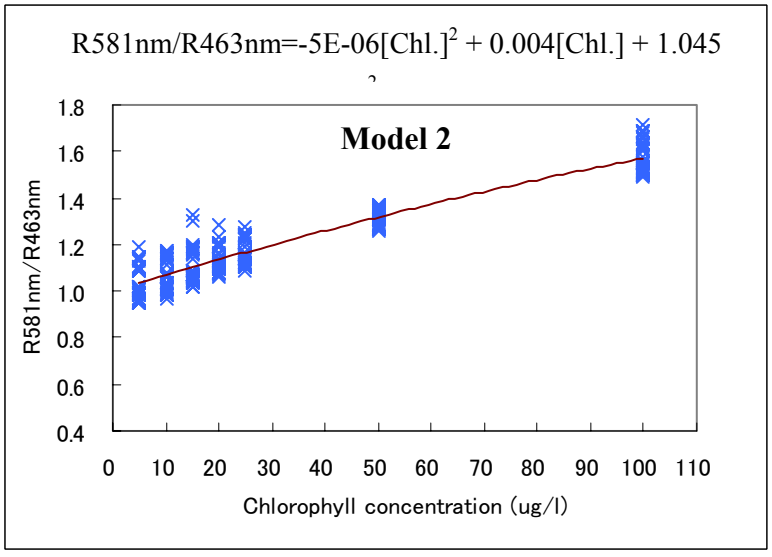

Fig. 4.14 Regression model for chlorophyll estimation using band ratio values R581nm/R463nm

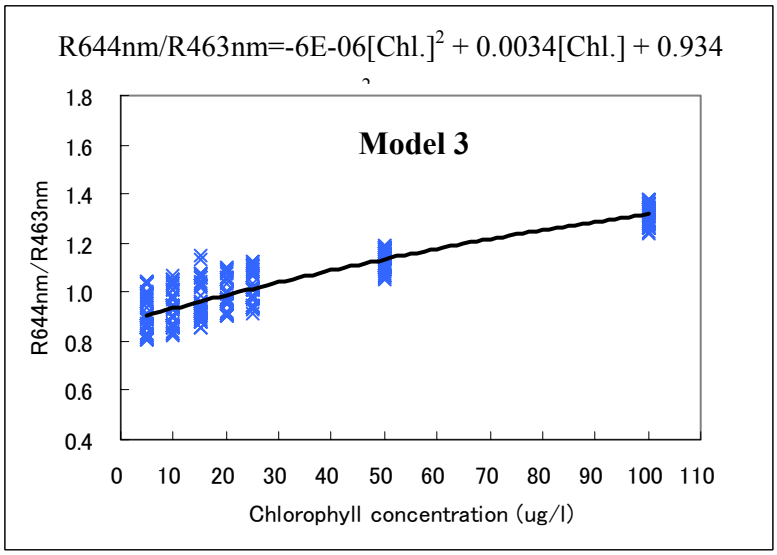

Fig. 4.15 Regression model for chlorophyll estimation using band ratio values R644nm/R463nm

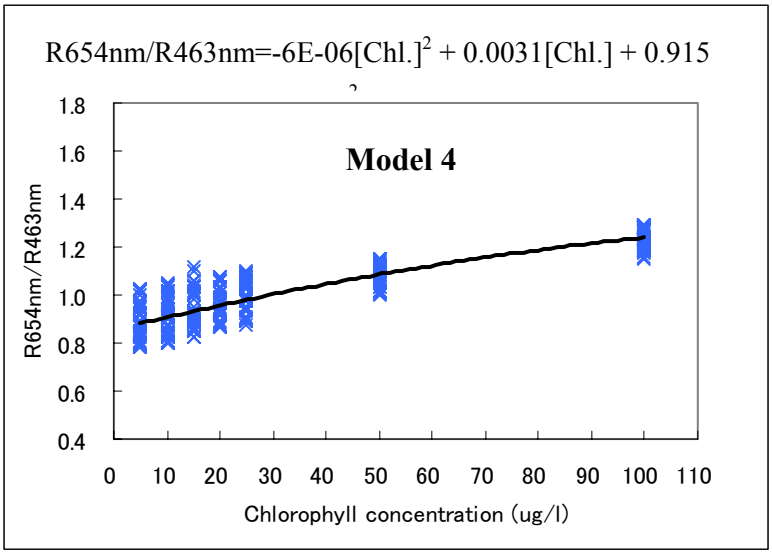

Fig. 4.16 Regression model for chlorophyll estimation using band ratio values R654nm/R463nm

Appendix D: Probability densities of spectral data for different chlorophyll concentrations

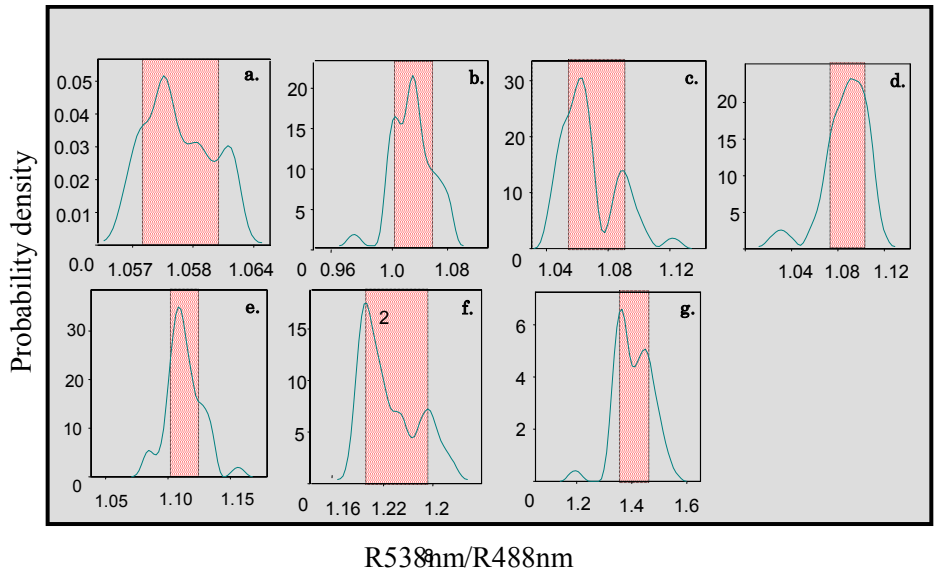

Fig. 4.17 Probability densities of spectral data for different chlorophyll concentrations

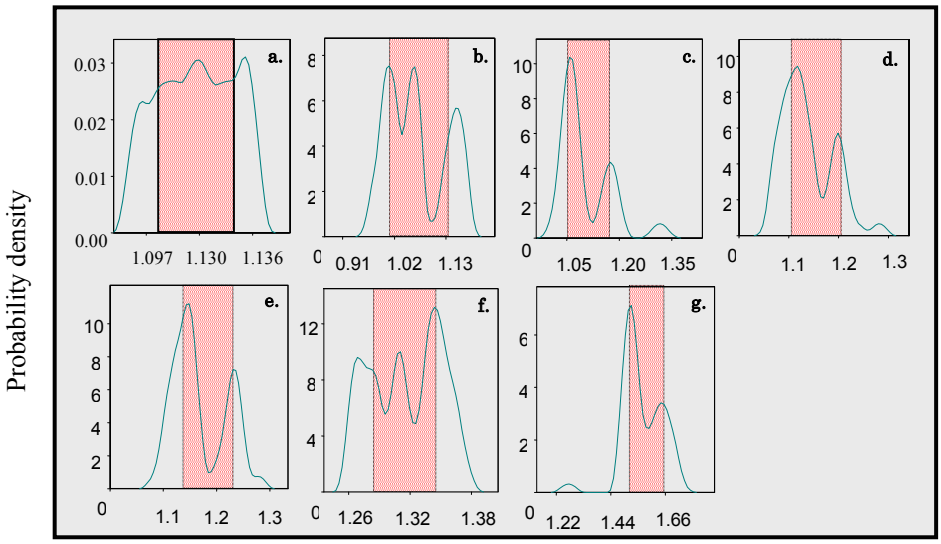

Fig. 4.19 Probability densities of spectral data for different chlorophyll concentrations

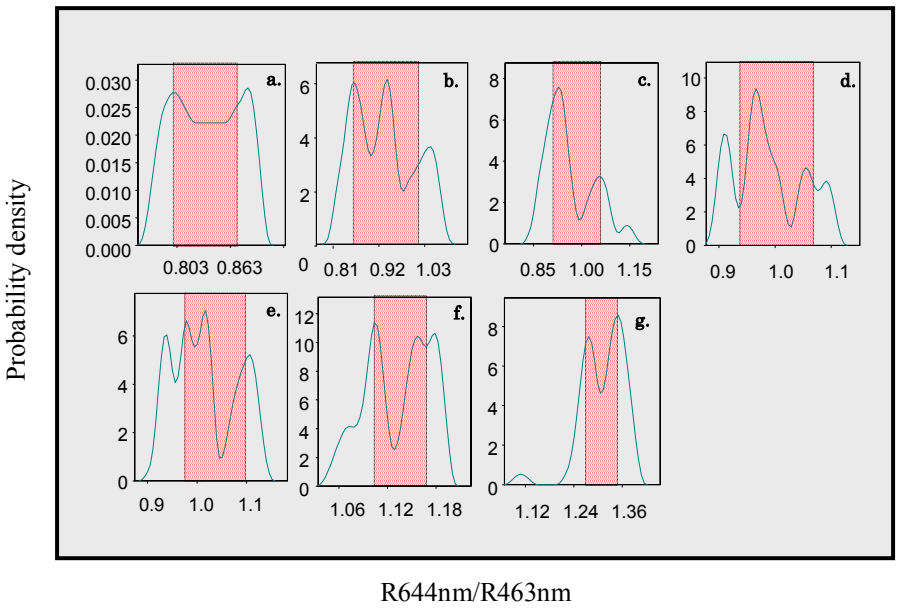

Fig. 4.21 Probability densities of spectral data for different chlorophyll concentrations

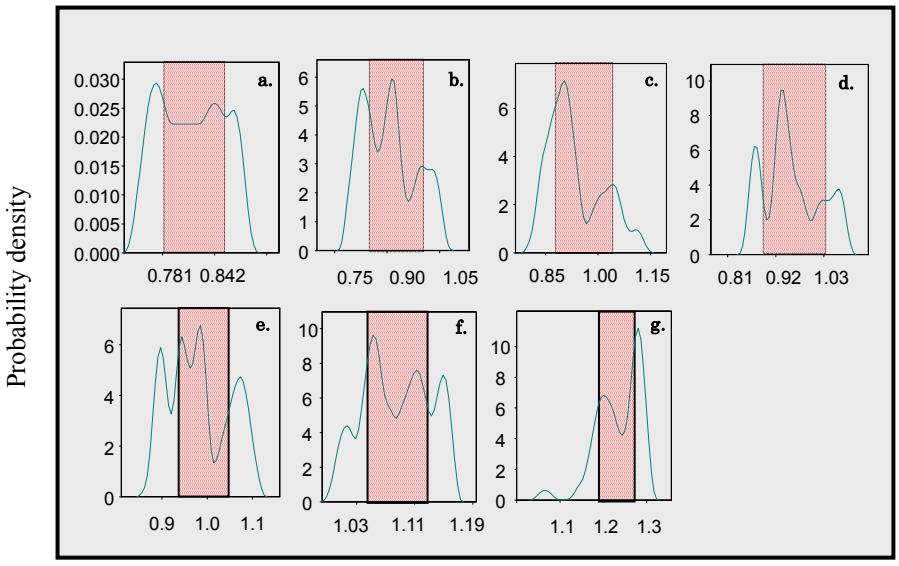

Fig. 4.23 Probability densities of spectral data for different chlorophyll concentrations

Appendix E: Model prediction accuracy obtained with 50% probability distribution of the spectral data set

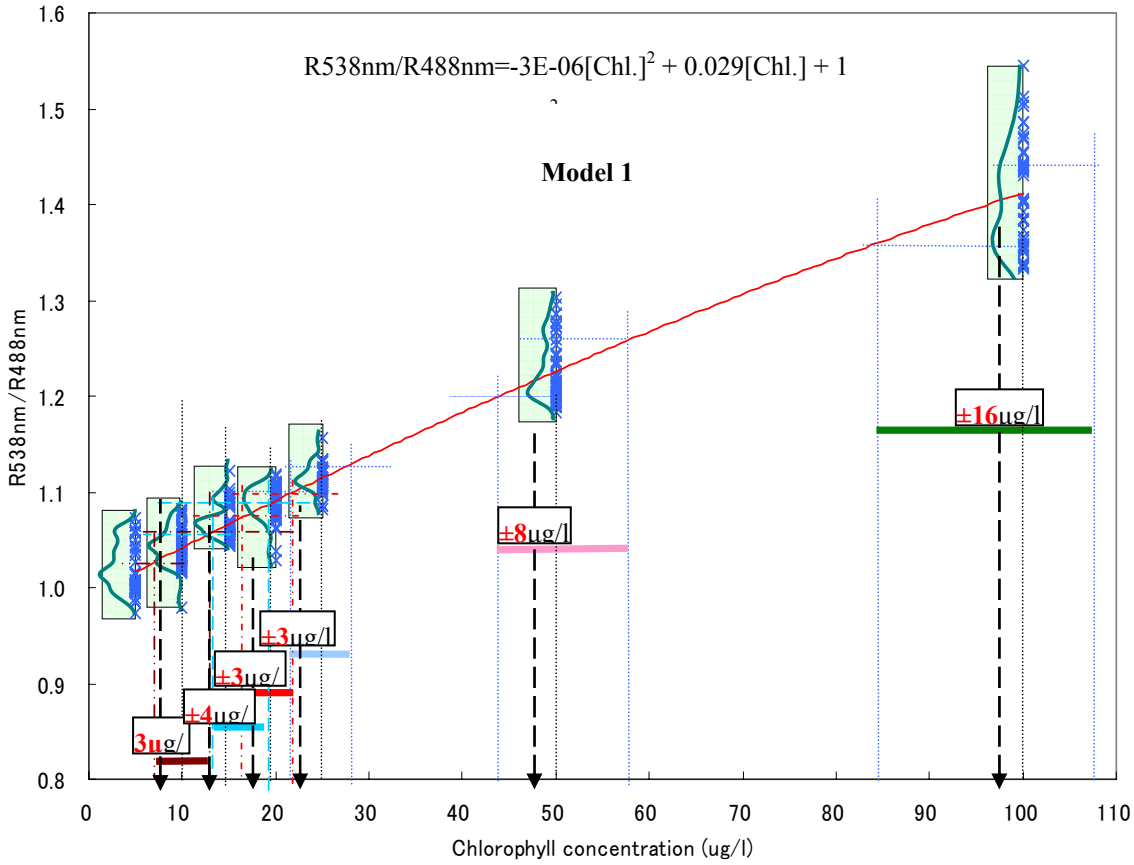

Note: The curve in red color represents the regression line, the curves in green color represent the probability density of band ratio R538nm/R488nm data distribution for each class of chlorophyll concentration. The ranges of chlorophyll estimation accuracy for each class of estimated chlorophyll concentration are written in red.

Fig. 4.18 Improved model prediction accuracy obtained with 50% probability

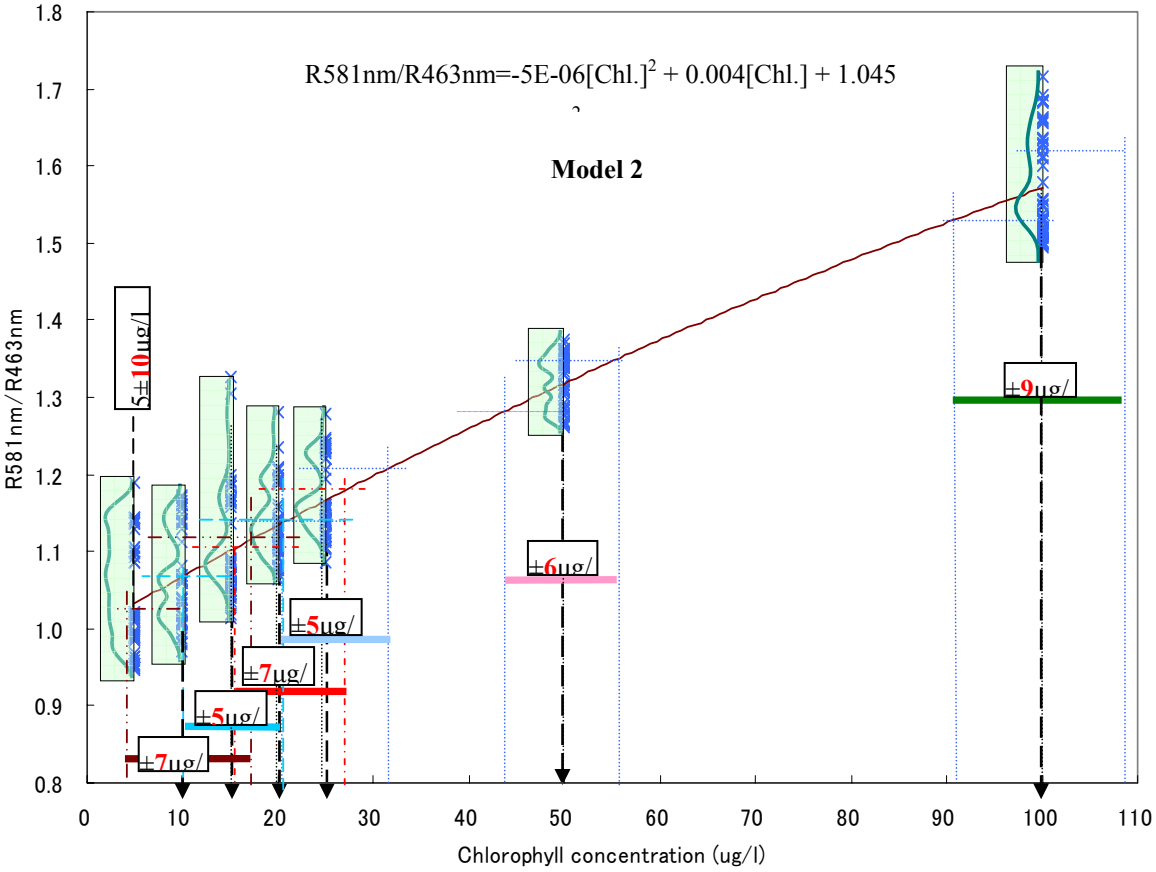

Note: The curve in red color represents the regression line, the curves in green color represent the probability density of band ratio R581nm/R463nm data distribution for each class of chlorophyll concentration. The ranges of chlorophyll estimation accuracy for each class of estimated chlorophyll concentration are written in red.

Fig. 4.20 Improved model prediction accuracy obtained with 50% probability

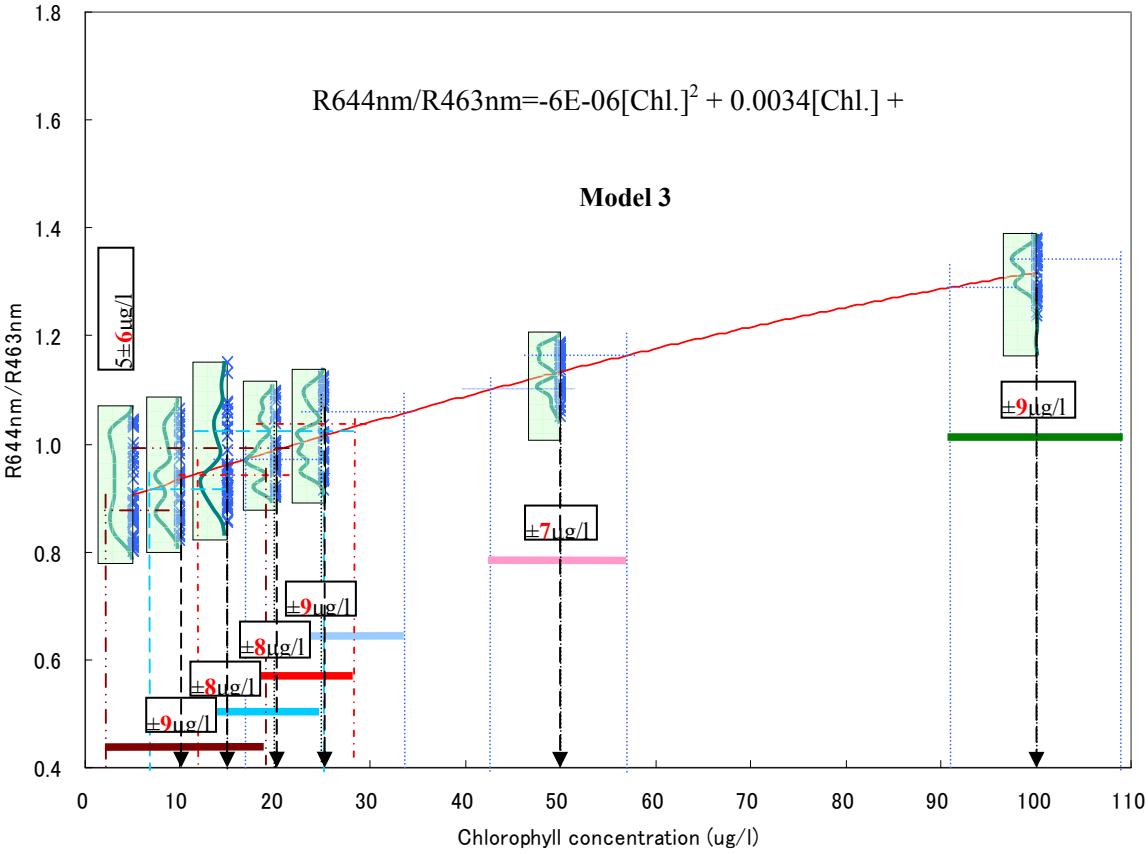

Note: The curve in red color represents the regression line, the curves in green color represent the probability density of band ratio R644nm/R463nm data distribution for each class of chlorophyll concentration. The ranges of chlorophyll estimation accuracy for each class of estimated chlorophyll concentration are written in red.

Fig. 4.22 Improved model prediction accuracy obtained with 50% probability

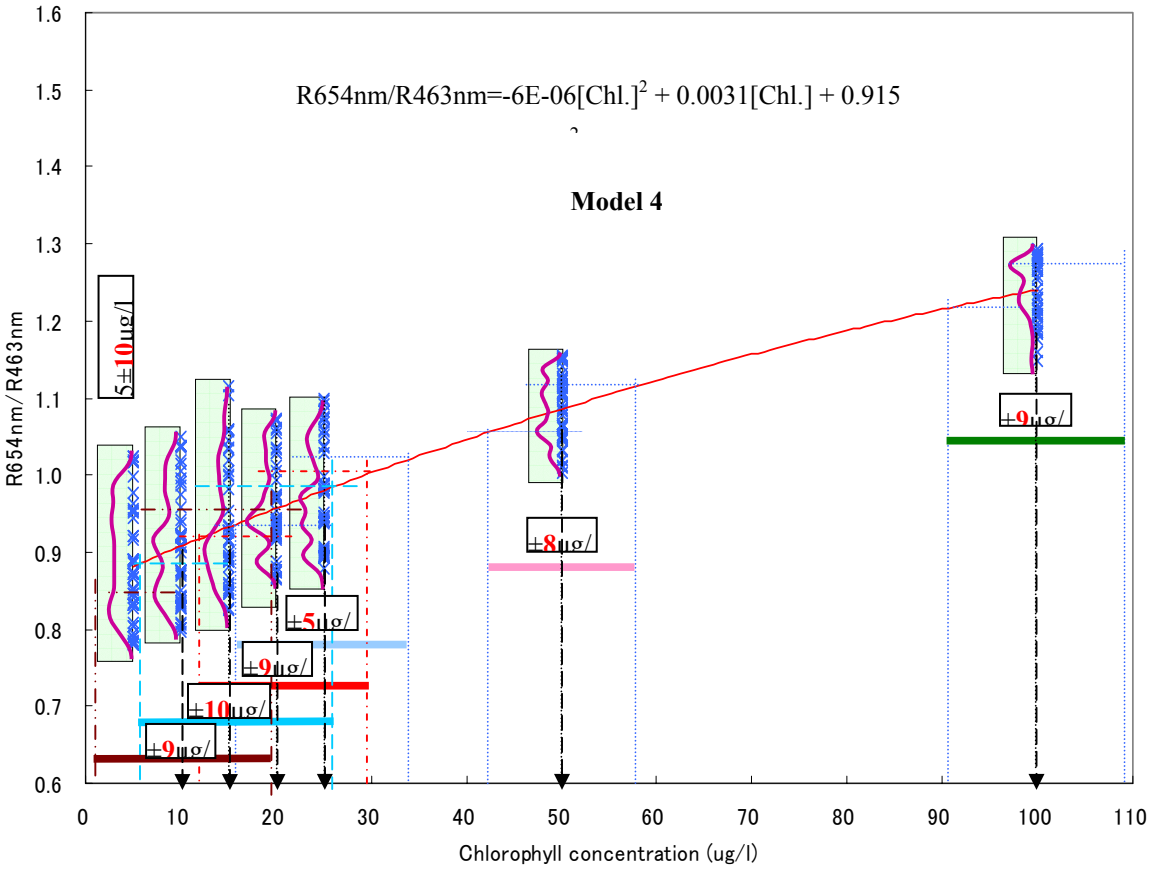

Note: The curve in red color represents the regression line, the curves in green color represent the probability density of band ratio R654nm/R463nm data distribution for each class of chlorophyll concentration. The ranges of chlorophyll estimation accuracy for each class of estimated chlorophyll concentration are written in red.

Fig. 4.24 Improved model prediction accuracy obtained with 50% probability

Appendix F. Phytoplankton culture media used for growing the monocultures

AF-6 medium

NaNO3	14 mg
NH4NO3	2.2 mg
MgSO4·7H2O	3 mg
KH2PO4	1 mg
K2HPO4	0.5 mg
CaCl2·2H2O	1 mg
CaCO3 [(2)]	1 mg
Fe-citrate	0.2 mg
Citric acid	0.2 mg
Biotin	0.2 µg
Thiamine HCl	1 µg
Vitamin B6	0.1 µg
Trace metals [(2)]	0.5 ml
Distilled water	99.5 ml
pH	6.6 [(3)]

C medium

Ca (NO3)2·4H2O	15 mg
KNO3	10 mg
β-Na2glycerophosphate	5 mg
MgSO4·7H2O	4 mg
Vitamin B12	0.01 μg
Biotin	0.01 μg
Thiamine HCl	1 μg
PIV metals [(1)]	0.3 ml
Tris (hydroxymethyl) aminomathane	50 mg
Distilled water	99.7 ml
pH	7.5

CA medium

Ca (NO3)2·4H2O	2 mg
KNO3	10 mg
NH4NO3	5 mg
β-Na2glycerophosphate	3 mg
MgSO4·7H2O	2 mg
Vitamin B12	0.01 μg
Biotin	0.01 μg

Thiamine HCl	1 µg
PIV metals [1]	0.1 ml
Fe (as EDTA; 1:1 molar) [2]	0.1 mg
HEPES	40 mg
Distilled water	99.9 ml
pH	7.2

CB medium

C medium with pH adjusted to 9.0 by buffering with Bicine instead of Tris (hydroxymethyl) aminomethane.

Csi medium

C medium with pH adjusted to 7.0 by buffering with 50 mg HEPES instead of Tris (hydroxymethyl) aminomethane. Thereafter, 10 mg $Na_2SiO_3 \cdot 9H_2O$ is added.

Appendix G: Short explanation about the importance of the future study points.

The roadmap (see Fig. 7.1) shows how far this study has been dealing with the problems of hyperspectral remote sensing technology for the monitoring and estimation of eutrophication in the shallow lakes and reservoirs.
Highlighted in red color are the problems which are not discussed in this research. These problems need further attention in future studies because they can generate some error in the spectral data.

- Most of the phytoplankton classification problems have been studied, while additional problems include how to evaluate the spectral contributions of skylight and the variations in sunlight intensity. These two points are especially important for field applications of the remote sensing technology to classify the phytoplankton species.

- For the chlorophyll density estimation, only the equipment error have been discussed and evaluated. One important source of error is the effect of the water column constituents on the spectral data because most of the other constituents have their spectral information mixed with the chlorophyll spectral information. The water column constituents susceptible to generate large error in the chlorophyll estimation results include (i) the suspended sediments such as inorganic matter and algal particulates, (ii) the dissolved substances such as the organic matter and yellow substances (degradation products of aquatic plants) (iii) the sediments which may be re-suspended from the bottom owing to biological activities or wind interaction with the shallow water surface, and (iv) the difference in the phytoplankton species. This difference is expressed in terms of specie-specificity of the chlorophyll density, and specie-specificity of the optical properties of the phytoplankton group. Another important factor to be discussed in future studies include the packaging effect of the chlorophyll pigment. This can be explained simply by saying that the chlorophyll measured directly on the phytoplankton

without breaking the cell appear to have lower density than the chlorophyll measured after destroying the phytoplankton cell. Those problems need to be investigated.

- It is necessary to up-scale the findings of this research to field remote sensing. Even though the intensities of the signals in the raw spectral data from the field may appear very weak, the same methodologies which are used in this study to evaluate the errors may be applied to field data remote sensing. In near future, the satellite remote sensing will be able to provide hyperspectral images with a resolution which is similar to the resolution of the hyperspectral spectrometer.
- Wastewater treatment and monitoring are very closely related issues in the sense that monitoring is always necessary to evaluate the efficiency of the wastewater treatment process to restore and secure water environment. But both will require cost evaluation to be applied for environmental restoration aim. The cost is a delicate issue in new technologies that are still under development such as the tertiary water treatment process and the proposed monitoring way by remote sensing technology. Over the operational lifetime of the wastewater plant or the monitoring equipment, operation and maintenance costs are also as important as the construction cost or the equipment cost. It is proposed in the future studies to evaluate objectively the costs of these technologies taking into account that it will be worth-investment for the preservation of water resources.